

AN ABSTRACT OF THE THESIS OF

Jonathan M. G. Viducich for the degree of Master of Science in Water Resources Engineering presented on June 26, 2015.

Title: Spillway Staging and Selective Sediment Deposition in Sand Storage Dams.

Abstract approved: _____

John S. Selker

Rainfall scarcity and variability present serious challenges to water security for many rural communities throughout the world's drylands. Sand dams—weirs built across ephemeral or seasonal rivers—provide an appropriate water harvesting and storage option for many regions. The structures quickly fill with sediment during rainy season flow events and store water underground in interstitial pores, thereby limiting evaporation, contamination and the prevalence of disease-carrying vectors. The size of deposited sediment particles largely determines sand dam effectiveness; fine materials do not transmit or yield usable quantities of water under a dam's modest head conditions. Many researchers and practitioners propose building sand dams in stages to limit capture of fine particles. I apply field and remotely-sensed data and statistical analysis to evaluate hypotheses about the catchment and reach-scale conditions required to optimize sediment deposition. I also use the results of unsteady HEC-RAS flow models to quantify the sensitivity of sedimentation processes to spillway height. The results of the statistical analyses show a negative correlation between mean catchment slope and median particle size collected by sand dams. Modeled results indicate that sedimentation is relatively more sensitive to variations in spillway height than to changes in the hydrograph, especially when a dam is short. However, sensitivities to a given modeled parameter vary by site. Based on the results, I recommend that the need for spillway staging be evaluated on a site-by-site basis, accounting for costs and expected benefits, and that designs incorporate progressively taller stages.

©Copyright by Jonathan M. G. Viducich
June 26, 2015
All Rights Reserved

Spillway Staging and Selective Sediment Deposition in Sand Storage Dams

by
Jonathan M. G. Viducich

A THESIS

submitted to

Oregon State University

in partial fulfillment of
the requirements for the
degree of

Master of Science

Presented June 26, 2015
Commencement June 2016

Master of Science thesis of Jonathan M. G. Viducich presented on June 26, 2015

APPROVED:

Major Professor, representing Water Resources Engineering

Director of the Water Resources Graduate Program

Dean of the Graduate School

I understand that my thesis will become part of the permanent collection of Oregon State University libraries. My signature below authorizes release of my thesis to any reader upon request.

Jonathan M. G. Viducich, Author

ACKNOWLEDGEMENTS

I am indebted to many individuals for the invaluable aid I received in completing this thesis. First, thank you to my advisor, Dr. John Selker, for wanting to explore this topic with me, and for your enthusiastic support along the way. It's been a real pleasure to work with you, and I'm a more creative and passionate scientist-engineer because of our time together. Thanks too to my incredible committee members, Drs. Richard Cuenca and Gordon Grant—you both played major roles in helping me connect my ideas to reality.

Thank you to Betty Miner, the Evans family and OSU's Humanitarian Engineering program for your friendship and generous financial support, without which this research would not have been possible.

Thank you to all of the OSU WRGP professors and colleagues who helped me think through tough questions. Drs. Mary Santelmann, Desirée Tullos and Robert Kennedy, your support is especially appreciated. Alan Stanton, Andy Wentworth, Austin Hall, Giova Mosquera, Leah Tai, Theresa Ring and Dr. Yutaka Hagimoto, I'll remember our long office hours together with great fondness. Thanks to Ian Neal and Dr. Stephen Hussey for the years of fruitful and perplexing conversations which helped frame this research topic in my mind. A big thanks to Sahelian Solutions (SASOL), the African Sand Dam Foundation (ASDF), the Conselho Cristão de Moçambique (CCM), the Mennonite Central Committee (MCC), Erik Nissen-Petersen and Prof. G-C. M. Mutiso for your wisdom, logistical support and friendship as we visited dams and traded stories. I hope this research proves useful as you continue in your good work. Thank you to the many rural communities who welcomed and hosted me over the years; your generosity astounds and inspires. Thanks to all the friends who helped critique this manuscript and shared invaluable insights, including Dr. Gordon Godshalk.

Thanks to my family for all your encouragement and patient efforts to understand my work these past years, especially when I didn't always have a firm grasp myself. And finally, enormous thanks to my wife, Lindsey, for the kind of support that included trekking with me through East Africa and baking cookies during the most stressful times. I couldn't have done this without you.

TABLE OF CONTENTS

	<u>Page</u>
1 Introduction.....	1
1.1 Target group.....	1
1.2 Personal motivation.....	1
1.3 Research method in brief.....	2
1.4 Structure of the report.....	2
2 Background and related literature.....	4
2.1 Sand storage dams description and history.....	4
2.2 Sedimentation processes.....	7
2.2.1 Sediment transport in seasonal and ephemeral rivers.....	7
2.2.2 Sand dam sedimentation.....	10
2.2.2.1 Catchment controls on sedimentation.....	10
2.2.2.2 Reach-scale controls on sedimentation.....	11
2.2.3 Sediment quality and water availability.....	14
2.3 Spillway height staging.....	20
3 Study region.....	25
4 Methods.....	27
4.1 Site selection.....	27
4.2 Field data.....	30
4.2.1 Field data collection.....	30
4.2.1.1 General site data.....	30
4.2.1.2 Dam design.....	30
4.2.1.3 Riverbed slope.....	31
4.2.1.4 Channel, flow and sedimentation history.....	31
4.2.1.5 Soil samples.....	33
4.2.2 Sediment characterization.....	35
4.2.2.1 Hydrometer method.....	35
4.2.2.2 Dry sieve method.....	37
4.2.2.3 Particle size distributions.....	37

TABLE OF CONTENTS (Continued)

	<u>Page</u>
4.2.3 Analysis.....	40
4.3 Remotely-sensed data.....	43
4.3.1 Catchment delineation and area.....	44
4.3.2 Catchment slope.....	46
4.3.3 Catchment land use.....	47
4.3.4 Analysis.....	48
4.4 Flow and sedimentation modeling.....	49
4.4.1 Site descriptions.....	50
4.4.2 Channel geometry reconstruction.....	55
4.4.3 Hydrograph reconstruction.....	57
4.4.4 Hydraulic flow models.....	61
4.4.5 Analysis of model outputs.....	63
4.4.6 Statistical analysis of maximum flow data.....	66
5 Results.....	68
5.1 Catchment characteristics.....	68
5.2 Local hydraulic conditions.....	70
5.2.1 Static flow data.....	70
5.2.2 Hydraulic flow modeling.....	72
6 Discussion.....	76
6.1 Recommendations for sand dam spillway design.....	76
6.1.1 Costs vs. benefits.....	76
6.1.2 Spillway stage design.....	77
6.2 Recommendations for further research.....	82
6.2.1 Larger sample sizes.....	82
6.2.2 Drainage options.....	82
6.2.3 Dam rehabilitation.....	83
6.2.4 Dams built in series.....	84
6.2.5 Bank management.....	84
6.2.6 Flow measurement.....	85

TABLE OF CONTENTS (Continued)

	<u>Page</u>
7 Conclusion.....	86
Bibliography.....	87
Appendices.....	92
Appendix 1: Site drawings.....	94
Appendix 2: Site photos.....	98
Appendix 3: Channel cross-section and stage profiles.....	100
Appendix 4: Variation in median particle size by location and depth.....	104
Appendix 5: Particle size distribution plots for bulk site sediment.....	110

LIST OF FIGURES

<u>Figure</u>	<u>Page</u>
2.1 Cutaway view of a mature sand dam.....	5
2.2 Traditional abstraction method.....	6
2.3 Common sand dam sedimentation process.....	12
2.4 Riverbed stratification.....	12
2.5 Suspended fines in open pool.....	13
2.6 Evaporation, depth and particle size.....	16
2.7 Threshold particle sizes for drainage.....	19
2.8 ALDEV spillway design.....	20
2.9 Spillway staging method.....	23
3.1 Kenya county map.....	26
4.1 Study site map.....	28
4.2 Silted sand dam.....	29
4.3 Site drawing.....	30
4.4 Soil core sample.....	33
4.5 Sand harvesting.....	34
4.6 Hydrometer test.....	36
4.7 Buried bottomset bed.....	41
4.8 Bulk particle size distributions.....	42
4.9 Stream and watershed delineation.....	45
4.10 Slope calculation.....	46
4.11 Land classification.....	47
4.12 Site 2 sand dam.....	50

LIST OF FIGURES (Continued)

<u>Figure</u>	<u>Page</u>
4.13 Site 2 sediment profile.....	51
4.14 Site 8 sand dam.....	52
4.15 Site 8 sediment profile.....	53
4.16 Site 9 sand dam.....	54
4.17 Site 9 sediment profile.....	55
4.18 Site 2 HEC-RAS reach geometry.....	56
4.19 Site 2 HEC-RAS dam geometry.....	56
4.20 Flow section area.....	58
4.21 Flow section wetted perimeter.....	59
4.22 Site 2 hydrographs.....	60
4.23 Site 8 hydrographs.....	60
4.24 Site 9 hydrographs.....	61
4.25 Variation in Rouse numbers.....	65
5.1 Catchment slope and particle size.....	69
5.2 Spillway height and particle size.....	71
5.3 Time fraction results.....	72
5.4 Actual particle size distributions.....	73
5.5 Surface plot comparison.....	74
6.1 Staging design flow chart.....	78
6.2 Failed sand dam.....	79
6.3 Sabo dam.....	83

LIST OF TABLES

<u>Table</u>	<u>Page</u>
2.1 Typical hydraulic properties of sediments.....	14
2.2 Capillary rise by sediment size class.....	15
2.3 Standard spillway heights.....	21
2.4 Comparison of staging methods.....	23
4.1 Site selection criteria.....	27
4.2 Particle size data.....	38
4.3 Processed hydrometer data.....	40
4.4 Particle size distribution.....	40
4.5 Characteristic bulk sediment results.....	43
4.6 Catchment characteristics.....	48
4.7 Model runs.....	61
4.8 Rouse number.....	63
4.9 Reach-scale characteristics.....	67
5.1 Catchment correlation results.....	68
5.2 Reach-scale correlation results.....	70
5.3 Sensitivity analysis.....	75

Chapter 1. Introduction

The objective of this work is to develop new understanding about sediment transport processes associated with sand dams at both catchment and reach scales, testing the sensitivity of selective deposition to a number of previously-proposed hypotheses and providing recommendations for the use of spillway staging.

1.1 Target group

This thesis is written primarily for sand dam practitioners and funding agencies, and assumes basic knowledge of hydraulic and hydrologic principles and vocabulary.

1.2 Personal motivation

Prior to beginning my graduate studies at Oregon State University, I spent three years working as a water engineer in Mozambique, partnering with the Mennonite Central Committee and the Conselho Cristão de Moçambique. During that time, I collaborated with communities in Mozambique and other countries to site, design and build over 35 sand dams, and I visited many more dam sites around the region.

Because sand dams represent a little-studied technology, many technical questions remain unanswered in the relatively small body of available academic literature. Over the years, I have shared many ongoing and lively conversations about various aspects of design with colleagues from around the world. Many points of confusion were resolved as a result of conversations with more knowledgeable engineers or by lessons learned in the field, but one question in particular remained unanswered and somewhat controversial: what is the importance and proper application of “spillway staging”, the trapping of sand in sequential lifts by adding to the dam’s height over time?

My personal motivation to address the topic of spillway staging stems in part from my own curiosity about a rather opaque aspect of sand dam design, and in part from my desire to continue supporting colleagues working to increase water security in arid and semi-arid regions through the application of sand dam technology.

1.3 Research method in brief

I collected field data, including channel geometries, flow records and samples of deposited sediment, at 13 established sand dams constructed using different techniques in two counties in Kenya. I then used remotely-sensed data to calculate catchment characteristics for 11 of the sites, and applied statistical tests to evaluate hypotheses that catchment characteristics (slope, area and land cover) and reach-scale hydraulic conditions at peak reported flow (peak reported discharge, flow cross-section and average velocity, spillway width and spillway height) provide good predictors of the sediment particle sizes trapped by sand dams. Finally, I used HEC-RAS to model dynamic hydraulic conditions at three sand dam sites, using field data to construct the models and validate the results. I applied calculated variations in a dimensionless descriptor of sediment transport, the Rouse number, to determine the relative sensitivities of sedimentation processes to spillway height, flow magnitude and peak flow duration.

1.4 Structure of the report

The report consists of seven chapters, a bibliography and five appendices.

Chapter 1 presents a short introduction to the research topic and methods, along with background about my personal interest in the subject.

Chapter 2 provides a survey of related literature, and contains sections describing the function and history of sand dams, sedimentation processes associated with arid and semi-arid regions in general and with sand dams in particular, and the impacts of deposited sediment quality on a sand dam's performance. The chapter concludes with an introduction of spillway staging for sand dams and a discussion of current views, methods and challenges.

Chapter 3 presents a brief description of the study region, including general information about climate and topography.

Chapter 4 describes my research methods in detail, and contains sections describing site selection, field data collection and sediment characterization, remotely-sensed data

collection and analysis, analysis of peak reported flow data, and the development and evaluation of hydraulic flow models.

Chapter 5 presents the results of the catchment characteristics and local hydraulics statistical analyses, as well as the results of the sensitivity analysis based on the unsteady flow modeling.

Chapter 6 discusses the implications of the results from Chapter 5, and includes sections with technical recommendations for sand dam practitioners and suggestions for further research.

Chapter 7 concludes the report with final recommendations for funding agencies, organizations and communities, and ends with closing remarks about the future of sand dams.

Finally, the bibliography section presents the primary sources of information referenced during the research, and the appendices present additional, detailed information about each of the study sites.

Chapter 2. Background and related literature

2.1 Description and history of sand storage dams

In the social and political economies of the world's drylands, water represents one of the most precious assets. Groundwater is frequently used where surface water is scarce, but in regions where existing groundwater resources are insufficient or too expensive to develop, rural communities frequently collect and store surface water during wet periods for use during dry periods [Lasage et al., 2008; Nilsson, 1988; Wipplinger, 1953]. Open water reservoirs are commonly used as rainwater harvesting solutions. However, surface dams face two primary obstacles, evaporation and siltation, which can drastically reduce effective storage capacity and efficiency [Quilis et al., 2008; Wipplinger, 1953]. Silt can be removed from reservoirs, but rehabilitation is usually prohibitively costly. Dam walls can sometimes be raised to increase a structure's storage capacity, but this actually increases evaporative losses as the surface area of the reservoir grows. As such, open water dams lose much or all of their cost-effectiveness over their lifetimes, a process often accelerated in dry regions.

Sand dams provide an alternative to open water dams. Sand dams are reinforced concrete or stonemasonry weirs constructed across intermittent, sand-bedded streams underlain by bedrock or another stable, low-permeability layer (Figure 2.1, next page).

Rather than filling with clay and silt, which limit conventional reservoir storage, well-designed sand dams fill primarily with coarser materials like sand and gravel, raising the level of the riverbed upstream of the structure.

The accumulation of coarse particles is key to a sand dam's success. Water quickly infiltrates the sediment and is stored in the pore spaces between grains. The hydraulic properties of the coarse sediment allow for the water's subsequent abstraction. In addition to overcoming most of the limitations typically associated with siltation, coarse sand also protects collected water against evaporation [Hellwig, 1973; Wipplinger, 1953]. Burger and Beaumont [1970] calculated very comparable annual yields for equal-sized open water and

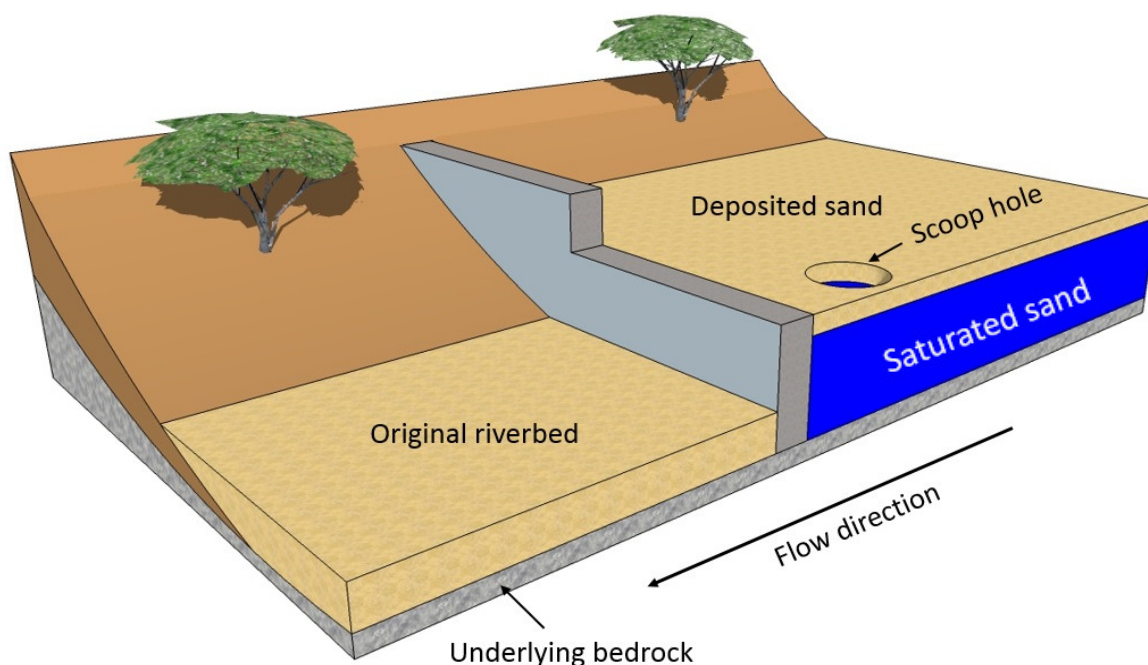


Figure 2.1: Cutaway view of a mature sand dam. Sand dams fill with sediment during flow events, and store water underground for the dry season.

sand storage dams, suggesting that the loss of storage volume when a sand dam fills with coarse sediment is often offset by the reduction in evaporative losses during a water year. Finally, sub-surface storage also limits the prevalence of disease-carrying vectors such as mosquitoes, and may prevent and reduce contamination [Avis, unpublished thesis, 2015; Hofkes and Visscher 1986].

Depending on reservoir capacity and sediment quality, sand dams can store tens of thousands of cubic meters of water [Quilis et al., 2008]—a volume typically representing only a small fraction of total annual stream runoff [Hut et al., 2008]—and create permanent or semi-permanent shallow aquifers in the riverbed which serve as dry season water sources for people, animals and small-scale agriculture. Water is often abstracted using traditional, hand-dug scoop holes (Figure 2.2, next page). Higher-cost, protected sources may also be used, such as large diameter wells or piped distribution systems passing through the dam wall, hydraulically connected to the aquifer by an infiltration gallery [Hussey, 1997; Nilsson, 1988]. Over time, sand dams can recharge existing aquifers and raise both upstream and downstream water tables [Borst and de Haas, 2006; Forzieri et al.,

2007; Hut et al., 2008; Nilsson, 1988; Quilis et al., 2008], permitting abstraction using different methods and creating an enhanced environment for plant and animal life. The establishment of localized water resources can be life-changing in hot, dry areas. Sand dams provide an important form of adaptation in the face of climate change and increasing rain variability [Lasage et al., 2008].



Figure 2.2: Traditional abstraction method. *After a sand dam fills with sediment and water, water is commonly abstracted using hand-dug scoop holes.*

Sand dams have been constructed and used for millennia in arid and semi-arid regions, including locations in Africa, North and South America, Asia and the Middle East. The structures are referred to by a variety of names, including, but not limited to, sand storage dams, sand dams, check dams, trap dams, sponge dams and desert water tanks [Van Haveren, 2004]. Their roots in modern community development water projects can largely be traced to Kenya, where the African Land Development Board (ALDEV) built the first sand dams between 1954 and the country's independence in 1964 [Mutiso, personal communication, 2014; Nissen-Petersen, 2006]. Since the early 1950s, a number of organizations and individuals have worked with communities to construct in excess of 3000 sand dams throughout Kenya's drylands [Nissen-Petersen, personal communication, 2015], though the exact number is unknown. Kenya features what is almost certainly the greatest concentration of sand storage dams built in modern times, and many recent publications related to sand dams have focused on Kenyan case studies (see Chapter 3). However, the structures are currently used throughout the continent, and in many of the world's other dryland regions.

While some sand dams are built by private landowners, especially for commercial purposes (e.g. watering cattle or irrigating crops), the majority of sand dams today are probably built by rural community associations or self-help groups, in partnership with non-governmental organizations (NGOs). Community engagement models vary widely by organization and region, but communities wishing to build a sand dam are typically responsible for sourcing locally-available materials (sand, water, stones etc.) and unskilled labor. NGOs provide other construction materials (cement and reinforcement steel), tools and technical support [Ertsen and Hut, 2009]. Community members are frequently involved in almost every step of the process, often by necessity, navigating land use issues, lending local knowledge to the siting process, and making decisions about abstraction methods and other aspects of design. This model of sharing cost and responsibility has proven effective in developing local ownership, which is closely linked to the sustainability of water supply projects [Hofkes and Visscher, 1986; Marks, Onda and Davis, 2013]. Also, due to their minimal maintenance and long life, sand dams frequently retain their effectiveness for many decades. Some sand dams have been reported to store water for over a century [Nilsson, 1988; Wipplinger, 1953]. The structures' long life, low maintenance and high level of community involvement often contributes to their value in low-resource contexts [Van Haveren, 2004] while reducing the cost-per-benefit [Nilsson, 1988].

2.2 Sedimentation processes

2.2.1 Sediment transport in seasonal and ephemeral rivers

Sand dams are typically constructed in arid and semi-arid regions, which are characterized by annual rainfall depths ranging from 100–300 mm and 200–800 mm, respectively, and precipitation to potential evapotranspiration ratios of 0.03–0.2 and 0.2–0.5 [Salem, 1989]. As such, the regions are highly prone to drought conditions. Most dryland precipitation falls during one or two annual rainy seasons, sometimes representing only a few (or no) significant storm events, and is highly variable both spatially and temporally. Rainfall is often intense and erosive; Edwards *et al.* [1983] found that 70% of total precipitation near Gatab, Kenya, fell at intensities greater than the 25 mm/hr erosive threshold as defined by

Hudson [1971], while *Mansell and Hussey* [2005] report typical rates of over 100 mm/hr for their arid and semi-arid study region in southern Zimbabwe.

Due to the relative lack of water during large portions of the year, along with wind erosion, soils in arid and semi-arid regions often exhibit low infiltration rates and high drainage densities [*Reid and Frostick*, 1987; *Rodier*, 1994]. Near-instantaneous ponding and the formation of a crust lead to a rapid onset of overland flow in response to rain events. For catchments with moderate to steep slopes, overland flow quickly accumulates in otherwise dry streambeds, resulting in relatively flashy hydrographs. *Reid and Frostick* [1987] describe rising limb times of only 4 to 16 min from dry bed to peak flow in their third-order stream in northern Kenya. As a result of intense rainfall and the large shear stresses applied by fast-moving overland flow, erosion rates are often very high in dry regions [*Hofkes and Visscher*, 1986; *Moore*, 1979], especially when slopes are steep and long [*Kinnell*, 2000].

Seasonal and ephemeral streams in arid and semi-arid regions often approach or slightly exceed critical flow (Froude number ≈ 1) around their peak [*Reid and Frostick*, 1987], likely due to interactions between hydraulic conditions and mobile beds as described by *Grant* [1997]. Discharges are extremely turbulent throughout much of the rising and falling limbs, with reported Reynolds numbers above 10^5 [*Reid and Frostick*, 1987]. Storms are typically short-lived, and river discharges drop quickly due to the lack of catchment storage. However, small, baseflow-driven surface flows may persist for days, weeks, or months following precipitation events, especially as a rainy season progresses and baseflow increases [*Jansen*, 2007]. Total annual runoff and flood intensity return periods vary widely from catchment to catchment [*Wipplinger*, 1953].

Sediment transport can generally be understood as the relationship between four factors: sediment supply (or load, q_s), sediment grain size (D , typically D_{50} , or the median grain diameter), stream discharge (Q) and channel slope (S_0). Lane's Balance

$$q_s D \propto Q S_0 \quad (\text{Eq. 1})$$

(Eq. 1) [Lane, 1955] provides a helpful framework for understanding the dynamic equilibrium maintained by a stream, as well as the mechanistic responses to perturbations like anthropogenic changes.

Like the storm discharges that drive them, sediment transport processes are highly dynamic in intermittent streams with mobile beds, and transport rates are often very large¹. Most sediment travels as suspended load during storm flows. Powell *et al.* [1996] showed that suspended sediment frequently comprises more than 90% of total sediment load for dryland ephemeral rivers. Sediment transport is often hysteretic—suspended and bedload transport rates often peak before or after discharge—and hysteresis observed in the field is most often related to different sediment availability conditions between the rising and falling limbs [Alexandrov *et al.*, 2003; Mao, 2012]. The direction of hysteresis may actually vary for a given stream over time, though suspended sediment concentrations typically dominate during the rising limb, especially early in the runoff season when supply is essentially unlimited [Alexandrov *et al.*, 2003; Negev, 1969].

Due to the near-unlimited supply of sediment early in a rainy season, streams in semi-arid and arid zones may hold more potential for deterministic modeling than those in regions with humid climates. As indicated by Eq. 1., when sediment supply is abundant, suspended sediment load concentrations and median grain sizes are primarily controlled by hydraulic processes and vary systematically with flow parameters [Reid and Frostick, 1987].

However, a few challenges to successful deterministic modeling of sediment transport in intermittent dryland streams remain. First, spatio-temporal sediment supply and rainfall-runoff patterns associated with heterogeneous catchments and sporadic rainfall are sometimes very complex, resulting in uncertainties [Alexandrov *et al.*, 2003]. Additionally, data useful for the characterization of seasonal and ephemeral flows in arid and semi-arid regions remain scarce, due to the lack of extensive gauging networks in most developing countries [Reid and Frostick, 1987]. Sand dams are most often built on intermittent streams

¹ According to compiled records of suspended sediment yields for medium-sized basins in a range of climates, semi-arid catchments export 36 times more material than humid-temperate and 21 times more than humid-tropical equivalents [Reid and Frostick, 1987].

falling in the 1st to 4th order range, and any one stream has relatively limited regional significance. Because of the lack of widespread data, most studies of seasonal river processes, including those concerning sediment transport and sand dam hydrology, are restricted to one or just a few highly-monitored sites, and a single rainy season.

2.2.2 Sand dam sedimentation

2.2.2.1 Catchment controls on sedimentation

The sediment which deposits in a sand dam originates in the catchment area, and only some catchments produce desirable, coarse-textured sand. *Gijsbertsen* [2007] notes that the availability of sand in a riverbed prior to construction represents a crucial component for functional sand dams. He used remotely-sensed data to identify catchment characteristics best correlated with sand-bedded, intermittent streams for a region in southern-central Kenya. *Gijsbertsen* found that mean catchment slopes greater than 2 degrees provide the strongest predictor of sandy riverbeds, and that mean particle sizes in a riverbed strongly correlate with those on the riverbanks. He concluded that coarse-grained sediment is mainly sourced from riverbanks eroded by surface runoff. *Nissen-Petersen*, however, suggests that sediment is predominately sourced from the larger catchment area, and points to basin land use as among the most important factors in sand dam sedimentation². Based on his field experience, *Nissen-Petersen* proposes that sand dams with watersheds dominated by farmland are more likely to fill with fine sediment than those characterized primarily by rocky outcrops. Regardless of their source, the most favorable parent rocks are coarse granite, quartzite and sandstone, while basalts and rhyolites tend to produce less favorable sediment for sand dams [*Nilsson*, 1988].

As Lane's Balance (Eq. 1) indicates, riverbed particle sizes are typically proportional to channel slope. Coarse particles found in steep, mountain catchments typically transition to fine silts in lower-lying floodplains. Due to the inverse relationship between particle size and potential dam storage volume along the length of a stream, *Nilsson* [1988] and others

² From *Nissen-Petersen*, E. (2011), Sand Dams or Silt Traps, ASAL Consultants Ltd., available at <http://www.samsamwater.com/library/Sand_dams_or_silt_traps.pdf>.

recommend siting sand dams in transitional zones between mountains and plains, where intermediate slopes permit the transport of coarse material while allowing for sufficient storage volume.

While precipitation is clearly important for sand dam success, and rainfall must be of sufficient intensity and depth to erode and transport coarse sediment and fully recharge sand dams, *Gijsbertsen* [2007] did not find a correlation between precipitation depth or intensity and the presence of sandy riverbeds for southern Kenya. In addition, *Gijsbertsen* visited a number of sub-optimal sand dams located in areas with positive catchment characteristics and concluded that local conditions had a greater impact than broader catchment characteristics for those sites.

2.2.2.2 Reach-scale controls on sedimentation

The construction of a dam creates a backwater, or an upstream river section which is characterized by increasing cross-sectional flow area, decreasing flow velocity and decreasing turbulence. Because turbulence provides the principle force keeping particles in suspension³, the reduction in turbulence allows coarse sediment to drop out of the flow, often resulting in the formation of a delta at the upstream end of the backwater⁴ (Figure 2.3, next page). Meanwhile, smaller, lighter particles which remain in suspension at the top of the backwater are either deposited closer to the dam wall, where velocities and turbulence continue to decrease, or they remain in suspension and flow over the top of the structure. The fine sediment particles which settle near the dam wall typically form a wedge-shaped layer called a bottomset bed. As sediment-laden water continues to flow over the delta and enters the deeper, slower-moving pool upstream of the dam, coarse

³ Many sand dam practitioners refer to high flow velocities transporting particles or keeping them in suspension. While velocity is an important factor in drag and turbulent forces (the latter due to the velocity-related transfer of momentum through shear stresses in the water column), velocity itself is not a force capable of lifting or transporting sediment, so this language is imprecise.

⁴ I am unaware of literature describing the differences between sedimentation patterns in sand dams, but my own field experience and anecdotal evidence from community members suggest that a small percentage of sand dams fill uniformly, with deposition occurring nearly simultaneously throughout the backwater. This phenomenon also occurs occasionally in large, open-water reservoirs with narrow channels, frequent water level fluctuations and limited fine sediment loads [*Morris and Fan*, 1998]—common conditions in streams suitable for sand dams.

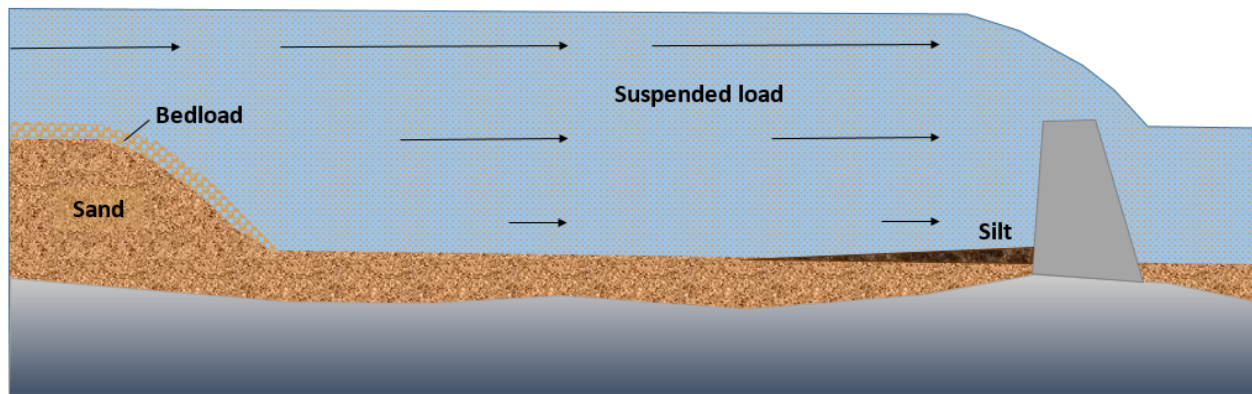


Figure 2.3: Common sand dam sedimentation process. As a sand dam fills with sediment, coarse particles often form a delta, which migrates downstream towards the dam. Meanwhile, fine particles either settle near the dam wall or continue in suspension and are discharged.

sediment particles traveling as bedload are deposited on the forward edge of the delta (known as the foreset), and the bedform migrates downstream until it eventually reaches the dam wall and fills the structure to the level of the spillway.

Of course, the terms “fine” and “coarse” are relative, and the actual sizes of particles which are either trapped by a dam or remain in suspension vary with a number of factors.

Because the construction of a new sand dam results in decreased stream competence and transport capacity upstream of the structure, sand dams ultimately trap some percentage of the fine sediment which would have otherwise traveled as washload, resulting in aquifers with more fine particles than the original riverbeds. Likewise, because a storm’s falling limb

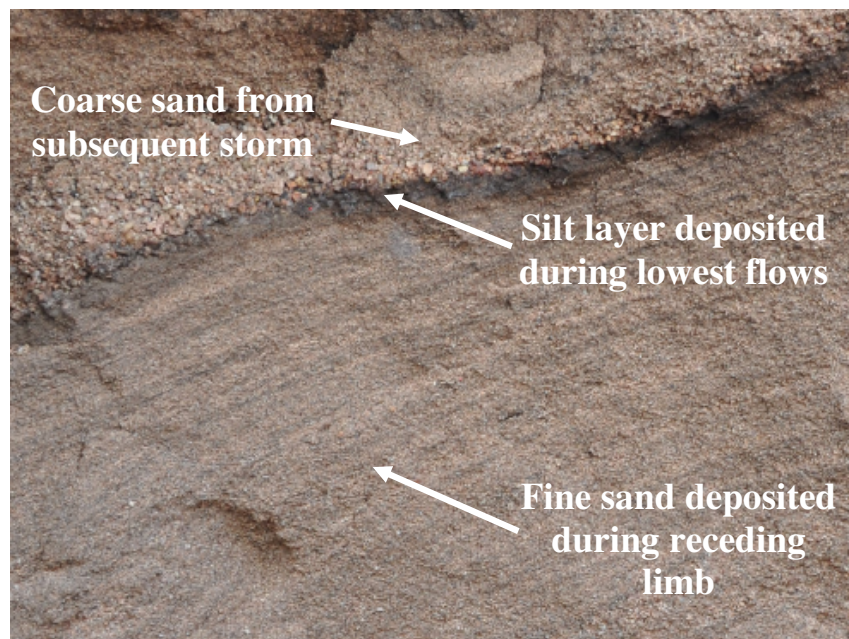


Figure 2.4: Riverbed stratification. Sediment is often deposited in visibly stratified layers upstream of a sand dam.

transports and deposits progressively finer sediment, and small storms may only transport fine particles, localized deposits of fines are common within a generally coarser bed. This is especially apparent when a dam requires many storms to fill: the coarsening-fining cycle resulting from the multiple storms often results in visible stratification (Figure 2.4, previous page). Fine sediment left suspended in the open water upstream of a partially-filled dam may settle out at the end of a rainy season and add fine material to the bottomset bed [Borst and de Haas, 2006].



Figure 2.5: Suspended fines in open pool. *At the end of a rainy season, some suspended sediment is often left in the open pool upstream of a partially-filled sand dam, and settles out during the dry season.*

Figure 2.5 shows a partially-filled sand dam at the end of a rainy season, with a high concentration of fine sediment left suspended in the surface pool.

Virtually all sand dams trap some fine sediment, and the fines do not necessarily present a problem for dam performance. As a sand dam fills with sediment, the flow's cross-sectional area upstream of the structure progressively decreases. This process results in increased velocity and turbulence for a given discharge, often leading to the scour of finer particles and replacement with coarser particles near the surface of the riverbed [Wipplinger, 1953]. Likewise, baseflow-controlled discharge at the end of one storm, along with the highly turbulent and powerful rising limb of the next storm, often scour fine particles deposited during the low flows produced by sediment-bearing runoff [Gijsbertsen, 2007]. A thin layer of silt sometimes remains on the bed surface after the end of a surface flow event; however, the reservoir is typically saturated before fines are deposited, so aquifer recharge is not affected. Any remaining silt is often eroded by animals, people, wind or the next storm [Borst and de Haas, 2006].

While fine sediments are frequently scoured, the competence of flows to erode silt and clay from the thicker bottomset bed, while often assumed, is not well documented. In many cases, the bottomset bed is simply buried by coarse sand, effectively reducing the structure's storage capacity in what might otherwise be the most productive location for water abstraction (see Chapter 4).

2.2.3 Sediment quality and water availability

The particle size distribution of deposited sediment, and the sediment's resulting hydraulic properties, dramatically affect a dam's ability to store, transmit and yield water. First, sediment should be highly porous, with the ability to store significant quantities of water. Second, the sediment captured by a successful sand dam must be highly permeable in both the vertical and horizontal directions, permitting the dam to fully recharge during flow events (this is especially important for sites with limited baseflow) and transmit useful quantities of water in a reasonable period of time to abstraction points during the dry season⁵. Third, the sediment must have a high specific yield, and easily release stored water for use. Table 2.1 gives typical values of porosity, permeability and specific yield for the sediment classes typically found in sand dams. Note that silts are more porous than some sands, but have much lower permeabilities and specific yields, illustrating some of their negative impacts on sand dam performance [Hofkes and Visscher, 1986; Nilsson, 1988].

Table 2.1: Typical hydraulic properties of sediments.
The sediments trapped by sand dams are characterized by a range of porosity, permeability and specific yield values [Mays, 2011].

Size class	Porosity (%)	Permeability (m/day)	Specific yield (%)
Gravel	25-35	100-1000	12-25
Sand	30-42	1-50	10-25
Silt	40-45	0.0005-0.1	5-10

⁵ Sediment with very high permeability may actually limit the duration of water availability during the dry season, especially when dams with small storage volumes are constructed on rivers with little baseflow. If subsurface baseflow quickly drains from upstream reaches and enters the reservoir, some will likely be discharged and lost before it is used. By contrast, less-permeable sediments restrict upstream flow, providing slower recharge throughout the dry season as water is gradually abstracted [Mansell and Hussey, 2005].

The reported values represent broad generalizations, and actual values may be higher or lower depending on the shape, size, compaction and grading of sediment particles. For example, *Mansell and Hussey* [2005] measured somewhat larger permeability values for sandy riverbeds in southern Zimbabwe. *Wipplinger* [1953] measured specific yields of around 25% for typical sandy riverbeds in Namibia. He describes a sand dam constructed south of Windhoek with sediment specific yields reportedly ranging as high as 33%. Most sediment mixtures trapped by sand dams have somewhat lower yields, however, especially when they are poorly sorted and compacted, and the values in Table 2.1 may be considered appropriate for most cases⁶. The particle size distribution of sediment trapped by a given sand dam can be used to predict many of the sediment's hydraulic properties [*Todd*, 1964], but direct testing of riverbed samples may be simpler and more effective for most cases.

The particle size distribution of sediments trapped by a sand dam also strongly affects capillarity and evaporative losses. Capillarity, which results from the adhesive forces between water molecules and solid materials, causes moisture to rise above the water table when it is stored in small pores (such as those between sediment grains in an aquifer). The strength of capillarity, and thus the height of the capillary rise above the water table, is determined by the size of the pore spaces. Table 2.2 gives approximate heights of capillary rise in different granular materials.

Table 2.2: Capillary rise by size class.
Due to the range of pore sizes, capillary rise varies by sediment class [Heath, 1987].

Material	Capillary rise (m)
Coarse sand	0.1
Medium sand	0.2
Fine sand	0.4
Silt	1

⁶ *Nissen-Petersen* [2006] reports commonly-quoted specific yield values of up to 35% for coarse sand, but defines the size class as particles ranging from 1.5 to 5 mm. Coarse sand is typically classified as particles ranging from 0.5 to 1 mm [*Vanoni*, 2006]—which *Nissen-Petersen* classifies as fine sand—and *Nissen-Petersen*'s measured specific yield of 19% for fine sand agrees with Table 2.1.

Hellwig [1973] measured and quantified the daily loss of evaporated water from a sand aquifer as a function of both water table depth and sediment particle size. He found that sediment size has little effect on surface evaporation from fully-saturated sand, but that 8% less water evaporates from the surface of saturated sand compared to open water surfaces. *Hellwig* also found that evaporation of sub-surface water decreases with increasing particle size and better sorting—corresponding with decreasing capillary rise—and increasing water table depth. Finally, *Hellwig* found that evaporation effectively ceases for water stored 60 cm below the surface of a sand bed with a mean particle size of 0.53 mm. *Wipplinger* [1953] reports a cessation of evaporation from a sand aquifer with a water table 0.9 m below the surface of the bed, but does not specify the sediment particle size(s). Figure 2.6 shows measured evaporative losses as a function of depth and mean particle size.

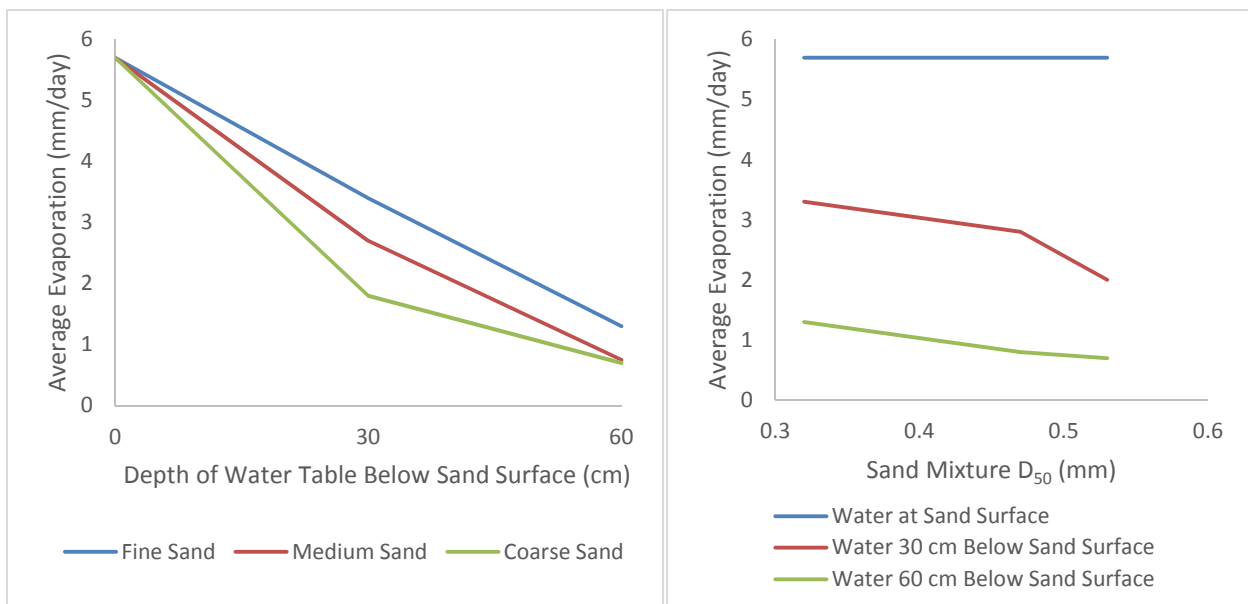


Figure 2.6: Evaporation, depth and particle size. *Hellwig* [1973] measured evaporative losses as a function of aquifer particle size and water table depth, and found that evaporation decreases with coarser media and deeper water table surfaces.

In addition to evaporative losses, fine sediment containing organic material is more likely to support vegetation, leading to transpiration losses from phreatophytic plants [*Hellwig*, 1973]. Due to the increase in evapotranspiration resulting from fine sediments

accumulated near the riverbed surface, *Nilsson* [1988] recommends avoiding the deposition of fine materials at shallow depths.

While I am unaware of established standards for quantifying and comparing the performance of sand dams⁷, it is clear that many sand dams fill with relatively fine sediment, and their limited ability to store and yield water either restricts or prevents their useful function. Nissen-Petersen suggests that 90% of all sand dams built since the 1970s have failed, many due to sedimentation problems⁸. The leader of one sand dam-building organization told me that approximately 40% of their sand dams suffer from significant storage problems due to the deposition of fine sediment.

However, it is also important to recognize that performance is somewhat relative in an analysis of benefits. For community members who currently walk tens of kilometers during the dry season to fetch water for domestic use, a sand dam which only stores sufficient water for two months' supply may represent a notable benefit. The same dam might represent a failure if built by a self-help group wishing to complement existing local groundwater supplies and use the stored water for irrigation. Regardless, the accumulation of fine sediment represents one of the greatest limitations to a sand dam's success.

Given the variation in community goals and the range of acceptable performances, it is difficult to define a single objective in terms of the particle size distribution of trapped sediment. It seems important to maximize both storage and yield by making use of the full reservoir volume, so for the purposes of this report, I propose that a successful sand dam, defined solely in terms of its sedimentation profile⁹, is one which releases water from its entire aquifer depth under gravity. Based on capillary theory, the (negative) pressure at which water drains from pores is a function of the pore size, which is itself a monotone

⁷ For an example of a method which quantifies the suitability of a site before construction, see *Forzieri et al.* [2007].

⁸ Nissen-Petersen, E. (2010), Sand dams vs subsurface dams, available at <<http://www.thewaterchannel.tv/media-gallery/663-nissen-petersen-sand-dams-vs-subsurface-dams>>

⁹ Sand dams may also perform poorly for reasons unrelated to the particle size distribution of deposited sediment. Examples include river rerouting, leaky basement material underlying the riverbed and/or poor rains. A sand dam's impact on livelihoods (which is generally considered to be of greater importance than its technical potential) is also dependent on social factors like distance from homes, proximity to sacred sites [*Hofkes and Visscher*, 1986] and general community interest.

function of particle size for non-swelling soils with limited aggregation, clay content and structure [Nimmo, 2004; Wu, 1987].

The critical pore size for drainage can be written as

$$r_{crit} = \frac{2\sigma\cos(\theta)}{\rho gh} \quad (\text{Eq. 2})$$

where r_{crit} is the critical pore radius, σ is the surface tension of water, θ is the contact angle of water on the sediment (typically taken to be zero for draining media), ρ is the density of water, g is gravitational acceleration and h is pressure head in meters. Characterizing pore size based on sediment particle size distribution requires some assumptions about particle shape, sorting and compaction; generally, homogenous sediments comprised of spherical particles have much larger pore radii than do poorly-graded mixtures. Researchers propose a range of scaling factors relating pore diameter to particle diameter [Wu, 1987]. Eq. 3 provides a conservatively-fine estimate for the sediments likely found in most sand dams.

$$r_{pore} \approx \frac{1}{10} r_{50} \quad (\text{Eq. 3})$$

By assuming a contact angle of 0° and a soil water temperature of 25°C , the critical particle size required for drainage may be plotted as a function of depth in a theoretical sand aquifer with a depth of 3 m, as shown in Figure 2.7 (next page).

Using my definition of success as stated above, a successful sediment bed is one whose particle sizes remain above the threshold curve at all depths. While the curve must be recalculated for other aquifer depths, the results are clear: coarse sediment is more important near the bottom of the reservoir in order to allow drainage, while fining is more acceptable near the surface. This result stands in contrast to the desired surface coarsening required to minimize evaporative losses, and reconciling the two results is site-specific. Assuming that a sand dam aquifer is of sufficient depth to store adequate water below the depth of evaporative influence, finer sediment may be more permissible near the surface, but for relatively shallow aquifers, coarse sediment is desirable at all depths to limit evaporative losses.

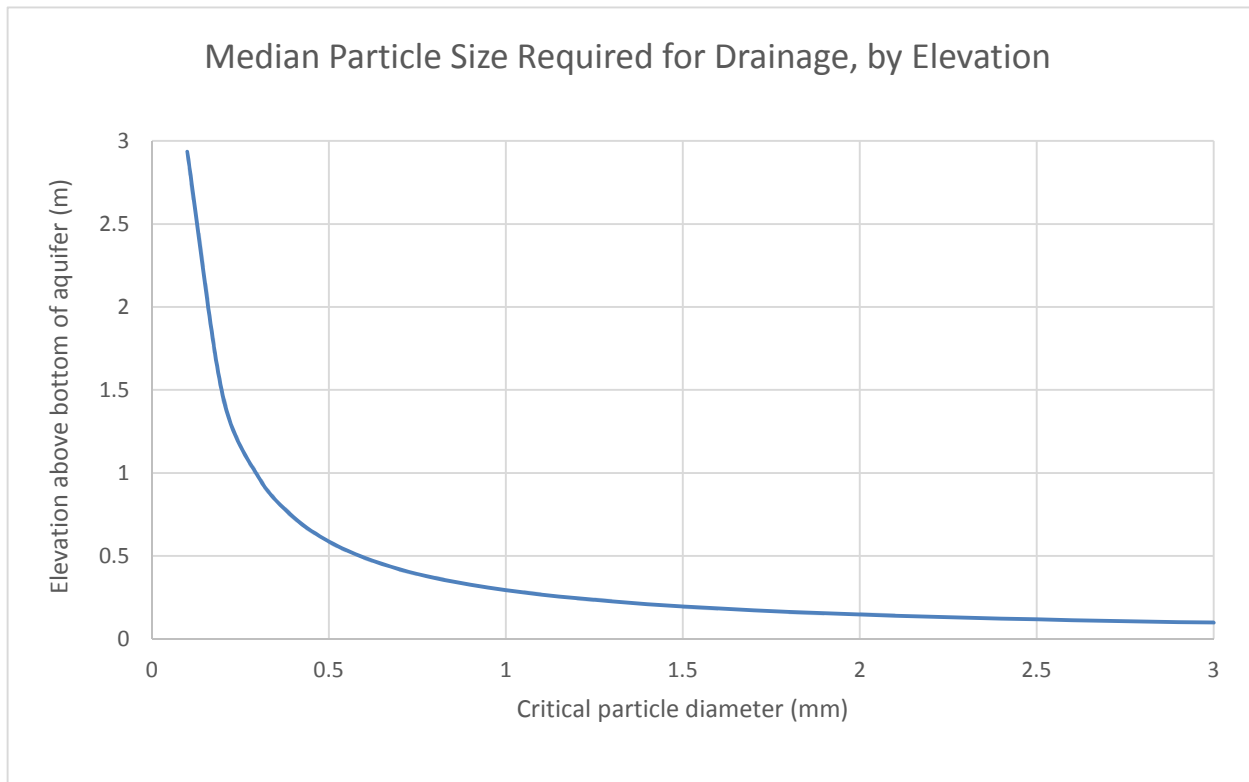


Figure 2.7: Threshold particle sizes for drainage. *The particle size required to allow pore drainage varies with depth; finer particles are more permissible near the bed surface.*

Nissen-Petersen [1997] recommends a minimum median particle size of 0.5 mm for sufficient storage and extraction, based on his extensive field experience. This value does not acknowledge the role of grading—a homogenous, coarse sand bed may have the same median particle size as a mixed bed of gravel, sand and silt, but perform very differently. Neither does the value consider baseflow, water demand, aquifer depth or the possibility of variation in median particle size with depth. Generally-speaking, though, Nissen-Petersen’s recommendation probably provides a reasonable value for many sites. Figure 2.7 suggests that the bottom 0.5 m of a 3 m-deep aquifer filled with this texture sand would yield little water, however.

2.3 Spillway height staging

Of the myriad factors affecting the size of deposited sediment particles in a sand dam, the height of the spillway represents one variable which may be easily controlled¹⁰. As was previously described, sand dams induce aggradation of the bed by reducing the forces required to keep sediment particles in suspension. In order to maintain a stream's ability to transport fine sediment, many sand dam practitioners and design manuals advocate building sand dams in stages. Using this method, a dam's spillway is initially built to some fraction of the final height, limiting the extent of the backwater and maintaining upstream velocity and turbulence, with the objective of discharging fine sediment and trapping predominately coarse particles. Then, after trapped sediment fills the dam to the level of the first stage (a process which may require only a single storm or many rainy seasons), a second stage is added, and the process is repeated until the final spillway height is achieved. The result, ideally, is a dam filled with relatively coarse and uniform sediment and enhanced aquifer performance.

Proponents of spillway staging suggest a number of different methods for staging design. Many practitioners recommend the use of a standard stage height for every dam, regardless of a site's particular characteristics. The earliest sand dams built in Kenya—those designed by District Agricultural Officer Eng. Classen as part of the 1950s and '60s ALDEV project—were themselves built using standard stage heights [Mutiso, *personal communication*, 2014; Nissen-Petersen, 2006], as depicted in Figure 2.8¹¹.

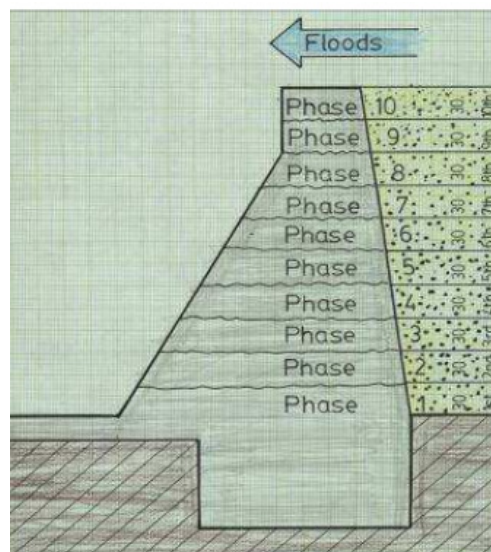


Figure 2.8: ALDEV spillway design. The original Kenyan sand dams were constructed in several phases using standard stage heights.

¹⁰ Siphons have also been used in an attempt to maintain flow velocities immediately upstream of structures, and to scour and discharge fine sediments which would otherwise deposit in the bottomset bed [Wipplinger, 1953]. Siphons are seldom used today, due to their technical inefficiency and high cost [Burger and Beaumont, 1970].

¹¹ From Nissen-Petersen, E. (2011), Sand Dams or Silt Traps, ASAL Consultants Ltd., available at <http://www.samsamwater.com/library/Sand_dams_or_silt_traps.pdf>.

Standard stage heights are advantageous in their simplicity, but the range of suggested values in Table 2.3 illustrates their disadvantage: every site is unique, and so standards vary by institution based on their experiences. A standard stage height which is universally appropriate for every sand dam must necessarily be overly conservative, and will incur extra costs for most sites.

Table 2.3: Standard spillway heights. *Practitioners and researchers recommend a range of standard spillway stage heights, based on their experiences in different regions.*

Source	Suggested stage height (m)
<i>Nissen-Petersen</i> [2006]	0.3
<i>Nissen-Petersen</i> [2011] ¹²	0.2-0.5
<i>RAIN Foundation</i> [2008]	0.3-0.5
<i>Hofkes and Visscher</i> [1986]	~2
<i>Diettrich</i> [2005] ¹³	2
<i>Maddrell and Neal</i> [2012]	<3

In contrast to a standard stage height approach, other researchers and practitioners identify a need for the development of site-specific approaches to spillway design. *Borst and de Haas* [2006] write:

“Experts should quantify processes of sedimentation behind a newly-built dam, and the risks of sedimentation of too fine materials in the reservoir behind the dam in relation to the height of the dam [...] Studies should be carried out to determine the optimal height of the dam and its spillway in relation to construction, sedimentation, water storage properties and costs.”

Several researchers and practitioners propose hypotheses regarding the most important catchment and site characteristics for consideration in staging. *The National Academy of Sciences* [1974] writes that “research is needed [...] for the height of stages in relation to the

¹² From Nissen-Petersen, E. (2011), Sand Dams or Silt Traps, ASAL Consultants Ltd., available at <http://www.samsamwater.com/library/Sand_dams_or_silt_traps.pdf>.

¹³ From presentation “Modern Design of Sand Reservoirs for Water Storage”, available at <http://www.sawea.org/pdf/2005/SpecialtySesstion/Session2/Modern%20Design%20of%20Sand%20Reservoirs.pdf>

extent of the catchment”, while *Gijsbertsen* [2007] says, “To define an optimal height of each stage more research is needed. The height is in many ways dependent on the amount of runoff.” *Gijsbertsen* also adds that baseflow-controlled flows during the falling limb ultimately produce the greatest scour of fine materials, so spillway staging is more necessary for upstream catchment areas with limited baseflow, and single-stage dams are more acceptable in downstream reaches.

Wipplinger, in his excellent 1953 doctoral dissertation *The Storage of Water in Sand* [Wipplinger, 1953], proposes a staging design principle based entirely on local hydraulic controls of sedimentation processes in sand dams. He suggests that sand storage dams should be designed so as to maintain a velocity of at least 0.46 m/s “a short distance upstream of the dam wall”, in order to prevent deposition of fine sediment. Wipplinger performed his velocity analysis on a single, very large sand storage dam located in Namibia, then South West Africa, which was built using a series of stages of varying heights over more than a decade. (Additional stages were also proposed at the time of writing.) Wipplinger calculated a single flow velocity for each successive stage using a design discharge—determined based on the catchment area and return frequencies—and the flow’s calculated cross-sectional area, and compared those with the particle sizes of the sediment trapped by each stage. Unfortunately, Wipplinger did not address the effects of dynamic flows within individual storm hydrographs. Also, the gains in accessibility Wipplinger made by simplifying analysis to a single discharge and a recommended threshold value were undermined by the more difficult calculations required to quantify design discharges and flow cross-sections.

In addition to decisions about whether or not to build sand dams in stages, and the height of those stages, project managers and community members are often faced with other choices about staging methods. Sand dam staging is completed using several different approaches, depending on the design of the dam and the project’s objectives. Some sand dams are built using a simple wall, as shown in Figure 2.9 (next page), and the entire length of the structure functions as a spillway, so the full length of the dam wall is raised between stages.

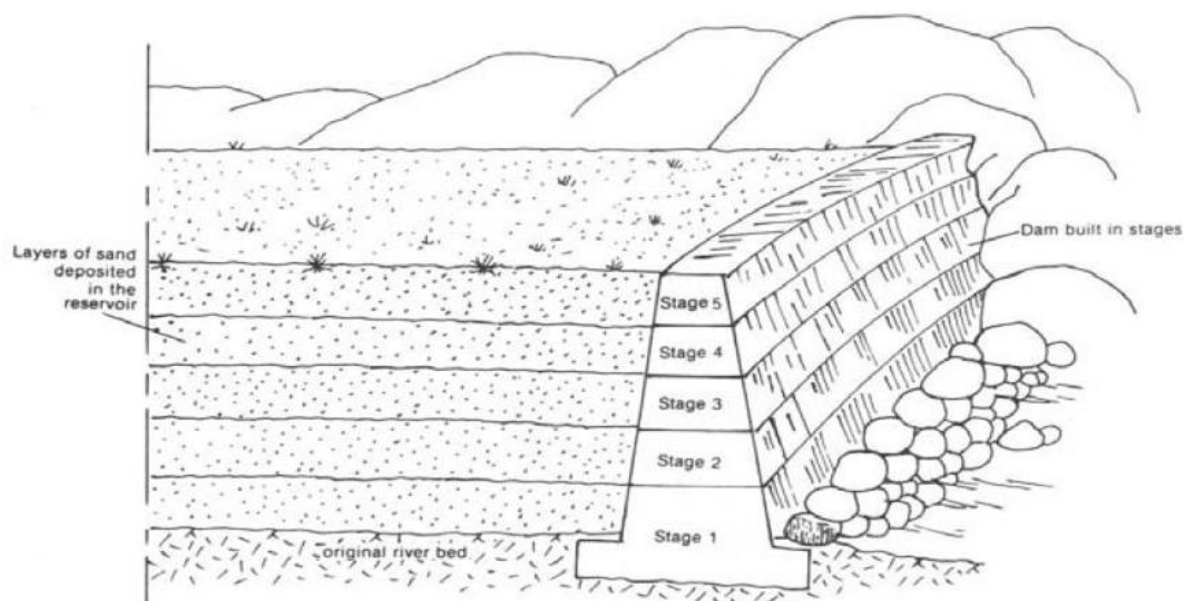


Figure 2.9: Spillway staging method. For sand dams built using a simple wall structure, building in stages requires raising the level of the entire dam [Nilsson, 1988].

Most sand dams built in East and Southern Africa today are constructed using single or compound rectangular spillways, with wing walls to protect the banks from erosion. For those structures which are built in stages, communities either raise the height of the entire dam, including both the wing walls and the spillway, or initially construct the wing walls to their final height, and only raise a smaller part of the dam in the center of the channel. Each method has benefits and drawbacks (Table 2.4).

Table 2.4: Comparison of staging methods. Sand dams with compound spillways can be constructed using different methods, and each method has benefits and drawbacks.

Construction Method	Advantages	Disadvantages
Raise both spillway and wing walls with each successive stage	More flexible option for communities; less wasted material if project is discontinued	More expensive for remote sites due to high transport costs; stages require technical expertise
Build wing walls to full height initially, and only raise spillway	Reduces construction complexity and quantity of materials for later stages; reduces overall transport costs; local artisans can complete without outside technical support	Risks waste if project is discontinued

Despite the common recommendation to build sand dams in stages, relatively few structures today are constructed using the method, primarily due to four factors.

1. Unclear methods and benefits: Many sand dams built to their final spillway height in a single stage function very well¹⁴, and with the general lack of consensus about an appropriate method for determining stage heights, the purpose and benefits of staging often remain unclear except in theory.
2. Cost: Building sand dams in multiple stages is more expensive than building them at a single time. Cornelius Kyalo of the African Sand Dam Foundation estimates building a dam in two stages instead of one could cost 60% more [*Kyalo, personal communication, 2015*]. For remote sites, transport costs represent a significant percentage of the total construction budget, and returning to a site many times is cost-inefficient. Also, some concrete must be removed from the previous lift with every successive stage in order to form a strong, impermeable connection, resulting in material losses [*Maddrell and Neal, 2012*].
3. Social constraints: Many community associations and self-help groups find it difficult to mobilize their members multiple times for the same project, especially when the benefits are not immediately apparent. Because initial dam stages may store relatively little water, it could take several years before a structure produces measurable benefits, and a loss of interest might result in wasted materials and time.
4. Funding constraints: Many sand dam projects are funded by international organizations, and must fit into 3- or 5-year project cycles. Because sand dams built in many stages may require a decade or more to complete, project managers would likely struggle to justify expenses and secure additional funding without measureable benefits [*Munguti, personal communication, 2014*].

¹⁴ The aforementioned Windhoek sand dam with the reported 33% specific yield was constructed to its final height of approximately 5 m in a single stage [*Wipplinger, 1953*].

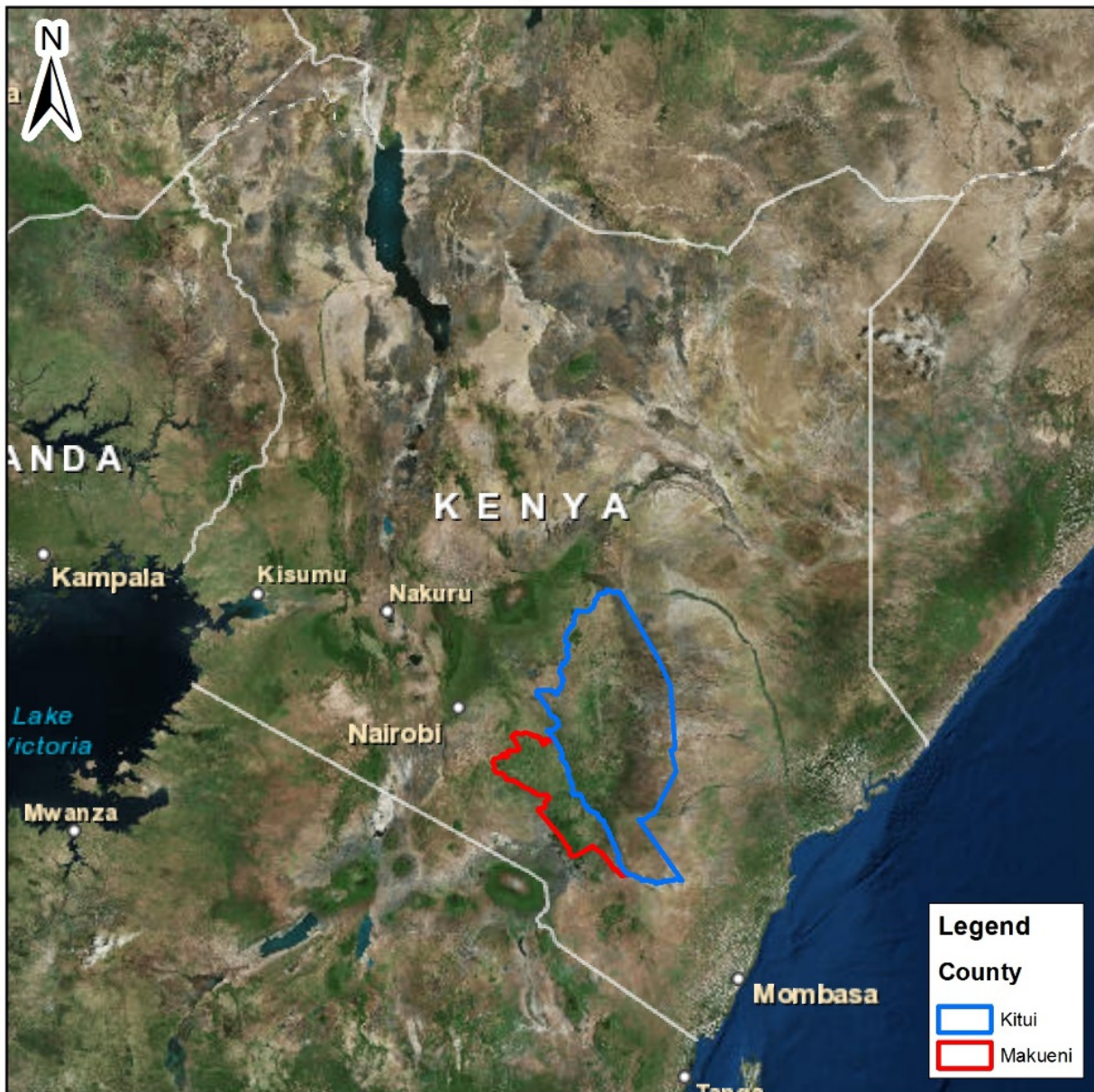
Chapter 3. Study region

I carried out my field work in Kenya to take advantage of the high concentration of mature sand dams in that country. Extensive research on sand dams in Kenya has already been completed by others in coordination with several Kenyan NGOs. [Some examples include *Aerts et al.*, 2007; *Arnold et al.*, 2002; *Avis*, unpublished thesis, 2015; *Beimers et al.*, 2001; *Borst and de Haas*, 2006; *Bossenbroek and Timmermans*, 2003; *Burger et al.*, 2003; *Ertsen et al.*, 2005; *Ertsen and Hut*, 2009; *Frima et al.*, 2002; *Gijsbertsen*, 2007; *Hoogmoed*, 2007; *Hut et al.*, 2008; *Lasage et al.*, 2008; *Quilis et al.*, 2008].

Kenya is divided into 47 counties; I collected data throughout Kitui and Makueni Counties (Figure 3.1, next page) in partnership with three sand dam-building institutions: Sahelian Solutions (SASOL), the African Sand Dam Foundation (ASDF) and Erik Nissen-Petersen's ASAL Consultants (ASALCON). As noted previously, most sand dam studies focus on a single case study site, but I hoped to study sedimentation relationships applicable to a range of dam designs built on rivers of various sizes.

The selected dam sites are located in a variety of arid and semi-arid landscapes, as both counties feature diverse, locally-specific climates. Kitui County has elevations ranging from 400 to 1800 m [*The County Government of Kitui*, 2015]; the study sites are located in the dry, lower-lying western part of the county. Makueni County has elevations ranging from 400 to over 2100 m, and site elevations range from 700 to 1500 m. All sites receive seasonal rainfall—historically, during two annual, increasingly-variable rainy seasons known as the “long rains” (approximately March through May) and the “short rains” (roughly October through December). Community members told me that most sites receive just a few storms, on average, during each rainy season, typically falling within a period of a few weeks, and rainfall appears to vary significantly due to topographical and other features. Droughts are also relatively common, occurring roughly every 4–5 years [*Lasage et al.*, 2008].

Study Region



Author: Jon Viducich
 Datum: WGS 1984
 Data source: Esri, David Muthami (2011)

0 80 160 320 Kilometers

Figure 3.1: Kenya county map. *Kitui and Makueni Counties form the study regions.*

Chapter 4. Methods

4.1 Site selection

I initiated my research by collecting field data to be used in analysis.

Sites were selected based on their diverse dam designs, channel geometries and sedimentation results, along with characteristics allowing for simplifying assumptions in data collection and analysis, as listed in Table 4.1.

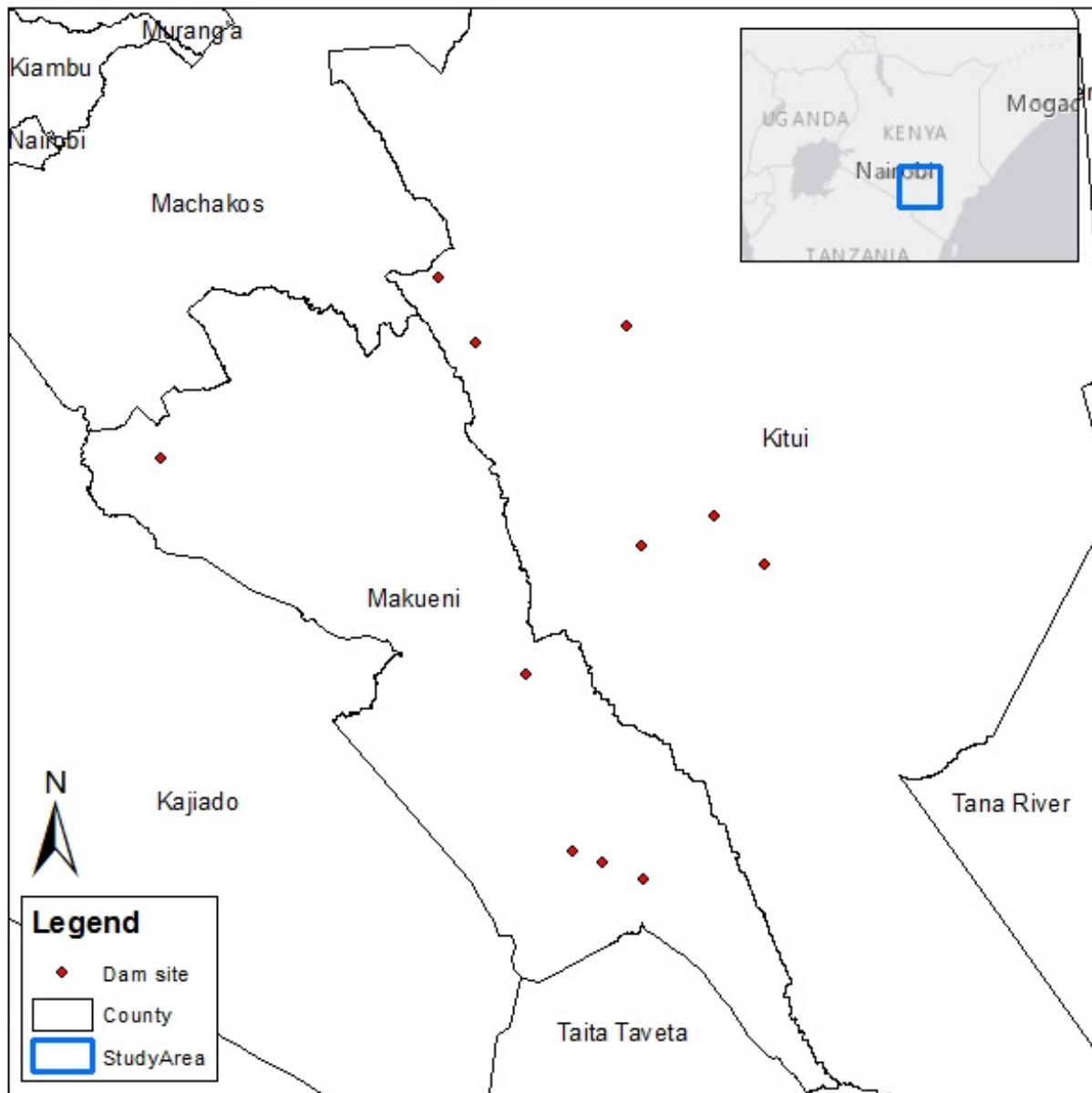
Table 4.1: Site selection criteria. *A number of criteria were used to select dam sites with characteristics allowing for simplifying assumptions.*

Criteria	Justification
Constructed on a sandy, intermittent stream	Limits scope of study to feasible sites as identified by <i>Gijsbertsen</i> [2007]
Constructed on a relatively straight reach	Minimize effects of secondary circulation; permits 1D flow modeling
Dam filled with sediment for several years	Assume re-establishment of channel equilibrium and original geometry downstream of structure
Furthest upstream structure on river	Minimize effects of upstream dams on downstream sedimentation processes

In total, I collected data at 13 sites. Unfortunately, several sites did not meet all of the site selection criteria. Due to the high density of sand dams in the study region and the lack of published inventories listing dams built by all organizations and community groups, I collected data at several sites before later discovering the presence of additional structures built further upstream. Given the relatively small total number of field sites, I retained the data collected for those sites, but only when the upstream dam(s) had either a) filled completely with sediment before the downstream structure was constructed or b) been constructed after the downstream dam had filled with sediment, and subsequently filled with sediment several years before the field visit. Four dams with upstream structures met

those additional criteria, resulting in a total of 11 field study sites. Figure 4.1 shows the location of the 11 study sites.

Sand Dam Study Site Locations



Author: Jon Vidulich
 Datum: WGS 1984
 Data source: GPS, Esri, David Muthami (2011)

0 15 30 60 Kilometers

Figure 4.1: Study site map. Data were collected at 13 sites, 11 of which were later deemed usable.

I collected data at sites representing a range of sedimentation results, including several which filled with fine sediment and do not perform well (Figure 4.2). This is clearly a sensitive issue, as most organizations depend on results-based, outside funding for their operations, and as such are typically incentivized to highlight the best-performing dams. However, all of the groups I partnered with are committed to improving their methods and results, and allowed me access to several older, low-benefit structures. Given the host organizations' willingness to show me a diverse set of sand dams, I agreed not to associate any particular dam's characteristics or results with its location or the funding organization. As such, I assigned a random number to each site, ranging from 1 to 11, and use those identifiers throughout the remainder of this report.



Figure 4.2: Silted sand dam. *Some non-functioning sand dams filled predominately with silt, as indicated by vegetation growing upstream of the structures.*

4.2 Field data

Given the high cost and high level of expertise required to collect rigorous field data over a multi-year period, I instead used simpler methods which may be reproduced by most NGOs. The methods were designed to permit collection of useful information in a single site visit consisting of just a few hours, and then processing of those data using low-cost and readily-available resources.

4.2.1 Field data collection

At each site, I recorded the following data:

4.2.1.1 General site data

Upon arriving at a dam site, I recorded several general site data, including the community name, river name, survey date and site coordinates. I used a Garmin GPSMAP 62s GPS while standing at the center of each dam's spillway to document its location, and waited until I achieved accuracy to within 3 m at each site. The accuracy of the coordinates was further verified using Google Earth.

4.2.1.2 Dam design

In order to document each dam's design, I sketched the structure from the downstream side, looking upstream, and labeled all relevant dimensions. Those included the width and aperture height of the spillway section(s), as well as the original spillway height above the riverbed. All

measurements were made using a Leica DISTO E7500i laser rangefinder and recorded to the nearest centimeter. Figure 4.3 shows one example of a site drawing; copies of the drawings for all sites

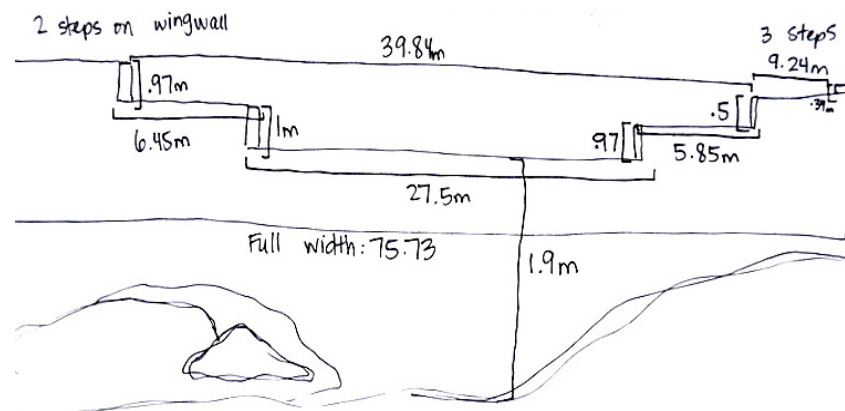


Figure 4.3: Site drawing. Each dam's physical dimensions were measured and noted in a drawing.

are presented in Appendix 1. A photo of each dam was taken from the same perspective to supply additional site information. Those photos are presented in Appendix 2.

4.2.1.3 Riverbed slope

I measured the riverbed slope profile upstream of each dam using a Leica DISTO E7500i laser rangefinder with the help of an assistant. Beginning at the center of the dam's primary spillway, I placed the rangefinder on a small tripod and aimed it upstream. The Leica DISTO E7500i shows the slope angle accurate to 0.1° , so I adjusted the tripod until the rangefinder was level. An assistant stood a short distance (<50 m) upstream of the dam, holding a piece of white paper, and located the laser point. I then used a tape to measure the height of the laser rangefinder above the riverbed and the height of the laser point on the assistant above the riverbed, and used the laser rangefinder itself to measure the horizontal span over the slope interval.

After taking the first slope measurement, I reset the tripod at the assistant's original location, and the assistant moved another interval upstream, staying in the thalweg of the riverbed. By repeating this process five to ten times at each site, we gathered information about the slope of the riverbed for a distance of 150 to 300 meters upstream of the dam. In addition to the current riverbed slope upstream of the dam, I recorded the pre-construction channel slope as measured by the partner organization.

4.2.1.4 Channel, flow and sedimentation history

Sand dams are built on seasonal and ephemeral streams with very dynamic flow levels. Unfortunately, no historic gauged flow data are available for the study reaches.

In order to characterize the flood flows which actually deposited sediment at the study sites, I developed an approach which combines crowd-sourced information with on-site measurements and an application of Manning's Equation (see Section 4.4.3).

I asked community members about the storm events and corresponding sedimentation results during the rainy seasons following their dam's construction. For most sites, community members were able to describe with great detail the number of times it had

rained each season, the durations of the rising limbs, the peak stage heights at a location downstream of the dam, the durations of the maximum reported discharges, the times required for the flows to recede to the primary channel, the durations of the falling limbs, and the location of the sand delta upstream of the dam at the end of each flow event.

While this research focuses on sediment transport and deposition processes upstream of sand dams, I took flow characterization measurements a short distance downstream of each dam, on a straight stretch where uniform flow could be reasonably assumed. I chose a downstream location for two reasons. First, because flood stage heights upstream of a dam increase after construction, community members with intimate knowledge of local streams often have better reference for flow levels on the downstream channel, where the riverbed has not changed drastically. Second, the water surface width typically increases upstream of a dam following construction, due to the shape of the channel and the increase in stage height. This increase in width complicates survey measurements and leads to greater error.

Most surveyed reaches consist of a primary channel characterized by a sandy riverbed and clay or rock banks and two overbank channels with some vegetation. After identifying a location near the top of an overbank channel, I stretched a tight string across the river at that level, using the Leica DISTO E7500i laser rangefinder to confirm the equivalent elevation height on the opposite bank. Next, beginning with the left side of the channel (facing downstream), I used a tape measure to determine the height of the string above the channel at 1-meter intervals, noting the surface type at each location. I also noted the height differences between the string, the maximum reported stage level and the primary channel bank elevations.

While relying on crowd-sourced flow data introduces some error, quantifying the uncertainty is difficult. In an effort to minimize bias and inaccuracy, I limited my interviews to adults who had lived near the river since at least the dam's construction (usually much longer), and attempted to find those who had actually participated in the construction. I found that people who depend on seasonal rivers for their livelihoods, and especially those who have a vested interest in their dam's performance (and thus its response to storm events), pay close attention to details like stage heights and timing. In addition to carefully

selecting interviewees, I also spoke with groups of at least two people at each site, assuming that reliance on consensus answers would help avoid obviously erroneous observations.

The community-supplied data were consistent from site to site. For example, two separate groups interviewed approximately 2 km apart on the Mukononi River, located near Kibwezi, provided remarkably similar answers about hydrograph timing for the previous year's storms. My calculated maximum discharge for the two sites, based on the interviews, varied by approximately 7% and the downstream site had the larger value. Further, natural signs, like debris left in low-hanging trees, often corroborated reported stage heights. The use of crowd-sourced data is not unprecedented—*Nilsson* [1988] also refers to the use of terrain marks and interviews for determining peak flows. Given the scarcity of gauged rainfall and flow data throughout much of the developing world, but especially in Sub-Saharan Africa, crowd-sourced data provide unique information about each site's hydrograph.

Appendix 3 presents profiles of each site's channel cross-section, along with stage levels at the primary channel and maximum reported flow.

4.2.1.5 Soil samples

In order to characterize sediment particle size distributions at different locations and depths, I took soil core samples (Figure 4.4) at locations 10, 50, 100 and 150 m upstream of each dam, at the thalweg, using an AMS soil probe and slide hammer. The maximum depth of each core was limited by the riverbed composition and saturation and the length of the sampler; for most sites, a depth of 1.5 m was achieved.



Figure 4.4: Soil core sample. Each soil core was partitioned into samples representing ~50 cm depth intervals.

I separated each 2.5 cm diameter core sample into 50 cm (or smaller) section lengths, making sure each sample included more than 100 g of sediment, and stored those in sealed, labeled plastic bags. In all, I collected 114 sediment samples at the 11 sites.

The 100 g mass required for the particle size distribution analysis, along with the relatively small diameter of the sampler, meant that the depth represented by each soil sample often failed to capture the bed's fine stratigraphy. Because thin silt layers affect vertical hydraulic properties in a way not clearly indicated by bulk samples, the required mass proved to be a limitation for the soil sampling method. The use of a larger diameter sampler and smaller depth intervals might have shed more light on the individual flow events responsible for the stratified sediments.

Another challenge for soil sampling upstream of sand dams was the prevalence of sand harvesting activities. Due to a recent surge in Kenya's construction sector, clean river sand is a very valuable commodity, especially near Nairobi, the capital city. Due to the steady, abundant source of sand



Figure 4.5: Sand harvesting. *A recent surge in Kenyan construction has resulted in increased sand harvesting at some sand dams in the study region.*

accumulated annually by sand dams, sand harvesting is common at some dam sites, and the riverbeds are pockmarked with pits and disturbed sediment. Because open pits excavated during the dry season, like those in Figure 4.5, are likely subjected to somewhat different sedimentation processes during floods than the rest of the bed, sampling in sites with active sand harvesting required extra care.

4.2.2 Sediment characterization

4.2.2.1 Hydrometer method

After returning from the field, I performed a particle size distribution analysis for each sample. To begin, samples were emptied into aluminum tins and air dried until none of the particles stuck to a stir stick—a process which typically required about 24 hours. Clayey soils were ground using a mortar and pestle, facilitating the drying process.

Because it is difficult to assess which proportion of clay and fine silt travels as aggregates with greater fall velocities than the constituent particles, I used chemical dispersion for the particle size analysis, in order to standardize the data for comparison. After the samples were dry, I weighed out 25 g of sodium hexametaphosphate (HMP) using an Ohaus SP202 Scout Pro Portable Balance (0.01 g resolution) and dissolved it in 500 mL of water, producing a 5% solution. I poured 100 mL of the HMP solution into each of five, 1 L graduated settling cylinders, and covered them to prevent evaporation.

Next, I weighed out 100 g of each dry soil sample using the electronic balance and added one 100 g soil sample each to four of the five settling tubes. The fifth settling tube served as a control, and no sediment was added. I stirred the soil/HMP solution in each settling tube to aid dispersion and allowed each sample to deflocculate for one hour.

After soaking the samples, I added water to each settling tube and filled it to the 1 L mark, producing a 0.5% HMP solution. While distilled water was not available in rural Kenya, I used water from the same source (either bottled or tap) for each batch of samples.

After filling each settling tube, I covered the top with Parafilm. I turned the control tube end-over-end once per second for sixty seconds to thoroughly mix the solution, and used a standard hydrometer (ASTM no. 152 H, with Bouyoucos scale in g/L) and glass thermometer to measure the specific gravity and temperature.

Next, I mixed each of the settling tubes containing soil samples, using the same end-over-end method, and started a timer as soon as the cylinder was set down on a flat surface. I used a hydrometer to measure the specific gravity of each undisturbed suspension after 30 s, 1 min, 3 min, 10 min, 30 min and 60 min, also periodically taking hydrometer and temperature readings for the control. Figure 4.6 shows the hydrometer test setup.



Figure 4.6: Hydrometer test. *Hydrometer tests were performed to measure the contribution of fine sediments to each sample's particle size distribution.*

While a longer hydrometer sampling period would have been ideal, I was limited by the number of samples to process, the time available for sampling, and my frequent movement from region to region. In addition, while it might have been interesting to distinguish between silts and clays with more precision, neither type of fine sediment is desirable in a sand dam, and I reasoned that a sand dam designed to discharge silt would by nature also discharge finer clays. As such, I decided more detailed classification within the fine sediment was unnecessary for my purposes.

After completing the 60 min hydrometer test, I wet sieved each soil sample using an 8 inch-diameter, U.S. Standard Mesh #200 (.074 mm) sieve, using tap water and a wash bottle to thoroughly rinse away all of the fines. I then washed each soil sample into another aluminum tin and allowed it to air dry for at least 24 hours, following the method previously described.

4.2.2.2 Dry sieve method

Following the drying process, I dry sieved each sample to determine the particle size distribution within the sand class size range, using the “End Point” hand sieving method described by the American Society for Testing and Materials [ASTM, 1985]. To begin, I weighed the samples, noting their dry mass after the wet sieving process. Next, I nested the U.S. Standard Mesh #18 (1 mm, 0 phi) and U.S. Standard Mesh #35 (0.5 mm, 1 phi) sieves, arranged from top to bottom, with a tight-fitting cap and pan. I placed the sand sample in the #18 sieve, held the sieves in a slightly inclined position in one hand, and struck the side of the sieves sharply and with an upward motion using the other hand at the rate of about 150 times/min. I turned the sieves about 1/6 a revolution at intervals of about 25 strokes, and continued with that process for 5 minutes.

Next, I carefully separated the sieves and poured the sand retained by each into a tared plastic container. Each sieve was tapped thoroughly to remove the sand grains stuck in the mesh. I weighed each sample using an electronic balance and recorded the masses.

After weighing the sediment fractions representing very coarse and coarse sand, I transferred the portion of the sample which had passed through both sieves from the collection pan to a plastic container. I then repeated the dry sieving process using U.S. Standard Mesh #60 (0.25 mm, 2 phi) and U.S. Standard Mesh #120 (0.125 mm, 3 phi) sieves. By weighing the portion of the sample which was retained by those sieves, as well as that which was retained by the collection pan, I further characterized the proportion of the total sample represented by medium, fine and very fine sand.

4.2.2.3 Particle size distributions

After the hydrometer and dry sieving processes, each soil sample’s particle size data appeared in two different forms. Table 4.1 (next page) presents those data for one sample, codified as Sample 6A0-0.4.

To calculate the sample's particle size distribution by combining data from both the hydrometer and dry sieve analyses, I first processed the hydrometer data using the method described by *Gee and Bauder* [1986]. First, C (g/L), the concentration of soil in suspension after each time interval, was calculated as the difference between R , the uncorrected hydrometer reading, and R_L , the equivalent hydrometer reading for the control cylinder.

Next, SP , the summation percentage for the time interval, was calculated as

$$SP = \left(\frac{C}{C_0} \right) * 100 \quad (\text{Eq. 4})$$

where C_0 equals the air-dried mass of the soil sample (for Sample 6A0-0.4, $C_0 = 100$ g).

The effective hydrometer depth, measured in cm, is defined as

$$h' = (-0.164R) + 16.3 \quad (\text{Eq. 5})$$

and represents the effective depth of settlement for particles of diameter D_{50} .

Stokes' Law, which describes the settling velocity of particles as a function of their size, depends in part on the density and dynamic viscosity of the fluid. In order to use Stokes' Law in conjunction with the hydrometer method, I first calculated the density and dynamic viscosity of the HMP solutions.

First, water's density and dynamic viscosity were approximated as a function of its temperature, using

$$\rho_0 = \frac{1000(1 - (T+288.9414))}{(508929.2*(T+68.12963))(T-3.9863)^2} \quad (\text{Eq. 6}) \quad [\text{McCutcheon et al., 1993}]$$

Table 4.2: Particle size data. *Following the hydrometer and dry sieve analyses, each sample's data required additional processing.*

Sample ID		6A0-0.4	
Initial mass of sample (g)		100	
Hydrometer Analysis			
Time (min)	R (g/L)	R _L (g/L)	Temp (°C)
0.5	7.8	4	25.1
1.0	7.2	4	25.1
3.0	7.0	4	25.1
10.0	6.9	4	25.1
30.0	6.4	4	25.1
60.0	6.4	4	25.1
Dry Sieve Analysis			
Initial mass after wet sieve (g)		95.87	
Mass remaining on #18 sieve (g)		25.59	
Mass remaining on #35 sieve (g)		35.79	
Mass remaining on #60 sieve (g)		23.33	
Mass remaining on #120 sieve (g)		9.02	
Mass remaining on #200 sieve (g)		1.75	
Mass loss (g)		0.39	

where ρ_0 is equal to the water's density at temperature T ($^{\circ}\text{C}$), measured in g/mL, and

$$\eta_0 = \frac{1000*(2.414*10^{-5})*10247.8}{((T+274.15)-140)} \quad (\text{Eq. 7}) \text{ [Al-Shemmeri, 2012]}$$

where η_0 is equal to the water's dynamic viscosity at T ($^{\circ}\text{C}$), measured in cpoise.

The corrected density for the HMP solution, ρ_l , was calculated as

$$\rho_l = \rho_0(1 + 0.630C_s) \quad (\text{Eq. 8}) \text{ [Gee and Bauder, 1986]}$$

where C_s is equal to the concentration of HMP (0.005 g/mL).

The corrected viscosity for the HMP solution, η , was likewise calculated as

$$\eta = \eta_0(1 + 4.25C_s). \quad (\text{Eq. 9}) \text{ [Gee and Bauder, 1986]}$$

The corrected density and viscosity values were used to calculate B , defined as

$$B = \frac{[30(\frac{\eta}{10})]}{[g(\rho_s - \rho_l)]} \quad (\text{Eq. 10}) \text{ [Gee and Bauder, 1986]}$$

where g is equal to the gravitational constant (980.665 cm/s^2) and ρ_s is the soil particle density (assumed here to be that of quartz, 2.65 g/cm^3).

I used B and h' to calculate the sedimentation parameter, θ ($\mu\text{m min}^{1/2}$), defined as

$$\theta = 1000(Bh')^{\frac{1}{2}}. \quad (\text{Eq. 11}) \text{ [Gee and Bauder, 1986]}$$

Finally, D (μm), the mean particle diameter in suspension at time t (min), was calculated as

$$D = \theta t^{-\frac{1}{2}}. \quad (\text{Eq. 12}) \text{ [Gee and Bauder, 1986]}$$

Table 4.2, next page, gives examples of calculated values for Sample 6A0-0.4.

To express the dry sieve data in an equivalent form, I calculated the summation percentage, SP (%), as the percentage of the total air-dried sample mass passing a given sieve, and used the diameter of the sieve openings as the mean particle diameter, D .

At this point, the hydrometer and dry sieve data were combined to provide a distribution spanning the full range of particle sizes of interest. Table 4.3, next page, presents the values

for Sample 6A0-0.4. Note that the mean particle size values resulting from hydrometer method calculations were converted to units of millimeters.

Table 4.3: Processed hydrometer data: *Density and viscosity corrections were used to calculate mean particle size distributions*

C (g/L)	SP (%)	h' (cm)	ρ_o (g/mL)	ρ_i (g/mL)	η_o (cpoise)	η (cpoise)	B	θ ($\mu\text{m min}^{1/2}$)	D (μm)
3.8	3.8	15.02	1.00	1.00	0.87	0.89	0.00	49.70	70.29
3.2	3.2	15.12	1.00	1.00	0.87	0.89	0.00	49.87	49.87
3.0	3.0	15.15	1.00	1.00	0.87	0.89	0.00	49.92	28.82
2.9	2.9	15.17	1.00	1.00	0.87	0.89	0.00	49.95	15.79
2.4	2.4	15.25	1.00	1.00	0.87	0.89	0.00	50.08	9.14
2.4	2.4	15.25	1.00	1.00	0.87	0.89	0.00	50.08	6.47

Table 4.4: Particle size distribution.

The processed hydrometer and dry sieve data are combined to form a complete distribution.

D (mm)	SP (%)
1.0000	74.4
0.5000	38.6
0.2500	15.3
0.1250	6.3
0.0740	4.5
0.0703	3.8
0.0499	3.2
0.0288	3.0
0.0158	2.9
0.0091	2.4
0.0065	2.4

4.2.3 Analysis

Particle size distributions vary by site, as expected. However, sediment samples for a given site also frequently vary widely by location and depth, often in unpredictable ways.

Appendix 4 presents plots showing variations by sample location and depth for all sites.

Many sites feature a thick, fine-textured bottomset bed overlain by coarser material—clearly, flows often fail to scour the fine material and simply bury it as the delta bedform

migrates to the dam wall. Figure 4.7 shows soil samples taken 10 m upstream of two dams, with silt and clay plainly visible.



Figure 4.7: Buried bottomset bed. *Many sand dam storage volumes feature a thick bottomset bed of silt or clay, overlain by coarse sand.*

Aside from the bottomset bed, few patterns emerged in the intrasite sediment data. Due to the relatively small number of sites, I combined each site's data to form bulk sediment profiles represented by values characterizing median particle size and sorting. Figure 4.8, next page, provides plotted comparisons of the bulk particle size distribution curves for each site, and Appendix 5 presents particle size distribution charts for each site.

I calculated four sediment variables for each site. Three of those are based on the D_{50} , or the diameter for which 50% of the sample is finer, by mass. The other is based on the average Hazen's Uniformity Coefficient (C_u), or D_{60}/D_{10} , of each site's samples in order to quantify and compare the relative grading of each site's sediment.

Unfortunately, some samples were coarser than expected, and the particle size analysis would have benefited from the use of one larger sieve size to differentiate between very coarse sand and gravel. For a few individual samples, over 40% of the particles (by mass) were larger than 1 mm, and it was not possible to calculate the D_{60} value. Likewise, for those samples with a high percentage of very fine sediment, it was not always possible to

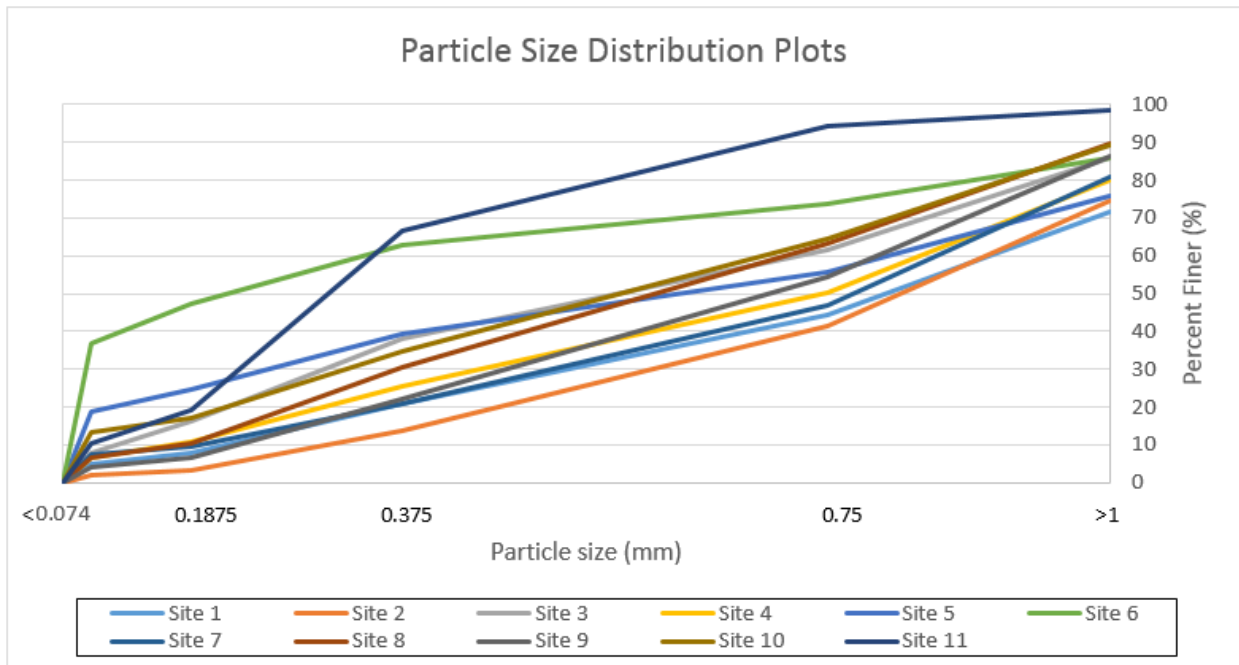


Figure 4.8: Bulk particle size distributions. *With two exceptions, most study sites have similarly-shaped particle size distribution curves.*

calculate the D_{10} value—this was often the case for the deepest sample taken closest to the dam. Rather than omitting those samples, which are generally biased towards larger C_u values (wider distributions), I instead estimated the missing values by assuming D_{10} values equal to half the smallest measured particle size (variable by sample) and D_{60} values twice the largest measured particle size (2 mm).

It was possible to calculate the D_{50} value for all samples, based on measured particle sizes. I first calculated the average D_{50} of all samples collected at a given site to represent the bulk median particle size trapped by the sand dam. In an effort to capture the presence of a thick, fine bottomset bed at some sites, I also calculated two additional average D_{50} values: one for all samples taken at the 10 m location alone, and one for samples collected at all locations other than those at 10 m.

Table 4.3 shows the D_{50} and C_U bulk values for each site; a few results immediately stand out. First, many sites have similar D_{50} values, and over half are coarser than the 0.5 mm threshold suggested by *Nissen-Petersen* [1997]. Some sites with very similar D_{50} values (such as Sites 5 and 9) have very different uniformity coefficients, suggesting different hydraulic properties. Also, a comparison of each site's three D_{50} values illuminates marked fining at the 10 m location for some dams, corresponding to the presence of a thick bottomset bed.

Table 4.5: Characteristic bulk sediment results. *Three characteristic D_{50} values, along with the bulk Hazen's Uniformity Coefficient, were calculated for each site.*

Site	D_{50} - All (mm)	D_{50} - No 10 m (mm)	D_{50} - 10 m (mm)	Hazen's C_U
1	0.643	0.632	0.665	5.77
2	0.653	0.671	0.618	3.62
3	0.428	0.523	0.205	4.04
4	0.529	0.534	0.525	8.72
5	0.516	0.643	0.177	20.28
6	0.184	0.287	0.116	96.63
7	0.612	0.560	0.569	11.17
8	0.433	0.435	0.428	9.74
9	0.513	0.588	0.289	9.18
10	0.384	0.408	0.334	7.10
11	0.219	0.225	0.200	13.03

While condensing the sediment data from entire sites into a few, simplified indicators may have resulted in the loss of some useful data, doing so facilitated the comparison of sites by establishing generalized parameters indicative of bulk sediment quality. This approach proved helpful for evaluating relationships between catchment and local hydraulic controls and the sediment trapped by a dam, but increasing the number of sites could possibly provide additional understanding of variations within a single sand dam aquifer.

4.3 Remotely-sensed data collection

In addition to field-sourced data, I assembled remotely-sensed data to study correlations between catchment characteristics and sedimentation results, and processed the datasets using ESRI ArcMap™ 10.2.2. The following sections describe the datasets and processing.

4.3.1 Catchment delineation and area

To delineate each site's watershed, I first used digital elevation data to identify stream networks throughout the study region. I began by creating a new project in ArcMap using the WGS 84 / UTM Zone 37S projected coordinate system, and imported 30-m elevation data from the Shuttle Radar Topography Mission (SRTM). The elevation data were captured in 2000 by the Space Shuttle Endeavor using C-band Interferometric Synthetic Aperture Radar (InSar) [USGS, 2004]. Data are available for download at no cost in 1 degree latitude x 1 degree longitude tiles; I mosaicked four scenes covering the full study area. While the 1 arc-second (~30 m) resolution is fairly coarse, it represents significant improvement over the 90-m data previously available before the release of the finer-resolution, continent-wide dataset in September 2014¹⁵. After importing the elevation data, I used the ArcMap Fill tool to remove sinks and peaks in the digital elevation model (DEM) and ensure continuity in the stream and catchment delineation.

Next, I created a flow direction map, which serves as an input for the flow accumulation tool. The flow direction function assigns one of eight possible values to each cell, indicating the direction of flow from that cell. I then used the Flow Accumulation tool, which calculates the number of upstream cells which flow into a given cell. I separated the results into two classes and set the break value to 500, thus delineating cells with at least 500 upstream cells (corresponding to an area of approximately 0.48 km²) and creating a stream network.

I imported the GPS dam site locations and visually confirmed the accuracy of the flow accumulation map for the catchment areas using satellite imagery. In general, the delineated stream networks align quite well with actual streambeds. I created a catchment outlet at the stream cell nearest to each dam location using the Snap Pour Point tool. Errors resulting from GPS inaccuracy or the coarse DEM resolution were negligible, and appropriate outlet locations were readily apparent in all cases. Finally, I used the

¹⁵ From Jet Propulsion Laboratory (2014), *U.S. Releases Enhanced Shuttle Land Elevation Data*, available at <<http://www.jpl.nasa.gov/news/news.php?feature=4305>>

Watershed tool to delineate the watershed for each site based on the flow direction map and pour points.

Figure 4.9 shows the results for Site 7, with the pour point visible near the northernmost edge of the catchment. The Watershed tool also calculates each catchment's surface area; for the 11 sites, basin areas ranged from 0.15 km² to 366 km², as shown in Table 4.4, on Page 48.

Site 7 Watershed

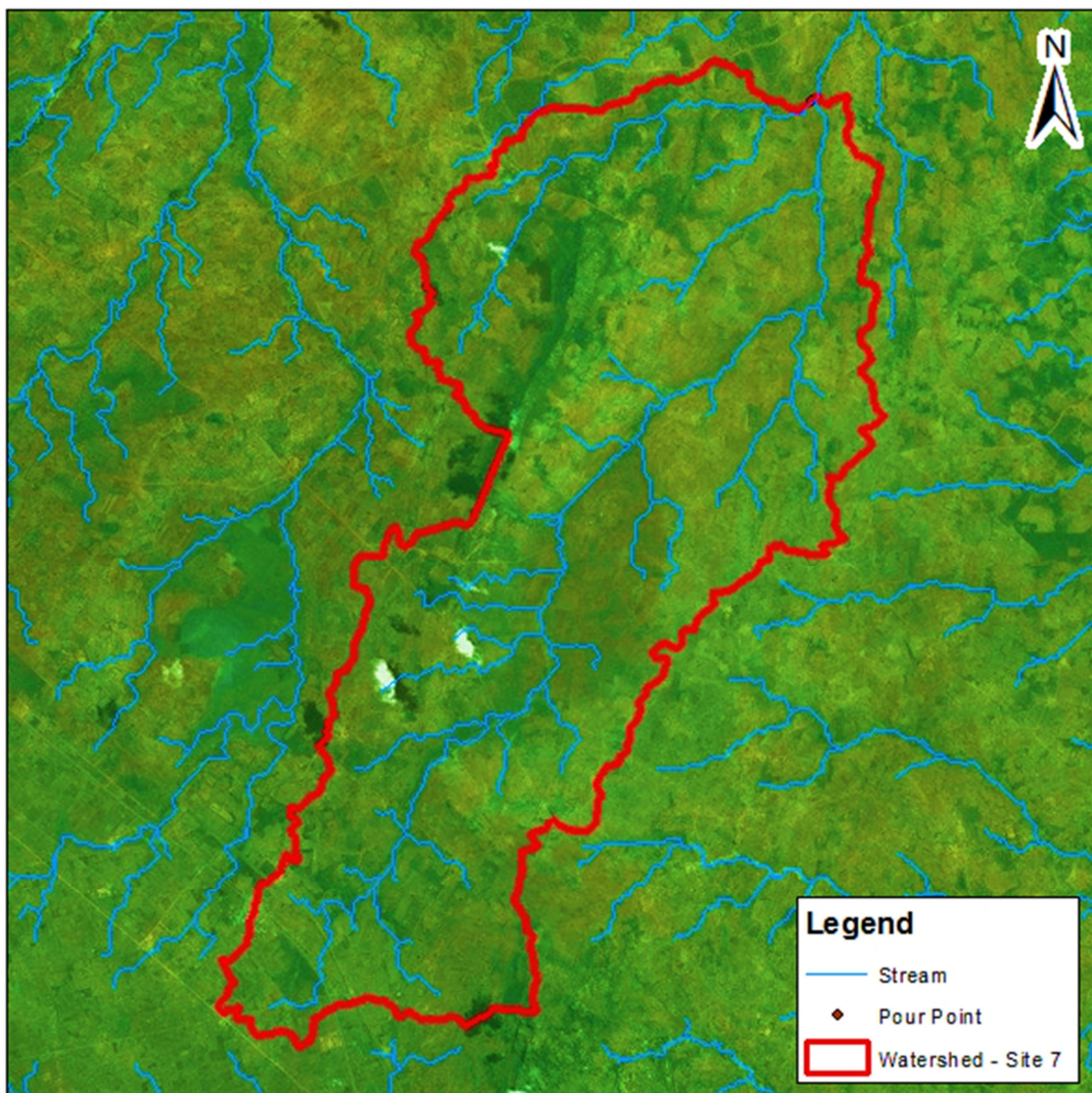


Figure 4.9: Stream and watershed delineation. *SRTM elevation data were used to delineate watersheds and stream networks for each site; this map shows the Site 7 watershed.*

4.3.2 Catchment slope

Next, I used the Slope tool in ArcMap to calculate land surface slopes throughout the study areas, based on the SRTM DEM data. The tool identifies the maximum change in elevation between each cell and its neighbors, and assigns the resulting slope gradient. I then used the Zonal Statistics tool to calculate the maximum and mean slopes for each catchment area.

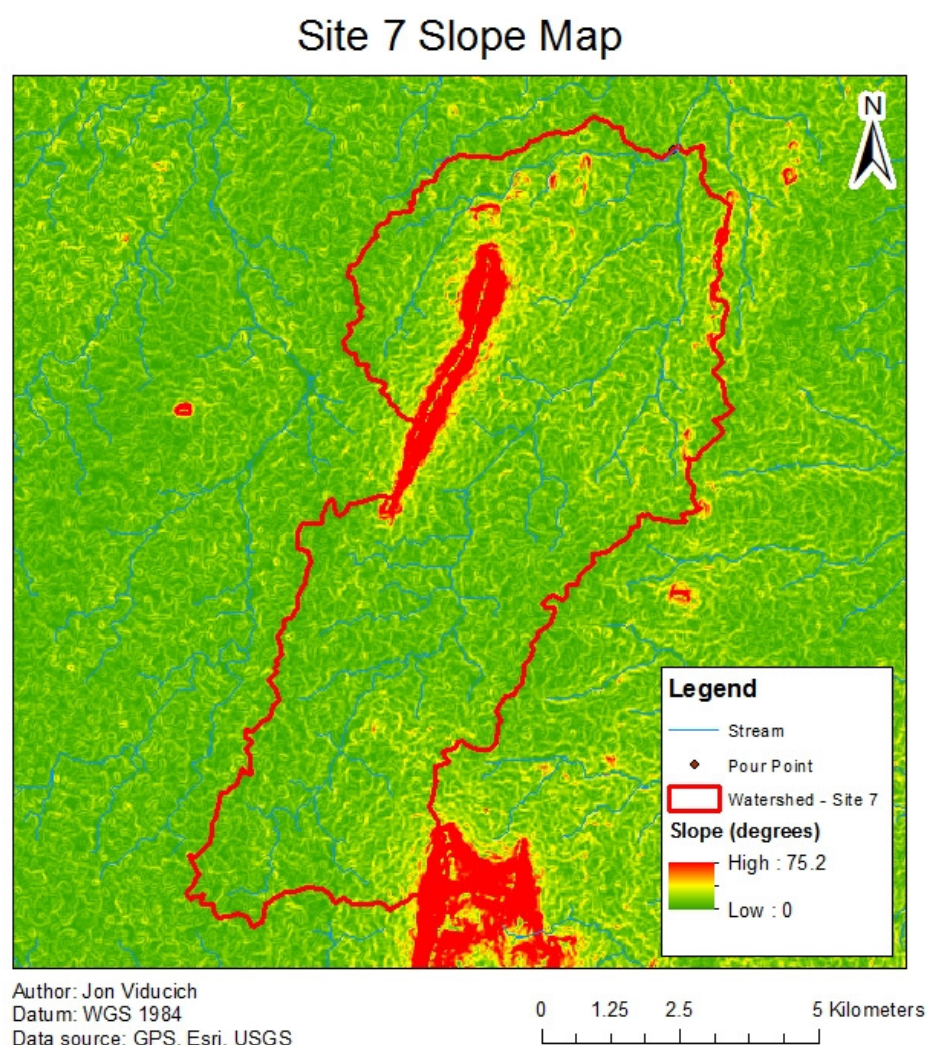


Figure 4.10: Slope calculation. *SRTM DEM data were also used to create slope maps, like this one for the Site 7 watershed.*

Figure 4.10 shows the slope map for Site 7, with a large rock outcrop visible in the northwest quadrant. Slopes ranged from 0° to 65.6° for all catchments, averaging 2.7° to 10.2° . All sites surpassed the 2° threshold requirement suggested by *Gijsbertsen* [2007]. Slope values for all sites are shown in Table 4.4, on Page 48.

4.3.3 Catchment land use

Catchment land cover and use represent important factors in determining sediment supply to a reach, and I initially planned to develop a land classification scheme for each watershed at the time of the sand dam's construction. Unfortunately, available datasets are relatively sparse for rural Kenya, and Advanced Spaceborne Thermal Emission and Reflection Radiometer (ASTER) data—those used by *Gijsbertsen* [2007] in his analysis of sandy riverbeds—are unavailable for the dates and regions of interest. Landsat 7 data do cover the study region for the dates of interest, and are freely available, but the sensor's scan line corrector

(SLC) failed in 2003, and many dam sites are located near the edges of scenes where data gaps are largest [USGS, 2013]. As such, the Landsat 7 data are not useable for land classification of the study area.

The Food and Agricultural Organization's (FAO) Global Land Cover Network (GLCN) Africover project produced a land classification map of Kenya using high-resolution LANDSAT

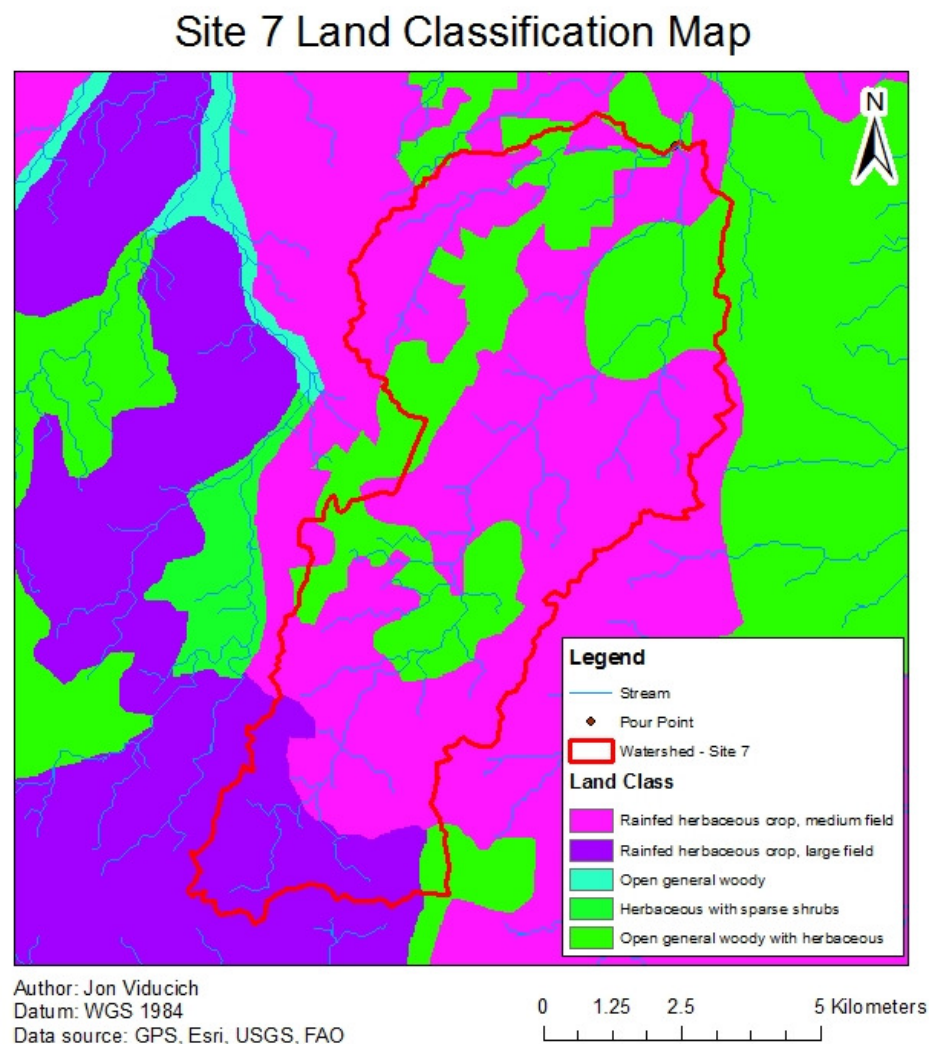


Figure 4.11: Land classification. Catchment land cover was classified using 1995 FAO data, shown here for Site 7.

TM images (Bands 2, 3 and 4) acquired primarily in 1995, based on the FAO/UNEP international standard LCCS classification system [FAO, 2014]. The dataset provides detailed classification of land cover and use, with over 80 categories for the country. In comparing the classified areas with present-day satellite imagery, it is apparent that land use has changed in many watersheds over the past twenty years, with a general trend towards increased cultivated area. However, the relative rankings of percentages represented by each land class type seem to have persisted in the majority of catchment areas, and I used the FAO data in lieu of better available resources. I combined the detailed classes into two broader categories representing cultivated cropland and all other cover types, to simplify analysis, and used the Zonal Histogram tool in ArcMap to calculate the percentage of each study catchment area represented by cultivated cropland.

Figure 4.11, previous page, shows the land classes present near Site 7. On average, 54.3% of catchments were comprised of cropland. Table 4.4 shows the land use compositions and other catchment characteristics for each site.

Table 4.6: Catchment characteristics. *Catchment characteristics were quantified for each study site.*

Site	<i>Catchment Characteristics</i>			
	Area (km ²)	Max. slope (degrees)	Mean slope (degrees)	Fraction cropland (%)
1	5.28	11.2	3.82	100
2	93.93	39.9	2.70	19
3	220.41	65.6	4.99	43
4	1.26	31.6	7.07	22
5	18.38	25.8	3.42	96
6	0.15	21.4	6.80	0
7	71.00	43.1	3.54	71
8	365.97	46.1	4.35	66
9	195.03	46.1	5.03	54
10	6.23	10.7	2.82	100
11	19.96	33.2	10.22	27

4.3.4 Analysis

In order to test hypotheses about the relationships between catchment characteristics and the need for sand dam spillway staging, I performed a statistical analysis to identify

whether catchment area, slope and land class are good predictors of deposited sediment quality for sand dams built in a single stage. In order to conclude that spillway stage heights should be determined based on a given catchment characteristic, one would expect median sediment particle sizes and/or the uniformity of particle size distributions to vary systematically with that catchment characteristic for a range of sites.

Using R [R Core Team, 2015], a free statistical computing tool, I performed univariate, linear regressions of each catchment characteristic and sedimentation combination using Pearson's correlation analysis. For a population sample, Pearson's correlation coefficient is defined as

$$r = cov(x, y) / s_x s_y \quad (\text{Eq. 13}) \quad [\text{Zaiontz, 2015}^{16}]$$

where *cov* is covariance and *s_x* is the sample standard deviation of the *x* variable. As defined, *r* is not an unbiased estimator of the population correlation coefficient, *ρ*, and given the relatively small number of study sites, I also calculated the p-value to evaluate the statistical significance of the results.

4.4 Flow and sedimentation modeling

After collecting and processing the available remotely-sensed data, I used the channel and flow data collected in the field, along with hydraulic flow models developed using HEC-RAS 5.0 (Beta 2014-10-01), to evaluate the impacts of static and dynamic hydraulic controls on sedimentation processes upstream of sand dams. The purpose of these tests was to evaluate hypotheses about the use of local hydraulic factors for staging design, and to develop understanding about the sensitivity of sedimentation processes to dam design.

¹⁶ From Zaiontz, C. (2015) *Real Statistics Using Excel*, available at <www.real-statistics.com>

4.4.1 Site descriptions

Of the 11 field sites, three were chosen for hydraulic modeling based on the completeness of their flow and sediment datasets, variation in their sedimentation profiles, and their relatively simple channel geometries. All three dams were built in a single stage.

The sand dam at Site 2 (Figure 4.12) was constructed in 2011, and filled with sediment over the course of two rainy seasons (one calendar year) consisting of four storms. The watershed has an area of 93.9 km² and is the smallest of the three modeled sites. Prior to construction, the upstream reach had a slope gradient of 0.005, and, with a constructed



Figure 4.12: Site 2 sand dam. *This photo depicts the Site 2 sand dam, taken from the downstream side, looking upstream.*

spillway height of 1.05 m, a backwater of 210 m. Two sediment samples taken upstream of the backwater, and assumed to represent the original riverbed, had an average D_{50} of 0.81 mm. The dam has a single rectangular spillway, and some flow overtops and passes around the wing walls during ordinary high flows, as evidenced by erosion to the banks and

supported by hydraulic computations. Based on community-sourced data, the flows which initially contributed to the dam's sedimentation peaked at approximately $65 \text{ m}^3/\text{s}$, remained at that level for three hours, and receded completely over the course of 50 hours (~ 2.1 days).

Figure 4.13 shows variation in the D_{50} particle sizes at different locations and depths upstream of the Site 2 structure. The dam does not have a visible bottomset bed and, with an average D_{50} of 0.65 mm and a C_U of 3.62 for all samples, it represents the most ideal of the sediment profiles for the three sites.

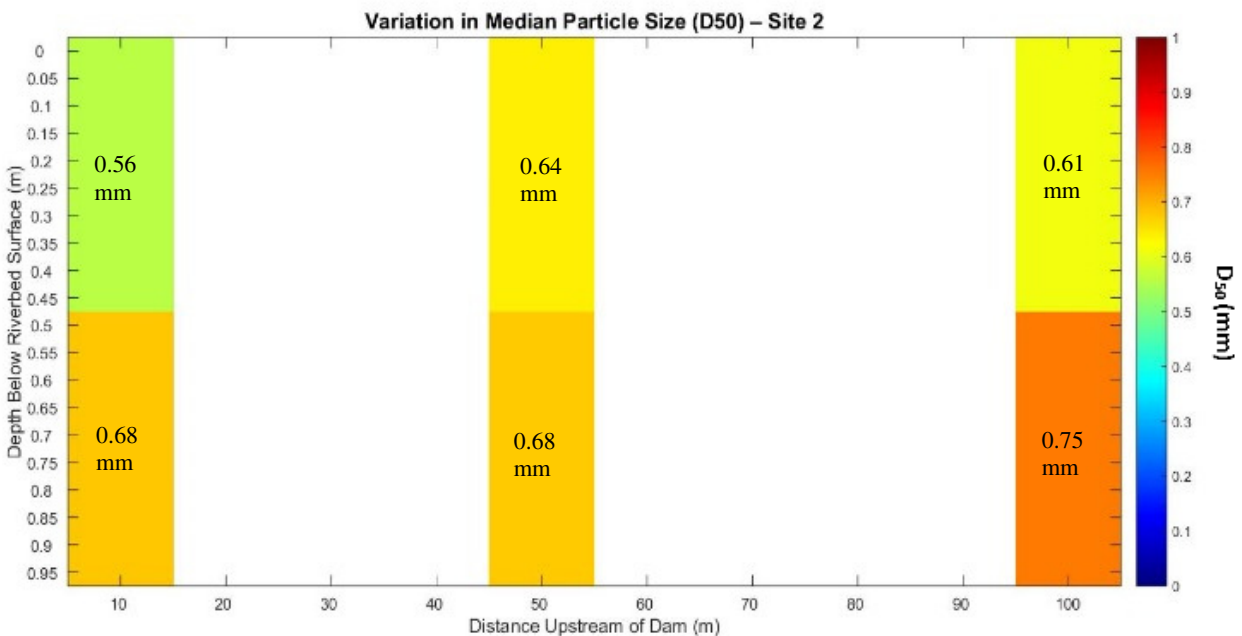


Figure 4.13: Site 2 sediment profile. This plot depicts the variation in D_{50} values by location and depth upstream of the Site 2 sand dam.

The Site 8 sand dam (Figure 4.14, next page) was also constructed in 2011, and filled with sediment over the course of two rainy seasons (one calendar year) consisting of three storms. (Two other precipitation events consisted of light sprinkles, and did not result in surface flow). The watershed has an area of 366 km^2 and is the largest of the three sites. Prior to construction, the upstream reach had a slope of 0.006, and, with a constructed spillway height of 1.9 m, the structure had a backwater of 317 m. A single sediment sample taken downstream of the structure, and assumed to represent the original riverbed, had a D_{50} of 0.46 mm. The dam has a compound rectangular spillway, and some flow overtops

the dam and passes around the wing walls during high flows, as evidenced by erosion to the banks and supported by hydraulic computations and community interviews. Based on community-sourced data, the flows which initially contributed to the dam's sedimentation peaked at approximately 204 m³/s, remained at that level for four hours, and receded over the course of two weeks.



Figure 4.14: Site 8 sand dam. *This photo depicts the Site 8 sand dam, taken from the downstream side, looking upstream.*

Figure 4.15, next page, depicts variation in the D_{50} particle size at different locations and depths upstream of the Site 8 structure. With an average D_{50} of 0.433 mm and a C_U of 9.74 for all samples, Site 8 had the finest median grain size of the three sites, and the least uniform particle size distribution.

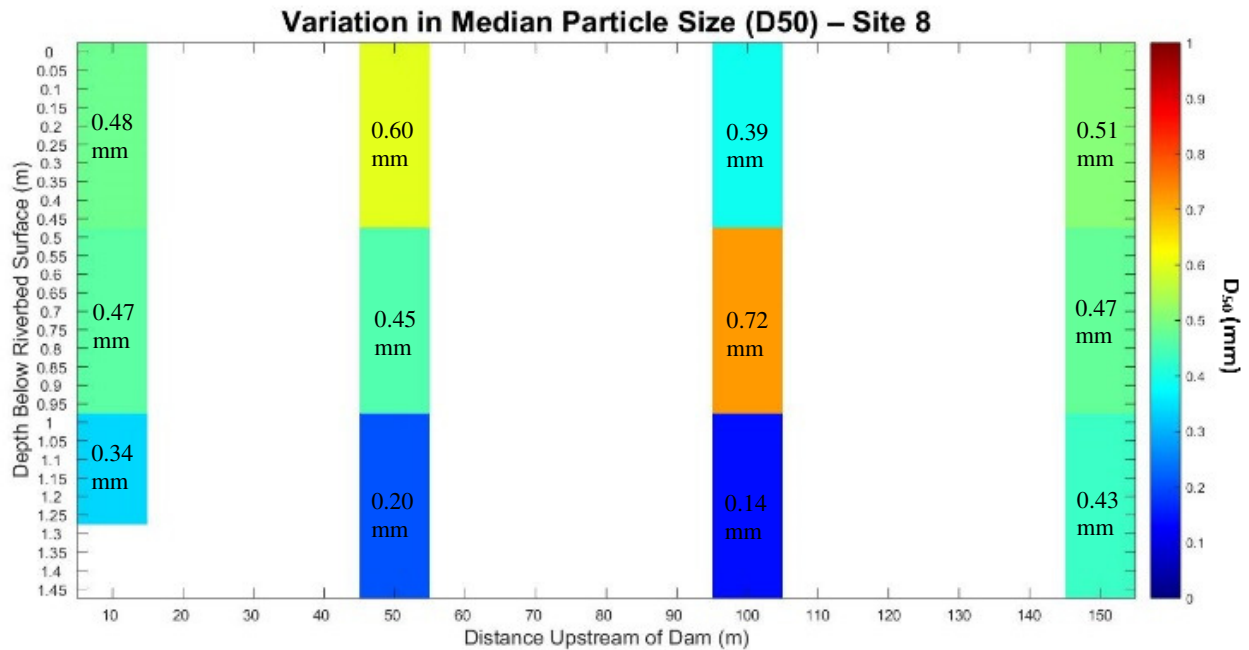


Figure 4.15: Site 8 sediment profile. This plot depicts the variation in D_{50} values by location and depth upstream of the Site 8 sand dam.

Finally, the Site 9 structure (Figure 4.16, next page) was constructed in 2012, and filled with sediment over the course of three storms spanning two rainy seasons. The watershed has an area of 195 km². Prior to construction, the upstream reach had a slope of 0.004, and, with a constructed spillway height of 1.7 m, a backwater of 425 m. Two sediment samples taken downstream of the structure, and assumed to represent the original riverbed, had an average D_{50} of 0.67 mm. The dam has a compound rectangular spillway, and some flow overtops the dam and passes around the wing walls during high flows, as evidenced by erosion to the banks and supported by hydraulic computations and community interviews. Based on community-sourced data, the storm hydrograph which initially contributed to the dam's sedimentation peaked at approximately 167 m³/s, remained at that level for three hours, and receded over the course of two weeks until the second storm began. Interestingly, the sand dam's construction ultimately resulted in perennial surface flow through the reach—some surface flow (~0.01 m³/s) was present at the time of the survey.



Figure 4.16: Site 9 sand dam. *This photo depicts the Site 9 sand dam, taken from the downstream side, looking upstream.*

Figure 4.17, next page, shows variation in the D_{50} particle sizes at different locations and depths upstream of the Site 12 structure. With an average D_{50} of 0.513 mm and a C_U of 9.18 for all samples, this represents the second-coarsest median grain size of the three sites, and the second-ranked site in terms of homogeneity. A bottomset bed is clearly visible in the sediment profile.

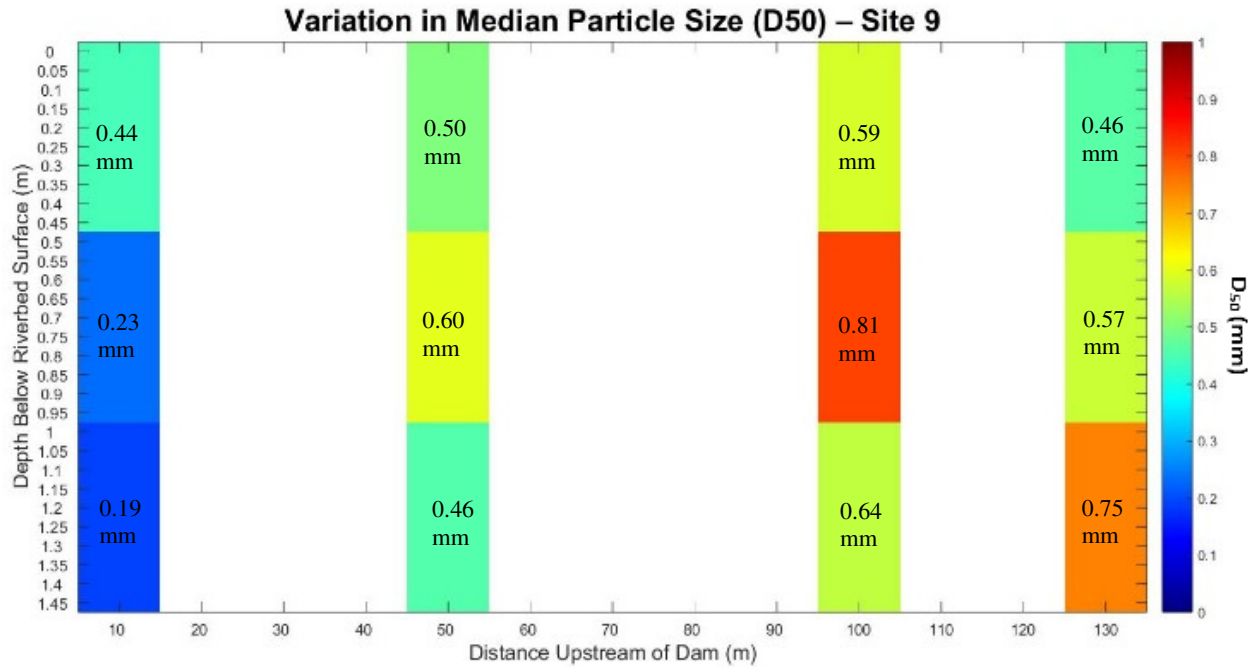


Figure 4.17: Site 9 sediment profile. This plot depicts the variation in D_{50} values by location and depth upstream of the Site 9 sand dam.

4.4.2 Channel geometry reconstruction

To reconstruct each site's original channel geometry in HEC-RAS, I used a cross-section surveyed 50 m downstream of the dam, assuming that any downstream channel degradation resulting from the short-term reduction in sediment supply was reversed after the dam filled with sediment and supply was restored. Beginning at a location 50 m downstream of the structure, I extrapolated the cross-section upstream through the dam site and over the full length of the backwater, using the original channel slope as recorded by the sand dam organization. Manning's n values for the riverbed and banks were estimated based on channel characteristics; most sandy riverbeds were assigned Manning's n values of 0.025, while bank values ranged from 0.03 to 0.06 [Chow, 1959]. Finally, I interpolated cross-sections at 5 m intervals throughout the reach, and added an inline weir structure at the dam location using dimensions measured in the field. In all, I created five geometry files for each site, representing cases with no dam, a dam with a 10 cm spillway, and dams with spillways $1/3$, $2/3$ and the full constructed height.

As an example, Figure 4.18 shows the geometry planform for the Site 2 reach, and Figure 4.19 shows the weir structure geometry with its full spillway height as constructed. Note



Figure 4.18: Site 2 HEC-RAS reach geometry. The HEC-RAS geometry for Site 2 shows the 53 cross-sections covering the reach, with the sand dam located at the 50 m river station.

that the cross-section labels are referenced to the location 50 m downstream of the dam, so the structure is located at the 50 m cross-section, and the backwater extends to the 260 m cross-section.

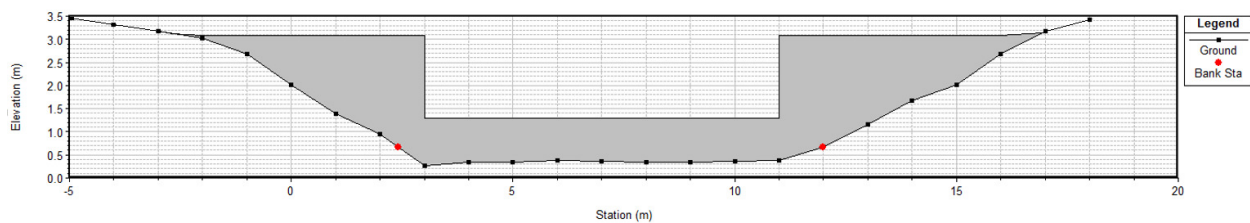


Figure 4.19: Site 2 HEC-RAS dam geometry. Sand dam spillway geometries were represented as inline weir structures. Site 2 has a relatively simple spillway geometry.

4.4.3 Hydrograph reconstruction

Because unsteady flow dynamics contribute to grain size variations within the deposited sediment, I used the detailed flood stage height information provided by community members during the field surveys to reconstruct the hydrograph for the first storm after each dam was constructed. The first flow event was chosen for several reasons. First, as described in Chapter 2, the assumption of unlimited sediment supply is probably most appropriate early in a rainy season, when soils are most susceptible to erosion. Second, modeling the first storm, before a dam has begun to accumulate sediment, allows for assessment of the conditions most likely to lead to the deposition of fine sediment, due to the maximum dam-induced reduction in flow velocity and turbulence. Finally, for each of the three modeled sites, the first storm deposited the greatest volume of sediment upstream of the dam, and the maximum reported discharge can be considered equivalent to the ordinary maximum flow.

To reconstruct each hydrograph, I first calculated the volumetric flow rates associated with the maximum reported stage height and the primary channel stage height using Manning's Equation. To do so, I created a spreadsheet to calculate the flow rate for each 1-meter subsection and sum those across the entire cross-section. The governing Manning's Equation for a compound channel may be written as

$$Q = \sum_{i=1}^N K_{Ni} \sqrt{S_0} \quad (\text{Eq. 14})$$

where Q is the total volumetric flow rate in cubic meters per second, S_0 is the flow's energy slope, and K_i is the conveyance of the channel for the i^{th} section of the flow cross-section. Assuming uniform flow—a common assumption for gradually-varied flows, even in ephemeral streams [Reid and Frostick, 1986]—the channel slope is substituted for the energy slope.

In S.I. units, the conveyance K_i is defined as

$$K_i = \frac{1}{n_i} A_i R_i^{\frac{2}{3}} \quad (\text{Eq. 15})$$

where n_i is the Manning's roughness coefficient (representative of channel characteristics which impede flow) for the i^{th} sub-section, A_i is the flow section's cross-sectional area and R_i is its hydraulic radius.

Because riverbeds are often quite irregular in shape and difficult to characterize algebraically, I estimated the cross-sectional area of each 1-meter flow section using the trapezoid rule, as illustrated in Fig 4.20.

$$A_i = \frac{(b)(y_i + y_{i-1})}{2} \quad (\text{Eq. 16})$$

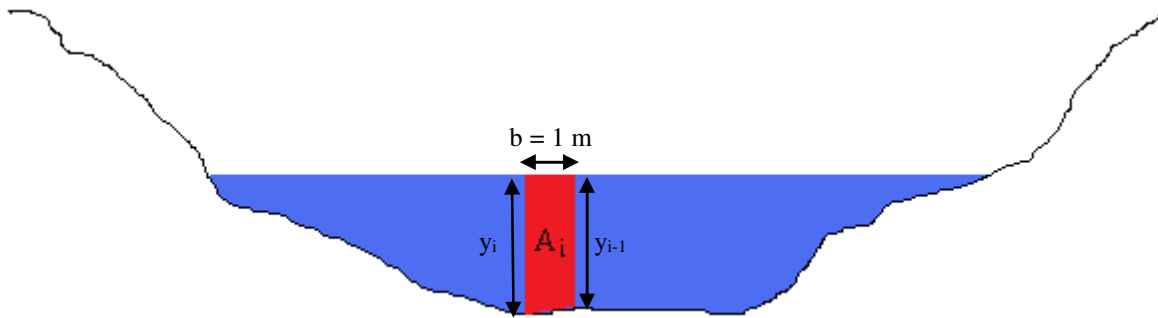


Figure 4.20: Flow section area. *The area of each 1-meter flow section interval was determined using the trapezoid rule.*

The hydraulic radius of each sub-section, which describes the section's flow efficiency based on its shape, is represented by

$$R_i = \frac{A_i}{P_i} \quad (\text{Eq. 17})$$

where P_i is the wetted perimeter, or the perimeter of the channel covered by water within the 1-meter section (Figure 4.21, next page). I did not consider the vertical boundaries between the 1-meter sections; in reality, lower velocities in the overbank channels may result in some shear resistance and a lower volumetric flow rate than that calculated. P_i was estimated using the distance formula, in meters.

$$P_i = \sqrt{(x_i - x_{i-1})^2 + (y_i - y_{i-1})^2} \quad (\text{Eq. 18})$$

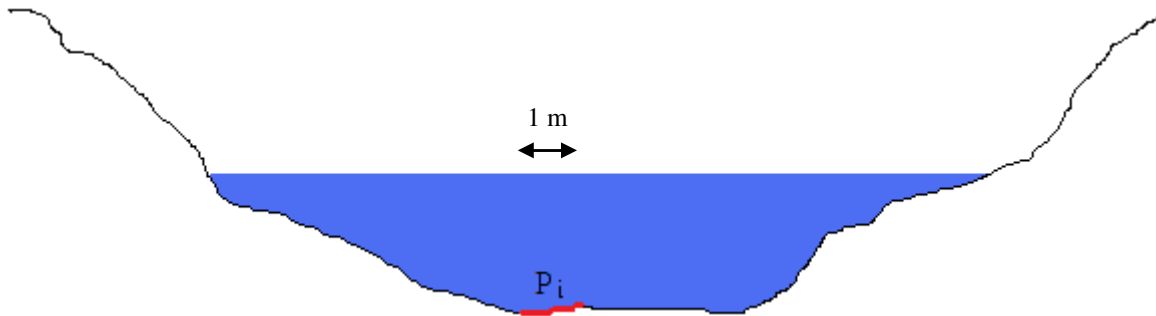


Figure 4.21: Flow section wetted perimeter. Each 1-meter interval's wetted perimeter, P_i , is used to calculate that section's flow rate.

To verify the method used to calculate discharges, I ran a HEC-RAS sub-critical steady flow model for each site using the maximum calculated volumetric flow rate, and compared the modeled water surface elevation with the reported stage height. The results compared very well, to within 10 cm.

Next, I reconstructed each site's hydrograph using a modified surge function of the form

$$Q(t) = ate^{-bt} \quad (\text{Eq. 19}) \text{ [Voytenko, 2011]}$$

where a and b are fitting parameters adjusted to interpolate the shape of each hydrograph at half-hour intervals between the start of flow and maximum reported flow, maximum reported flow and primary channel bankfull flow, and primary channel bankfull flow and end of flow. In the case of Site 9, the flow did not cease completely before the second storm started, two weeks later, so the storm hydrograph ends with a small, non-zero discharge value corresponding to the reported stage height. In addition to the reported hydrographs, I also created two modified hydrographs for each site. I varied the duration and magnitude of modeled flows in order to evaluate the relative sensitivity of sedimentation processes to hydrograph changes, in addition to changes in the spillway height. One modified hydrograph corresponds to a 10% increase in all discharge values over the course of the storm (hereafter referred to as the Tall case), and one represents a 50% increase in the

duration of the maximum reported flow (hereafter referred to as the Long case). Figures 4.22, 4.23 and 4.24 show the resulting hydrographs.

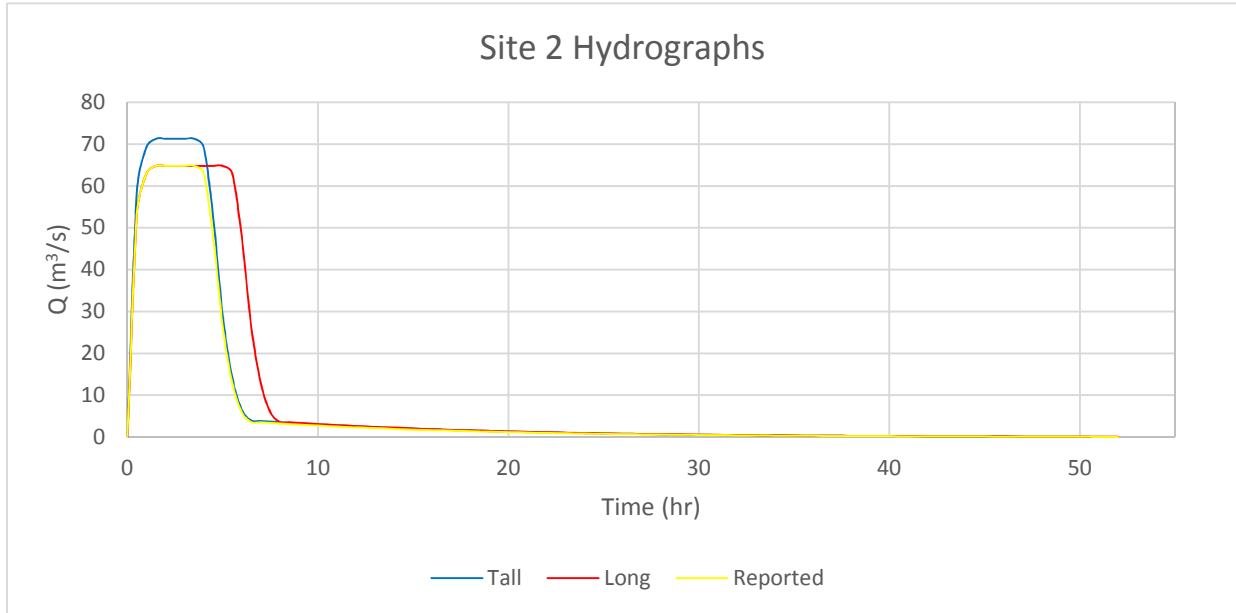


Figure 4.22: Site 2 hydrographs. Three distinct hydrographs are plotted for Site 2, including the reported case and two modified cases.

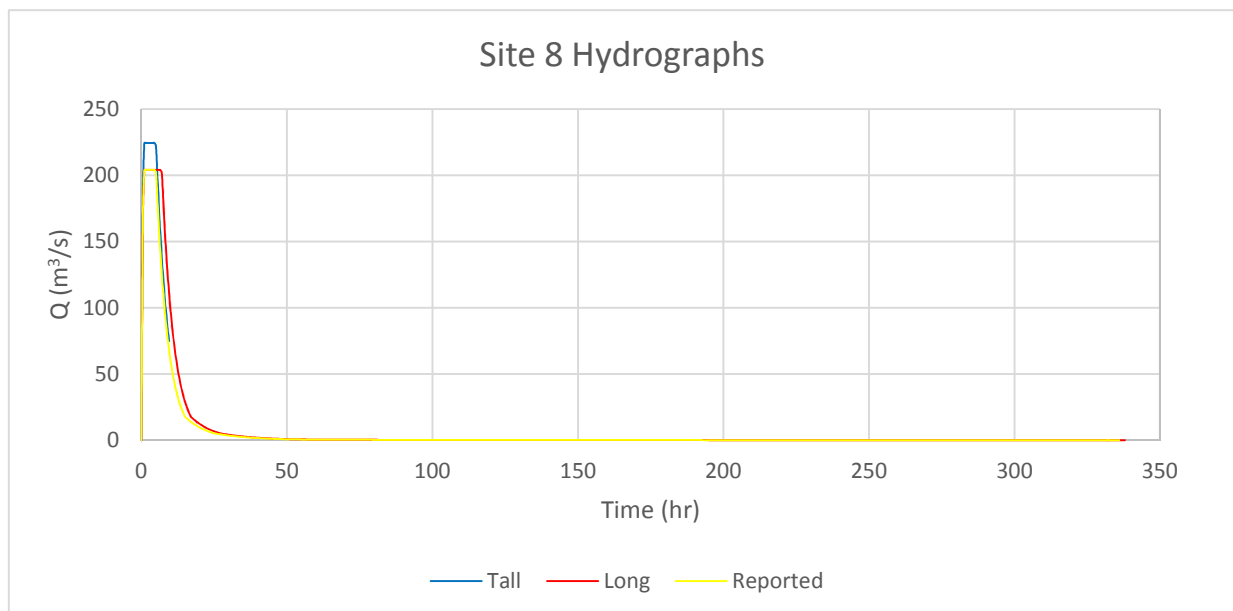


Figure 4.23: Site 8 hydrographs. Three distinct hydrographs are plotted for Site 8, including the reported case and two modified cases.

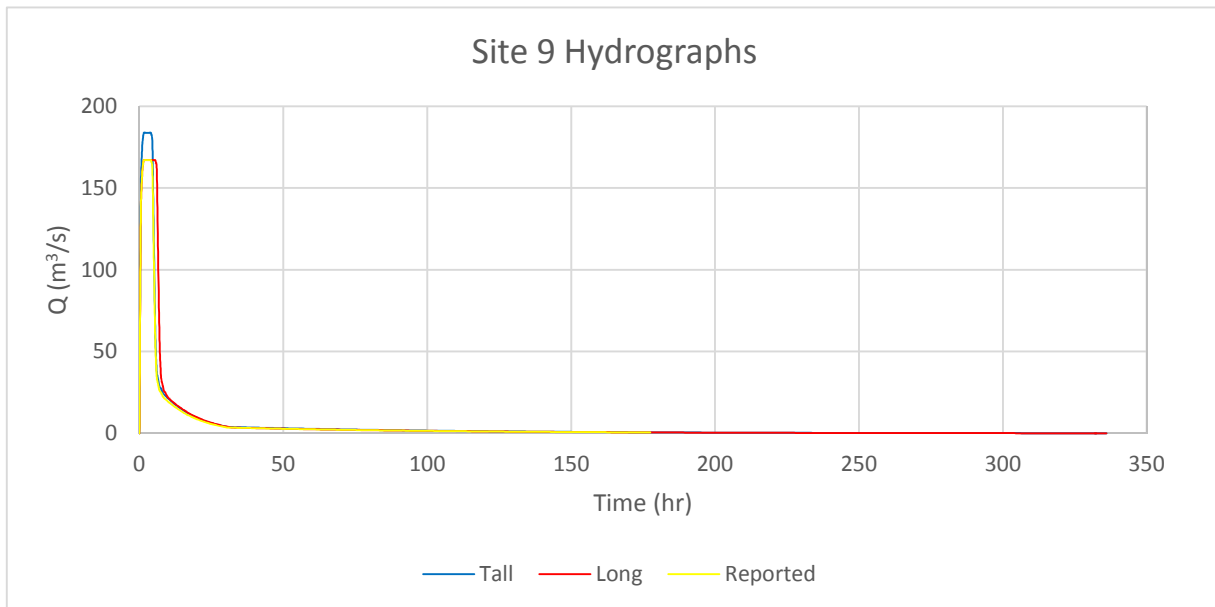


Figure 4.24: Site 9 hydrographs. Three distinct hydrographs are plotted for Site 9, including the reported case and two modified cases.

4.4.4 Hydraulic flow models

I ran a total of nine models for each site, alternatively varying flow and spillway height variables. Table 4.5 describes the altered parameters for each model run.

Table 4.7: Model runs. I ran 9 separate models tests for each site, varying spillway height and hydrograph parameters. Steady flow tests utilized the maximum reported discharge for the first storm after a dam's construction, while unsteady flow tests either used the hydrograph values as reported, the Tall case, or the Long case. Spillway heights ranged from zero (no dam) to the full height as the dam was constructed.

Test #	Flow model type	Spillway height
1	Steady flow (maximum reported discharge)	No dam
2	Unsteady flow (reported hydrograph)	No dam
3	Steady flow (maximum reported discharge)	Full spillway height
4	Unsteady flow (reported hydrograph)	Full spillway height
5	Unsteady flow (reported hydrograph)	10 cm spillway height
6	Unsteady flow (reported hydrograph)	1/3 spillway height
7	Unsteady flow (reported hydrograph)	2/3 spillway height
8	Unsteady flow (10% increase in peak discharge compared to Test #4)	Full spillway height
9	Unsteady flow (50% increase in maximum period compared to Test #4)	Full spillway height

For each test, I assumed a normal flow boundary condition at the bottom of the reach (50 m downstream of the dam site), based on the pre-construction channel slope. For the unsteady flow cases, I used 1-second computational time steps to avoid model errors, and 30-minute hydrograph output intervals. In addition to the standard tabulated output values, I also calculated channel shear stress—the bed shear stress applied to the sandy riverbed—resulting in a table of values with rows representing each cross-section at each 30-minute time step.

After exporting the model results, I used the shear stress to calculate the shear velocity at each cross section. Channel shear velocity, u_* , calculated as shown in Eq. 20, represents the channel shear stress expressed with units of velocity.

$$u_* = \sqrt{\frac{\tau_b}{\rho_w}} \quad (\text{Eq. 20})$$

where τ_b is the bed shear stress and ρ_w is the density of water, taken to be 998.2 kg/m^3 (corresponding to a temperature of 20°C). Next, I calculated the settling velocity, ω_0 , of four different sediment particle sizes representative of the collected sediment samples. Those particle sizes included 0.008 mm, 0.125 mm, 0.5 mm and 1 mm, corresponding to fine silt, fine sand, coarse sand and very coarse sand, respectively [Vanoni, 2006].

$$\omega_0 = -\sqrt{\left(\frac{4gd_s}{3C_d}\right)(s-1)} \quad (\text{Eq. 21}) \text{ [Chanson, 2004]}$$

where ω_0 is fall velocity, g is gravitational acceleration, d_s is the particle diameter, $s = \rho_s/\rho_w$, and C_d is a drag coefficient. C_d is calculated differently depending on the particle size and corresponding particle Reynolds number ($Re = \rho_w\omega_0d_s/\mu$), and due to the appearance of settling velocity in the Reynolds number, must be solved iteratively.

For natural sand and gravel particles with $Re < 1 \times 10^4$,

$$C_d = \frac{24}{Re} + 1.5 \quad (\text{Eq. 22}) \text{ [Engelund and Hansen, 1967]}$$

while for smaller particles with $Re < 0.1$, Stokes' law, defined below, is valid.

$$C_d = \frac{24}{Re} \quad (\text{Eq. 23}) \text{ [Chanson, 2004]}$$

Finally, I calculated the Rouse numbers for the four particle sizes at each cross-section and time interval, using

$$Rouse \# = \frac{\omega_0}{\kappa u_*}, \quad (\text{Eq. 24}) \text{ [Chanson, 2004]}$$

the ratio between a particle's settling velocity, ω_0 , and the product of the von Kármán constant, κ , and the shear velocity, u_* (Eq. 20). A von Kármán constant value of ~ 0.4 is typical for clear water flows, and has historically been considered a universal constant. Some evidence suggests that the von Kármán constant may decrease by 10% or more with increasing suspended sediment load, as sediment dampens the turbulence momentum transfer [Gaudio *et al.*, 2010], but this may only be true very near the bed, and the scientific community has yet to reach consensus [Castro-Orgaz *et al.*, 2012]. Given the lack of sediment load concentration data for the modeled sites, I assumed a constant of 0.4, with the understanding that the high suspended sediment loads transported by dryland streams may in reality affect the turbulent velocity profile, especially near the sandy bed.

4.4.5 Analysis of model outputs

I chose the Rouse number as an indicator with which to compare the effects of varying channel and dam configurations and stream discharges on sedimentation processes. As defined above, the Rouse number compares the relative effects of the forces acting on a sediment grain of a particular size in the vertical directions and provides a rough indication of the mode of transport, as show in Table 4.6 [Whipple, 2004¹⁷; Moore, 2006¹⁸].

Table 4.8: Rouse number. A particle's mode of transport is associated with its Rouse number.

Rouse #	Mode of transport
0 - 0.8	Wash load
0.8 - 2.5	Suspended load
2.5 - 7.5	Bed load
> 7.5	At rest

¹⁷ Whipple, K. X (2004), 12.163/12.463 Course Notes, MIT Open Courseware, available at <http://ocw.mit.edu/courses/earth-atmospheric-and-planetary-sciences/12-163-surface-processes-and-landscape-evolution-fall-2004/lecture-notes/4_sediment_transport_edited.pdf>

¹⁸ Moore, A. (2006), Fluvial Sediment Transport Course Notes, Kent University, available at <http://www.personal.kent.edu/~amoore5/FST_L_20.pdf>

Use of the Rouse number as an indicator is based on several important assumptions, including the following:

1. Any particle transported as bed load is trapped by the dam, while any particle that approaches the structure while traveling as suspended or wash load is ultimately discharged over the spillway. Thus, a Rouse number of 2.5 calculated for a particle of a given size represents the threshold value indicating the fate of that size class.
2. Varying transport rates (rates of sediment load supplied to a dam's backwater throughout the storm hydrograph) have little effect on the ultimate composition of the deposited sediment. As larger discharges deliver increased rates of sediment load to the dam backwater, a greater percentage of those loads will travel in suspension and ultimately bypass the dam, offsetting the effect. This is a necessary assumption as no transport rate data are available.
3. The sedimentation process described by the Rouse number represents the primary mechanism of deposition affecting the ultimate composition of the sand dam's stored sediment. Other processes, such as the settling of suspended sediment in the open water after flow has ceased, the scour of previously-deposited sediments by subsequent storms, and the import and export of sediment caused by animals or humans, play more minor roles in determining the bulk sediment characteristics throughout the dam's storage volume.

Predictably, for a given flow case and particle size, Rouse numbers vary both with time (corresponding to changes in discharge) and location. Figure 4.25 presents the variation in modeled Rouse numbers for a 0.125 mm (fine sand) particle transported throughout the Site 2 backwater over the course of the recorded storm hydrograph, with the spillway modeled at its full height. In the surface plot, the color yellow corresponds to Rouse numbers of magnitude 2.5 or greater, indicating cross-sections and times at which the particle either travels as bed load or ceases to move altogether—in other words, conditions leading to sediment trapping by the dam.

Variation in Rouse # for Site 2 (0.125 mm Particle, Gradually-Varied Flow, Full Spillway Height)

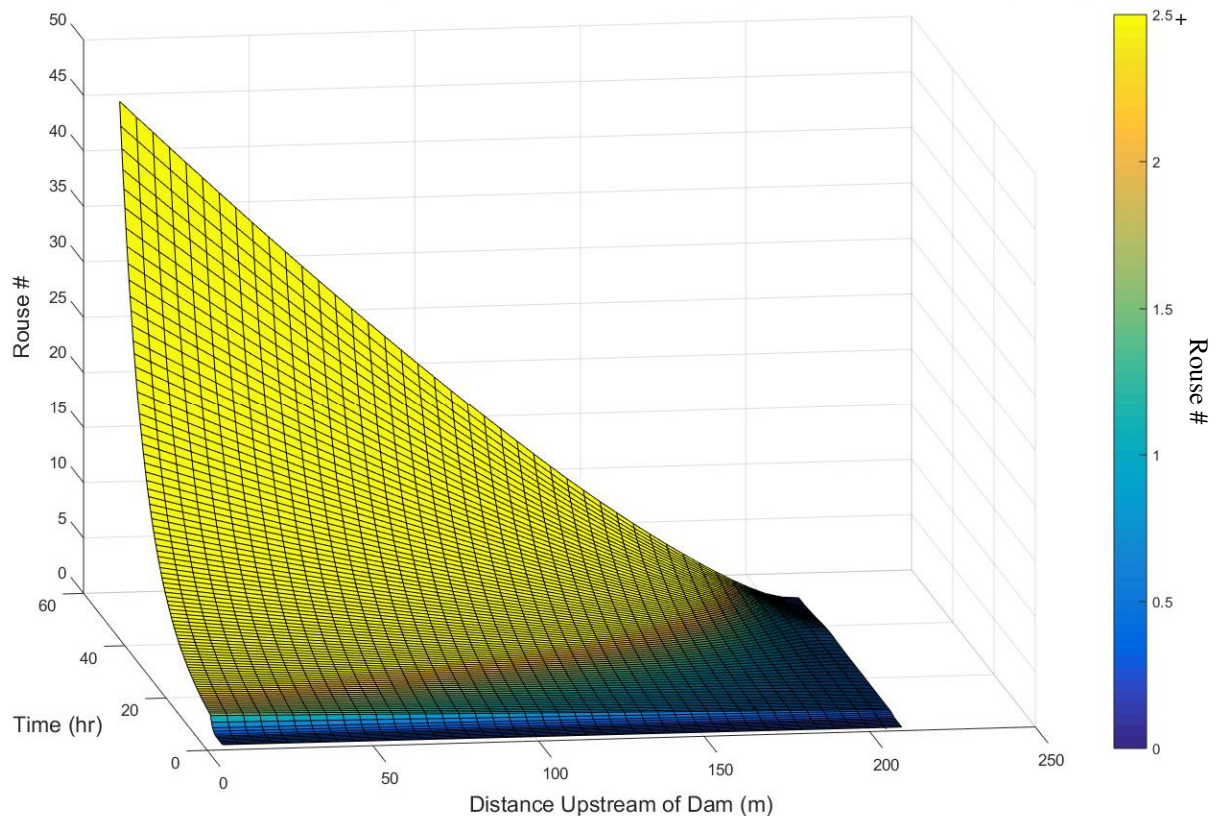


Figure 4.25: Variation in Rouse numbers. *Plotted Rouse number variations for a 0.125 mm sediment particle show dependence of sedimentation on location and time (discharge).*

As depicted in Figure 4.25, larger discharges at the beginning of a storm hydrograph result in larger channel shear stresses and shear velocities at a particular location, increasing the likelihood a particle will travel in suspension. The flow's cross-sectional area increases

closer to the dam, resulting in a decrease in the channel shear stress and shear velocity, so a particle is more likely to be trapped as it approaches the structure.

I analyzed each unsteady flow case by calculating the fraction of the total surface flow period during which particles of the four representative sizes traveled in suspension. In particular, I focused on a cross-section located 1/20th of the dam's total backwater length upstream of the structure. For the three structures, this represented distances of 10 m (Site 2), 15 m (Site 8) and 20 m (Site 9). Because Rouse numbers decrease (i.e. particles are more likely to travel in suspension) as distance upstream of the dam increases, choosing a scaled location close to the dam provided a bulk representation of sediment transport processes throughout the backwater. A particle transported in suspension near the dam wall will have traveled in suspension throughout the backwater.

I then performed a sensitivity analysis, evaluating the relative impacts of reduced spillway height, increased discharge magnitude and increased duration of maximum flow on sedimentation processes using the time percentage results for 0.125 mm particles. I calculated the relative sensitivity using Eq. 25, with the time results from Test 4 (full spillway height, hydrograph as reported) representing the nominal case.

$$Relative\ sensitivity = \frac{\left[\frac{Response_{Altered} - Response_{Nominal}}{Response_{Nominal}} \right]}{\left[\frac{Parameter_{Altered} - Parameter_{Nominal}}{Parameter_{Nominal}} \right]} \quad (Eq. 25)$$

For the spillway height parameter, I evaluated the sensitivity based on both the 1/3 and 2/3 spillway height cases to understand how sensitivities vary over a range.

4.4.6 Statistical analysis of maximum flow data

In addition to the hydraulic flow models, I also used the Pearson's correlation analysis described in Section 4.3.4 to evaluate possible statistically-significant univariate correlations between local hydraulic conditions, either measured during the field surveys or calculated from maximum reported flow data, and the resulting particle size distributions. As before, I used R [R Core Team, 2015] to evaluate correlations between the predictors shown in Table 4.7 and the site sediment parameters defined in Section 4.2.3.

Because the lateral extents of a sand dam's primary spillway are typically aligned with edges of the original riverbed, I assumed the spillway width provided an estimate of the original channel width. I used the pre-dam channel slope as reported by the NGOs and based the area, discharge and velocity values on surveyed data, an application of Manning's Equation and the continuity equation, respectively. The discharge, area and velocity values represent maximum reported flows for the reach before construction; in this way, the parameters differ from those calculated by *Wipplinger* [1953]. As with the correlation analysis described in Section 4.3.4, 11 sites were included in the analysis, though the maximum reported flow, area and velocity values for Site 6 were deemed unreliable due to the severe incision of the downstream channel after the dam's construction.

Table 4.9: Reach-scale characteristics. *Seven variables representing proposed, reach-scale controls on sedimentation were chosen for correlation analysis.*

<i>Local Reach Characteristics</i>							
Site #	Spillway Height (m)	Spillway Width (m)	# Rainy Seasons	Pre-Dam Slope	Peak Q (m ³ /s)	Peak A (m ²)	Peak U (m/s)
1	1.51	8.00	2	0.0001	46	19	2.47
2	1.05	7.93	2	0.0050	65	19	3.34
3	1.25	17.91	4	0.0003	28	26	1.08
4	1.19	5.00	4	0.0303	15	4	3.54
5	2.30	17.00	1	0.0001	80	24	3.40
6	1.37	4.27	2	0.0060	N/A	N/A	N/A
7	1.94	5.83	1	0.0050	98	46	2.13
8	1.90	27.50	2	0.0060	204	68	3.00
9	1.70	17.60	2	0.0040	167	49	3.39
10	2.25	6.13	5	0.0020	17	11	1.62
11	2.22	16.34	4	0.0050	96	46	2.08

Chapter 5. Results

5.1 Catchment characteristics

The results of the Pearson’s correlation analysis for catchment characteristics are surprising for two reasons. First, despite the relatively small number of sites ($n = 11$), I found a statistically-significant predictor of median sediment size: mean catchment slope. However, as shown in Table 5.1, mean catchment slope is *negatively* correlated with median particle size both throughout the entire backwater and at all locations not including that closest to the dam. Figure 5.1 presents plotted site data.

Table 5.1: Catchment correlation results. *The results of the Pearson’s correlation analysis for catchment characteristics showed a negative correlation between median particle size and mean catchment slope.*

		Pearson’s Correlation Coefficient				p-Value			
		D ₅₀ All (mm)	D ₅₀ No 10 m (mm)	D ₅₀ 10 m (mm)	Hazen's C _U	D ₅₀ All (mm)	D ₅₀ No 10 m (mm)	D ₅₀ 10 m (mm)	Hazen's C _U
Catchment characteristics	Area (km ²)	0.08	0.09	-0.02	-0.28	0.83	0.80	0.96	0.40
	Max Slope	0.1	0.14	-0.11	-0.28	0.78	0.68	0.75	0.40
	Mean Slope	-0.67	-0.71	-0.43	0.3	0.02	0.01	0.19	0.38
	Crops %	0.4	0.38	0.21	-0.46	0.22	0.25	0.53	0.15

This result is somewhat counterintuitive. As was described in Chapter 2, greater slopes are typically associated with greater transport capacities and competence, and thus larger particles supplied to (and found in) riverbeds. However, the analysis seems to suggest the opposite for the study sites: dams with steeper catchment slopes trapped finer particles. The mechanism behind this trend is unclear. On one hand, it may be the rare case that the statistical suggestion is not scientifically supported, and that random error has produced an apparent trend which does not in reality exist. On the other hand, it is possible that a scientific explanation does exist—for example, catchment slopes may be associated with different parent material types, which in turn produce different particle sizes. Another possible cause could be the increased infiltration and decreased drainage density associated with lower slopes, and the resulting increase in baseflow. As was discussed in

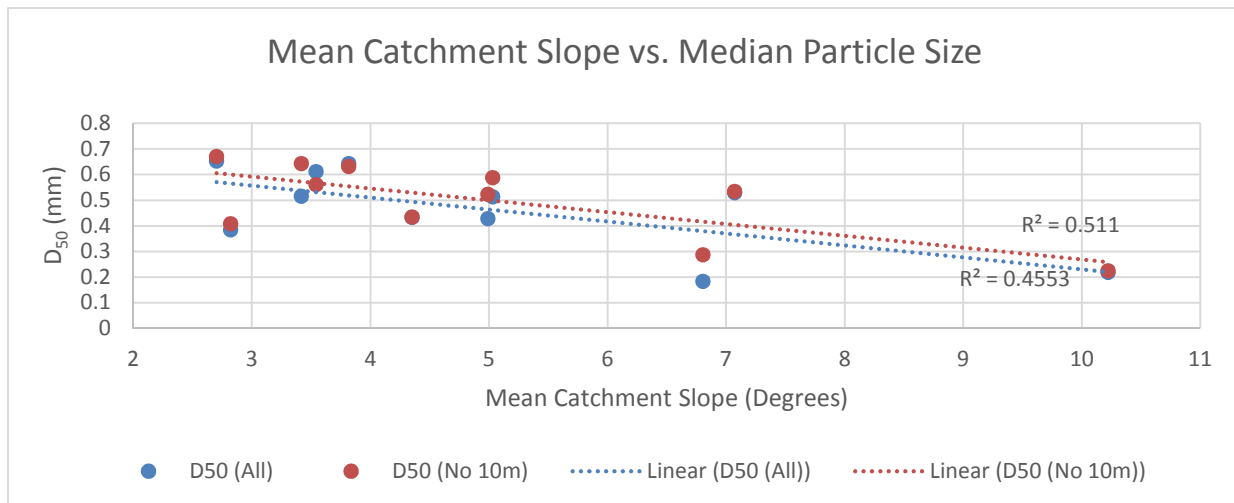


Figure 5.1: Catchment slope and particle size. *Pearson's correlation analysis reveals a statistically-significant, negative linear relationship between mean catchment slope and median particle size, especially when soil samples from 10 meters upstream of the dam are excluded.*

Section 2.2.2.2, because baseflow does not supply additional sediment to the stream, its excess energy may allow it to winnow fine sediment deposited by low runoff flows at the end of a storm's receding limb. This hypothesis could be tested by comparing suspended sediment concentrations at the top of the backwater and in the spillway during the baseflow-dominated receding limb of a flow event.

Interestingly, the median particle sizes at the 10 m locations do not correlate well with mean catchment slope, and the linear relationship between sediment size and mean slope improves when the 10 m location data are omitted from the analysis. This variability in sedimentation results appears to highlight the differences in sedimentation processes at work throughout the backwater at large and in the bottomset bed. The differing correlations support the conceptual model presented in Chapter 2, as well as the hypothesis about the role of baseflow in coarsening the bed. While increased baseflow associated with smaller slopes may scour fines throughout most of the backwater, especially where the cross-section is small, it seems less likely that the relatively small discharge will apply sufficient shear stress to the bottomset bed very close to the dam, where the cross-sectional area is greatest.

It is important to note that all of the study sites have mean catchment slopes of greater than 2°, which corresponds to the threshold identified by *Gijsbertsen* [2007] as necessary to produce coarse sand in catchments in Kitui County.

Other results also stand out. Notably, catchment area is the predictor variable least correlated with median particle size. Catchment land use is somewhat correlated with trapped sediment size, and cultivated lands are more often associated with coarse trapped sediment than are non-cultivated land cover types, but the result is not statistically significant.

5.2 Local hydraulic conditions

5.2.1 Static flow data

The statistical analysis of linear relationships between static local hydraulic conditions and deposited sediment did not result in any statistically significant correlations, as shown in Table 5.2. This is understandable. Given the small sample size and variability of the sedimentation processes, I expect a larger sample size would be needed to find any clear correlations, if they exist.

Table 5.2: Reach-scale correlation results. *The results of the Pearson's correlation analysis for local hydraulic characteristics did not illuminate any statistically-significant linear relationships.*

		Pearson's Correlation Coefficient				p-Value			
		D ₅₀ All (mm)	D ₅₀ No 10 m (mm)	D ₅₀ 10 m (mm)	Hazen's U.C.	D ₅₀ All (mm)	D ₅₀ No 10 m (mm)	D ₅₀ 10 m (mm)	Hazen's U.C.
Local characteristics	Spillway Height	-0.27	-0.30	-0.34	-0.11	0.42	0.37	0.30	0.74
	Spillway Width	-0.12	-0.05	-0.31	-0.30	0.72	0.89	0.35	0.37
	# Rainy Seasons	-0.41	-0.46	-0.19	-0.22	0.21	0.15	0.57	0.52
	Pre-Dam Slope	0.04	-0.06	0.25	0.00	0.90	0.87	0.46	1.00
	Peak Q (m ³ /s)	-0.10	-0.11	-0.12	0.29	0.78	0.75	0.74	0.42
	Peak A (m ²)	-0.27	-0.32	-0.20	0.25	0.45	0.36	0.58	0.49
	Peak U (m/s)	0.42	0.45	0.26	0.31	0.22	0.19	0.46	0.38

Despite the lack of clear relationships, some results are nonetheless interesting. The number of rainy seasons required for dams to fill completely with sediment, along with the

maximum reported average channel velocity before construction, may suggest a potential correlation. As one might expect, dams which filled in fewer rainy seasons were more likely to trap coarser sediment—this is supported by the inverse (but also statistically-insignificant) relationship between spillway height and median particle size, because smaller storage volumes are likely to fill with sediment more quickly.

The maximum reported average channel velocity before construction shows some correlation with median particle sizes throughout the backwater (less so at the 10 m location), likely reflecting the greater potential of relatively constricted channels to produce fast, turbulent flows capable of keeping particles in suspension.

It is worth noting that constructed spillway height is not well correlated with sedimentation results, as shown in Figure 5.2.

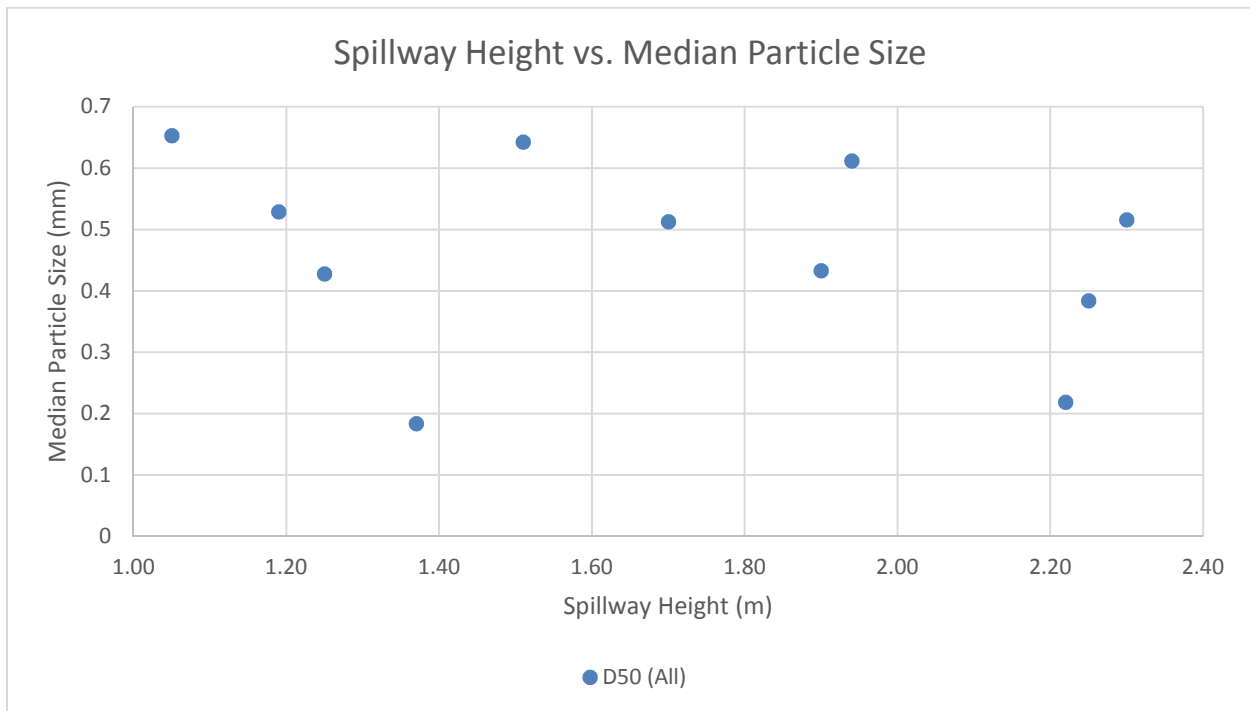


Figure 5.2: Spillway height and particle size. *Spillway heights for the 11 study sites were not well correlated with median particle sizes trapped by the dam.*

5.2.2 Hydraulic flow modeling

Of the various approaches used to model sedimentation processes in sand dams, the variation in Rouse numbers, based on unsteady HEC-RAS flow models, appears to be the most useful for capturing the impacts of dynamic flows and channel geometry.

Figure 5.3 presents the modeled time percentages for which particles of four different sizes traveled in suspension at a distance 1/20 of the backwater length upstream of the dam, for the reported hydrograph and constructed spillway height. As described in Chapter 4, this is assumed to represent the fraction of flow time during which the particles were discharged by the dams.

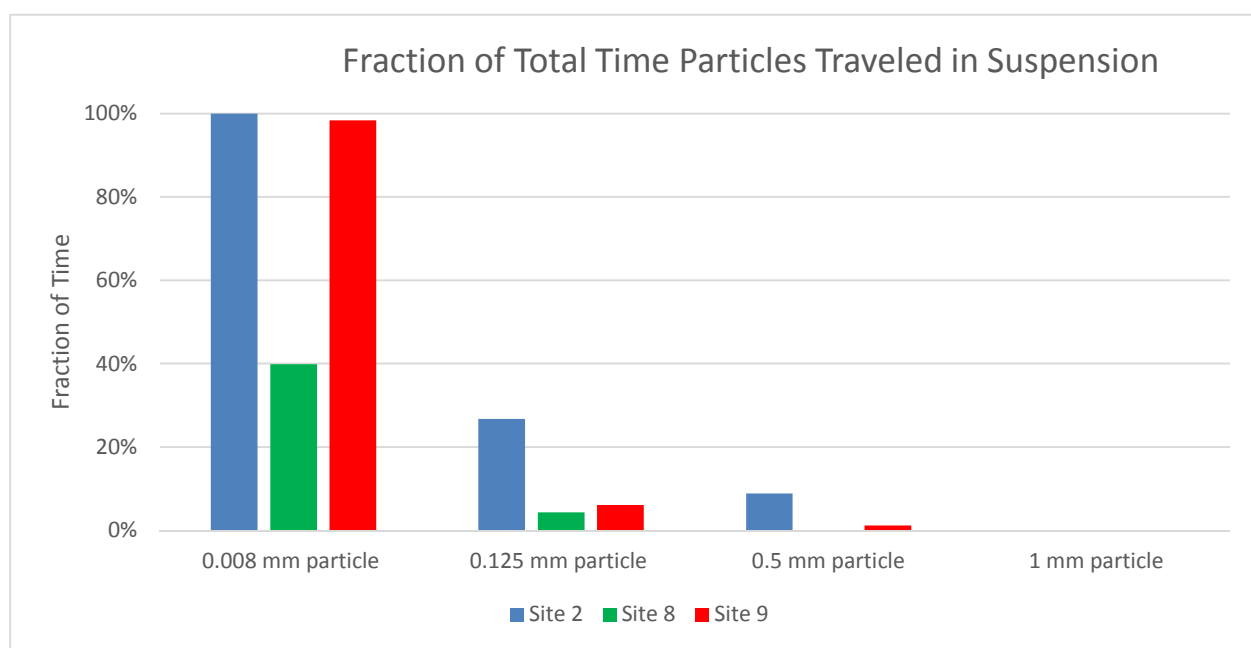


Figure 5.3: Time fraction results: Plot showing fraction of total surface flow time during which particles of four sizes were discharged by each of the three dams.

Fine particles were most often predicted to be discharged by Site 2, followed by Site 9, and Site 8 was predicted most likely to retain fine particles. Site 2 did not trap any 0.008 mm (fine silt) particles, while all three sites always trapped 1 mm (coarse sand) particles. As such, the model predicts that Site 2 will have the coarsest median particle size, followed by Sites 9 and 8. These results align well with actual sediment profiles for the three sites in ranking, as presented in Figure 5.4. It is more difficult to interpret and predict the spread of

the particle size distributions. However, due to the larger C_U values associated with finer samples (as in the case of samples from the bottomset bed), the sites' uniformity is ranked in the same order as their median particle size.

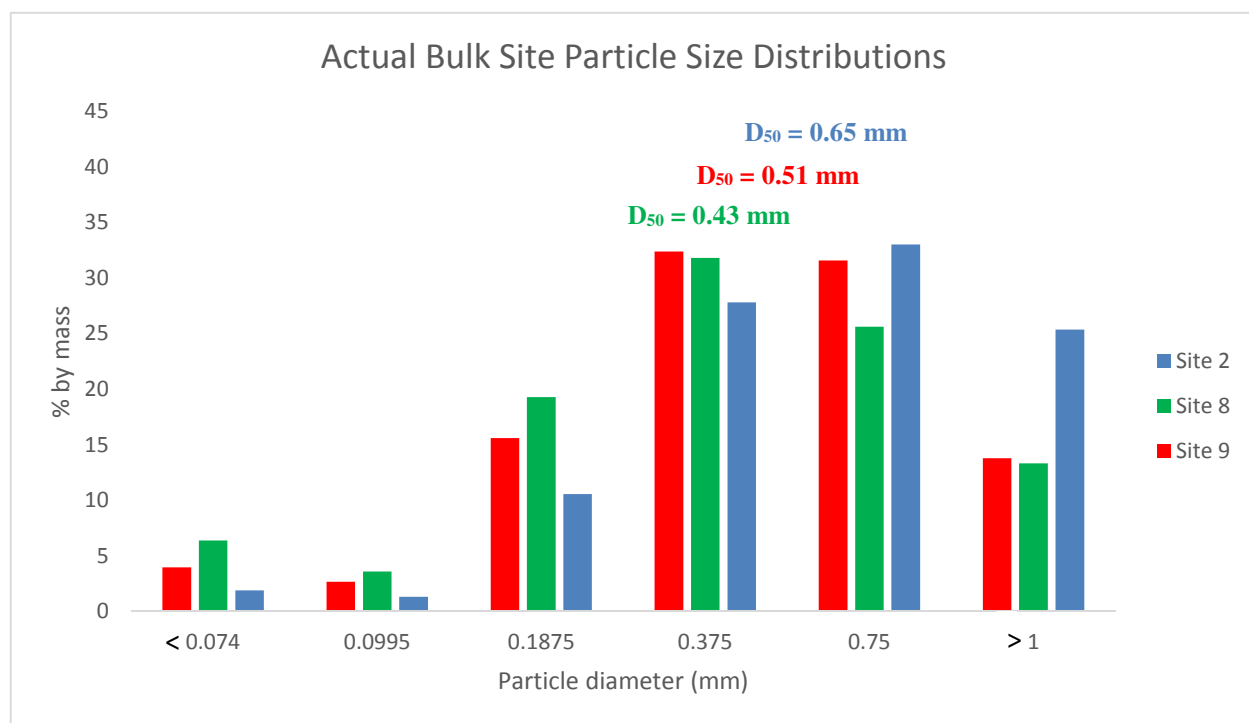


Figure 5.4: Actual particle size distributions. *Of the three modeled dam sites, Site 2 has the coarsest median particle size, followed by Sites 9 and 8.*

Based on the results of the model runs using the constructed spillway height, 0.125 mm particles appear best-suited as an indicator size for a sensitivity analysis, because fine sand is both discharged and trapped for some positive fraction of the total flow time for all sites. This is important; if 1 mm particles had been used, it would not be possible to compare the sites, because all particles would be trapped 100% of the time. Also, fine sand particles may represent a sort of theoretical minimum particle size, as communities may wish to limit deposition of anything finer than 0.125 mm.

Each dam's general response to varied spillway height and flow parameters was as expected: shorter spillway heights increased the likelihood that a 0.125 mm particle would travel in suspension throughout the entire backwater. Figure 5.5, next page, shows the same Rouse number surface plot presented in Figure 4.25, for the full spillway height case,

but also provides a visual comparison with the plot for a spillway modeled at 1/3 its actual constructed height. Once again, the color yellow corresponds to Rouse numbers of magnitude 2.5 or greater, indicating cross-sections and times at which the particle is trapped by the dam.

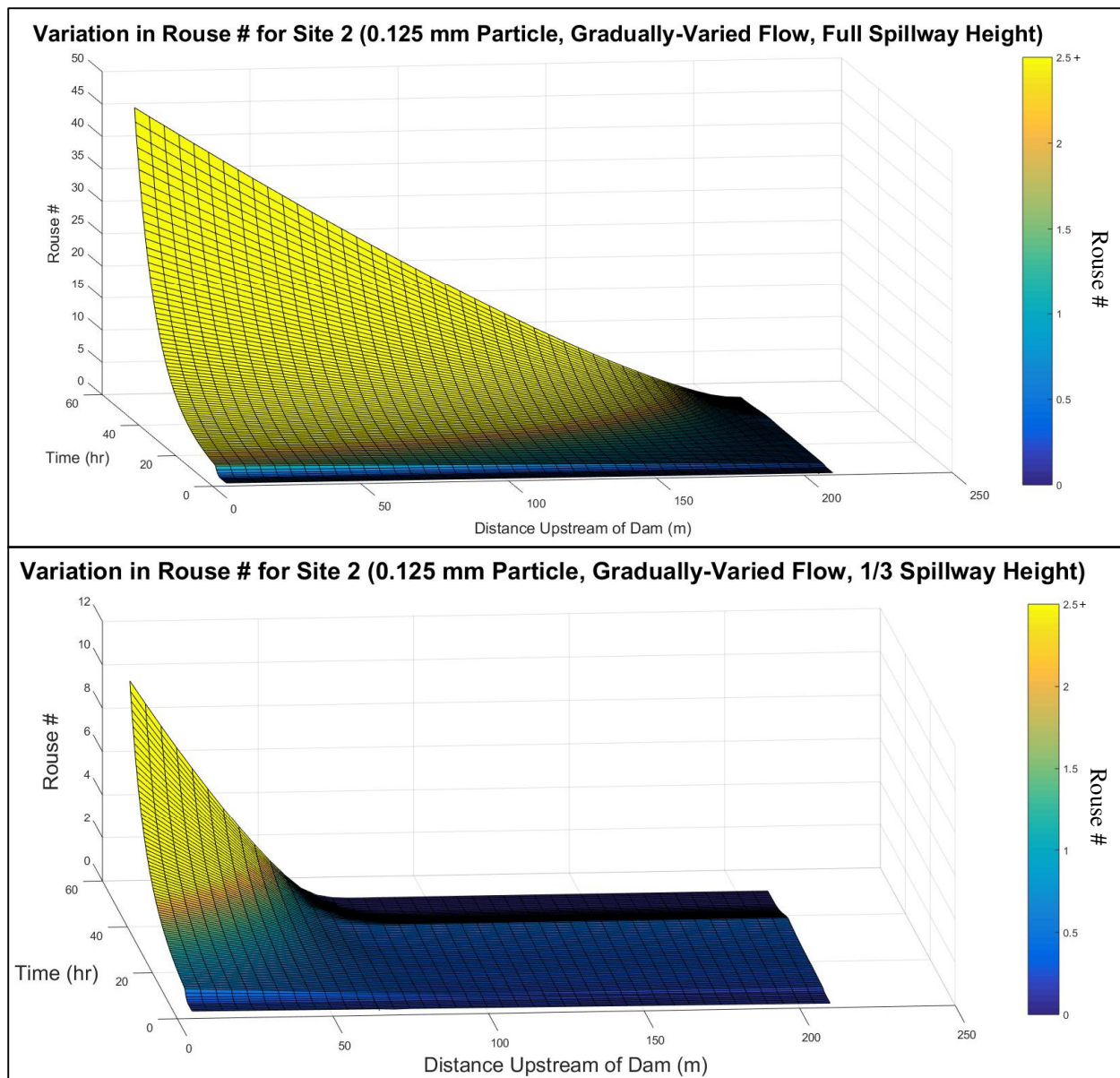


Figure 5.5: Surface plot comparison. *Sediment trapping for Site 2 is reduced, both temporally and spatially, when spillway height is reduced by 67%.*

Table 5.3 presents the results of the sensitivity analysis. The results provide useful insight into the relative importance of spillway height compared to changes in flood discharges, as

well as the differences in relative sensitivity at different spillway heights. For each site and model parameter, the table shows the time percentage a 0.125 mm particle traveled in suspension, and the relative sensitivity of that result compared to the nominal (full spillway height, reported hydrograph) case.

Table 5.3: Sensitivity analysis. *Simulation results predict that sedimentation processes are relatively more sensitive to spillway height than to changes in discharge, and that sensitivity increases as spillway height decreases.*

Sensitivity of Rouse # for 0.125 mm Particle to Spillway Height and Hydrograph Parameters							
Model Parameters		Site 2		Site 8		Site 9	
Parameter change	Range (%)	Response	Relative sensitivity	Response	Relative sensitivity	Response	Relative sensitivity
Nominal	0	26.7%	-	4.3%	-	6.1%	-
Spillway height	-33.3	39.6%	-1.4	6.0%	-1.1	8.2%	-1.0
Spillway height	-66.6	64.4%	-2.1	11.2%	-2.4	32.3%	-6.4
Discharge magnitude	+10	28.7%	0.7	4.5%	0.3	6.5%	0.7
Peak flow period	+50	28.8%	0.2	4.9%	0.3	6.5%	0.1

Several results stand out. First, for all three sites, sedimentation processes associated with 0.125 mm particles appear to be more sensitive to spillway height than to changes in the magnitude of the discharge and the duration of the peak flow, over the modeled ranges. Second, the relative sensitivity of sedimentation processes to spillway height appears to increase at lower heights; the sensitivities increased by factors of 1.5, 2.2 and 6.4 for the three sites between the 2/3 and 1/3 spillway height cases. Third, some sites are more sensitive to spillway staging than others. The relative response to a spillway built to 1/3 its constructed height is much greater for Site 9 than the other two sites, despite the fact that the actual reduction in spillway height for Site 8 is larger than the change for Site 9.

Chapter 6. Discussion

The results of this research suggest many general principles about sand dam spillway height staging, and also lead to several new questions about sedimentation processes and sand dam design.

6.1 Recommendations for sand dam spillway design

6.1.1 Benefits vs. costs

Based on the findings of this research, the use of spillway staging is predicted to result in measurable benefit at most sites, in terms of a sand dam's potential to store and yield water. While sand dam sedimentation does vary with many uncontrolled factors, the relatively strong modeled sensitivity of sedimentation processes to a given dam's spillway height suggests that uncertainties associated with other factors (such as increasingly-variable rainfall) do not justify disregarding the potential impact of spillway staging.

The relative benefit of spillway height staging is shown to be site-specific. Over half of the sites studied in this research did not need to be built in stages in order to store and yield sufficient quantities of water to achieve community aims. While the successful dams included in the research might produce measurably better results if they had been built in stages, the benefit could be small and vary significantly between sites. The same is true for study sites which trapped excessively fine material—spillway staging likely would have benefited all sites, but some would need to have been built using much shorter stages than others in order to achieve the desired particle size distributions and water availability results.

The costs of building sand dams in stages also vary by site. Material and personnel transport likely represents the biggest source of cost diversity between sites: some communities are located close to national highways and material supply centers, and are easily accessed by large trucks, while other sites are located far from supply hubs and require transport over rough terrain navigable only by smaller vehicles.

Finally, in addition to the site-specific range of benefits and costs, community members' willingness to build dams in stages over longer periods of time also appears to vary by site. According to Elijah Kamama, a community organizer with SASOL Foundation, communities with limited access to locally-available water resources, and especially those which have previously built a sand dam which does not function well, would likely be more willing to try building in stages [*Kamama, personal communication, 2014*].

Given the range of benefits per cost of staging, along with the diversity of social constraints, the use of staging should be evaluated on a case-by-case basis. Given the current rate of failure due to siltation and the expected benefit of staging, a greater percentage of sand dams should probably be built in stages. However, many sites do not require staging, and given the potentially high costs required to produce limited additional benefits, the universal application of staged designs should not be considered necessary nor appropriate.

6.1.2 Spillway stage design

Despite the site-specific nature of the costs and benefits associated with spillway staging design, many general principles appear to hold true for most locations when deciding whether or not to build a dam in stages. Figure 6.1, next page, presents a flow chart describing practical steps practitioners can use to evaluate whether staged construction is needed and, if so, how stages should be designed. The remainder of the section describes the components of the flow chart in greater detail.

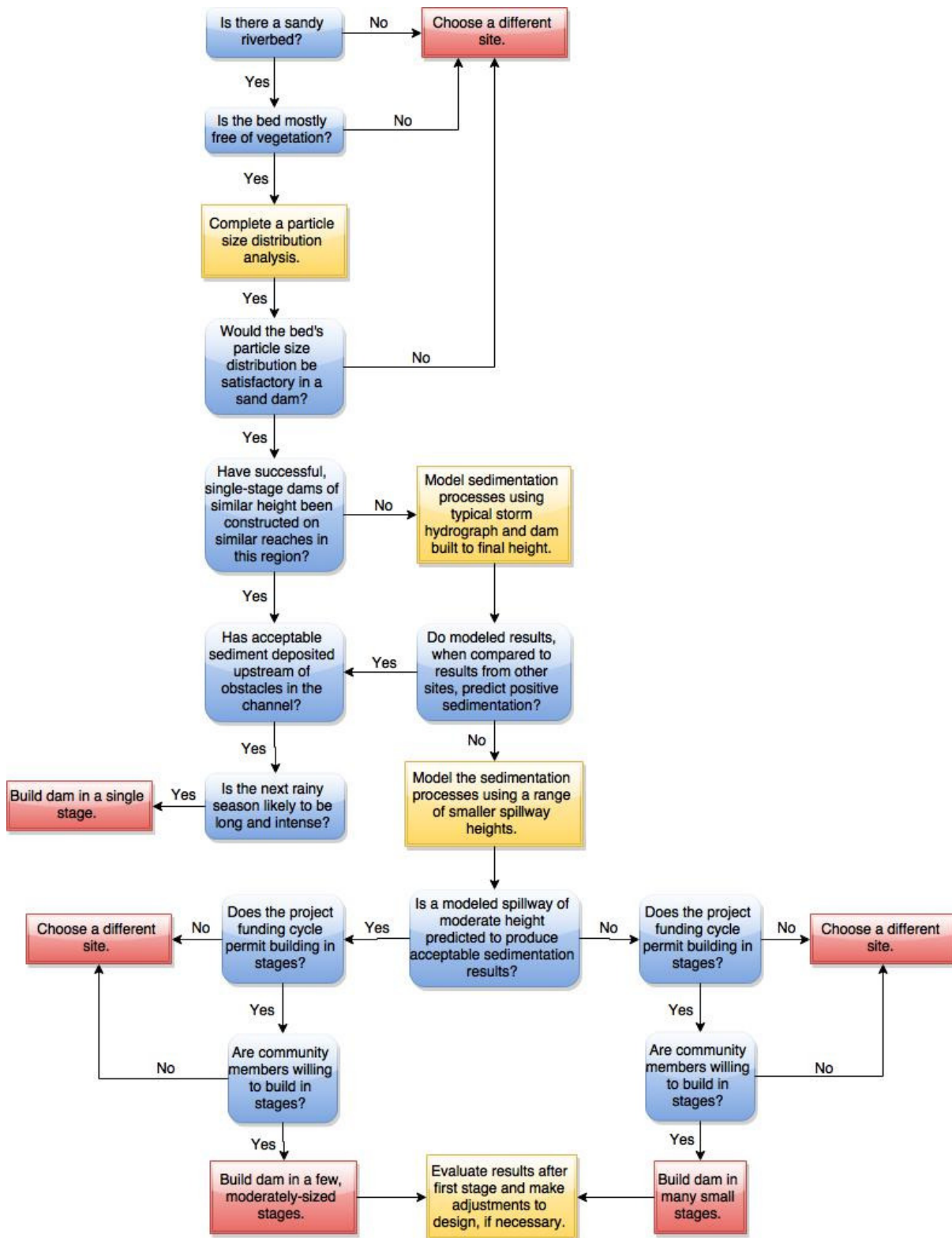


Figure 6.1: Staging design flow chart. Practitioners can apply a number of general principles to assess the need for and design of spillway stages for sand dams.

One important implication of the sedimentation processes described in Chapter 2 and supported by the hydraulic models is the role of the existing riverbed composition in understanding a site's potential. As described in Section 2.2.2.2, knowledge of the particle size distribution of an original riverbed is usually inadequate for making precise predictions about the particle size distribution of the trapped sediment, due to the deposition of fine sediment which otherwise would have been transported out of the reach as wash load. However, the existing riverbed does provide information about the upper limit of what can reasonably be expected to accumulate, in terms of coarseness, and the information can be used to eliminate some sites under consideration. Figure 6.2 shows a sand dam (not a study site) which was built in 2009 on a poorly-defined river without a sandy riverbed. Based on the understanding that construction of a sand dam will not



Figure 6.2: Failed sand dam. *Sand dams built on rivers without sandy riverbeds will not likely benefit from staged construction.*

typically result in a coarsening of the bed or accumulate sand where it does not exist¹⁹, this site's failure due to siltation could have been avoided.

For sandy riverbeds, a particle size analysis like the one described in Chapter 4, along with falling head permeability tests, may be useful for evaluating a river's potential. For sites where sediments seem marginal in their ability to store and yield water, spillway staging should be considered necessary. Vegetation in a riverbed can likewise be used as an indicator of fine and organic material, which is not ideal for sand dams [Gijbertsen, 2007]. Sites with extensive vegetation should be avoided altogether, and spillway staging should probably be considered for those with some plants growing in the channel. Finally, like sand dams, existing channel obstacles also trap sediment, and they may provide some insight into the type of sediment which can be expected to accumulate behind a dam of the same height [Nilsson, 1988].

Hydraulic modeling of local, dynamic flow conditions using the methods described in Chapter 4 may be useful in determining whether to build a dam in stages, especially for the first dam built on a given river. Many organizations have the technical capacity to survey rivers, set up HEC-RAS flow models and process data using spreadsheet software. By comparing modeled results of new sites with modeled and actual results of previously-built dams, sand dam practitioners can better understand the expected benefit of spillway staging for new sites. While it should not be assumed that dams located on the same river will have the same results, it does seem likely that sand dam practitioners will gain experience working on reaches with similar attributes, and may be able to make appropriate decisions about the need for staging simply by observing a site's geometry and learning about flows from community members.

After deciding that a dam should be built in stages, sand dam practitioners must decide how tall each stage should be, balancing anticipated benefits with costs and project restraints. Of all the results from this research, perhaps most striking is the weakness of the

¹⁹ Nilsson [1988] describes some rivers in India which transport sand but do not have sandy riverbeds, due to their large channel gradients. While this condition is not characteristic of rivers in the study region, it may be possible to infer sand transport in such a reach when coarse sand is found in downstream reaches with smaller gradients.

relationship between constructed spillway height and the median size of trapped sediment for the study sites, which appears to dispel the notion that a standard spillway height is appropriate for all dams.

Spillway stages, when necessary, should be designed on a case-by-case basis, with smaller stages used for sites more likely to trap fine sediment. However, based on the theoretical application of the drainage curve in Section 2.2.3, along with the results of the sensitivity analysis presented in the previous chapter, it appears that strategic stage design may actually lend itself to smaller initial stages, and increasingly taller stages as a dam is raised. For example, if, after reviewing costs and benefits for a given site, a community-NGO partnership decides to build a particular dam in two stages, it may be more effective to begin with a stage height $1/3$ the total planned height, and then add the last $2/3$ after the first stage has filled with sediment. Due to the evapotranspiration losses associated with fine material near the surface of the bed, this approach may be best suited to sites with adequate baseflow and relatively deep aquifers.

Another practical consideration when designing stage heights is the time of the year and the anticipated strength of the coming rainy season. While some Kenyan sites experience little difference between the short and long rains, in terms of flow magnitude, flow duration and the total number of storms, other communities describe significant and predictable differences between the seasons. If a sand dam will be built immediately before a rainy season historically characterized by a large number of intense storms, it may be possible to use larger stages, due to both the increases in stream competence during storm events and the increased baseflow near the end of the season.

Finally, one benefit of building sand dams in stages, especially when more than two stages are planned, is the opportunity to evaluate results between stages. If a sand dam is planned to be built in multiple stages, and the first stage captures predominately fine material during a normal series of storm events, community members and sand dam practitioners should be prepared to reduce the height of subsequent stages.

6.2 Recommended Further Research

While this report presents insights into sedimentation processes associated with sand dams, it also raises several new questions for further research. This section describes several areas of recommended study.

6.2.1 Larger sample sizes

Most sand dams will last several generations (or more), and replacement is costly and difficult. As such, the probability of success should be elevated to an acceptable level. While deterministic models appear useful for a dam's staging design when the channel is well-defined and reliable flow data are available, broad, programmatic decisions about the need to build sand dams in stages would be bolstered by a stronger statistical understanding of the uncertainties and risks of failure associated with certain regions, climates, designs etc.

Given the stochastic nature of the rainfall which drives the complex sedimentation processes at work in sand dams, developing such statistics will require much larger samples of successful and unsuccessful dams than the number of sites studied as part of this research. Based on an assumed population size of 5000 sand dams, a confidence level of 95% and a confidence interval of $\pm 5\%$ for some normally-distributed metric (such as, perhaps, the bulk median particle size), a sample of over 350 dams would be required. Care must be taken to avoid bias when selecting samples, and application of the results should be qualified by the sample's characteristics (e.g. if the sample is restricted to Kitui County, the results may not be applicable to dams in a different region). This type of sampling campaign could be coupled with a broader effort to record and categorize the location of sand dams throughout Kenya and other countries, to aid in regional water management.

6.2.2 Drainage options

Rainfall variability presents a major challenge when designing sand dams, and while quantifying uncertainties may help reduce the risk of small storms filling dams with fine sediment, another approach would be to include a drainage option in sand dam design. Using such an approach, communities could "reset" their dam if it fills with undesired

sediment. *Nilsson* [1988] recommends a flushing valve for dam cleaning, but it is unclear exactly what he has in mind, and how effective drainage options should be designed.

Successful drainage valves should induce scour and discharge trapped sediment quickly, without compromising a dam's structural integrity. One solution might be the use of clay brick inserts built into the dam wall at regular intervals, plastered on the upstream face, which could easily be chipped out and removed to leave openings in the dam wall. The result would be much like some sabo dams, which are used in Japan to capture and slowly

release sediment during and after debris flows (Figure 6.2). After the fine sediment in a sand dam has been successfully discharged, local artisans responsible for maintenance could replace the bricks and plaster the upstream face without further intervention by the NGO. To my knowledge, this approach has never been tried in sand dams, and it may hold some potential for draining silted structures.



Figure 6.3: Sabo dam. *Sand dams might employ drainage outlets like those of this sabo dam, constructed near Toyama, Japan (Shitaka.net)*

6.2.3 Dam rehabilitation

Assuming that half of all existing sand dams suffer from poor performance due to the trapping of fine sediment, thousands of structures might benefit from some form of rehabilitation, possibly at a fraction of the cost of building new dams. Given that most fine material is generally located near the bottom of sand dam reservoirs, effective rehabilitation strategies must penetrate the entire depth of the bed.

One such strategy might be a complete fluidization and mixing of the sand dam storage volume. For sand filters used for water treatment, this type of mixing action is accomplished through backwashing. Water is pumped upwards from the bottom of the

filter, liquefying the entire bed, and the coarsest, heaviest particles settle first, followed by the finer material. After a sand dam has finished filling with sediment, it may be possible to use a motorized pump during low flow events to systematically liquefy sections of the bed in this way, lifting silts and other fine particles to the surface where they can be entrained by surface flow. By reversing the gradation trend and depositing the coarsest material at the bottom of the aquifer, communities could potentially increase the volume of water which will drain from the sediment pores due to gravity (Figure 2.7).

Another, more invasive strategy for dam rehabilitation might entail cutting out a large notch to the base of a silted dam, allowing subsequent flows to scour the deposited material, and rebuilding the dam slowly, in stages. This strategy would probably be best suited to dams filled predominately with fine sediment, and given the relatively large economic and social costs associated with cutting out a new spillway and rebuilding the dam, it may or may not be cost-effective. However, by facilitating a direct comparison of the results of staged vs. unstaged construction for a given site, the method might provide additional validation of the benefits of staging.

6.2.4 Dams built in series

When a hydraulic structure traps sediment, even for a relatively short period of time, the disruption to the stream's dynamic equilibrium (as represented by Lane's Balance, Eq. 1) often results in downstream sediment deficit and scour. Sand dams are frequently built in series on the same rivers, and it seems likely that construction of a new sand dam could limit the supply of coarse particles to partially-filled downstream dams and possibly affect the sediment already deposited in other structures. Future research could address the interconnected sedimentation processes within networks of sand dams and propose strategies for improving sediment quality by controlling the timing and location of each dam's construction, perhaps through integrated regional planning.

6.2.5 Bank management

Bank management likely influences sand dam sedimentation in many ways. In particular, banks appear to supply much of the sediment ultimately deposited in dams [Gijsbertsen,

2007], and bank characteristics affect runoff ratios and the availability of river baseflow. Many Kenyan communities terrace the banks upstream of newly-constructed sand dams, hoping to increase infiltration and trap fine sediments during small storm events. The cumulative effects of terracing and other land practices on sand dam sedimentation are not well documented, however, and should be further studied.

6.2.6 Flow measurement

As described in Section 2.2.1, sand dams are built on seasonal and ephemeral rivers which are rarely gauged. However, a structure's spillway provides a fixed cross-section in an otherwise dynamic channel, and sand dams may offer potential as flow measurement devices useful to scientists, engineers and regional water managers. Future research could evaluate the effects of sediment deposition and spillway shape on stage-discharge relationships, and establish methods for integrating low-cost, robust sensors with sand dam design or crowd-sourcing data based on stage markings and submitted via text messages.

Chapter 7. Conclusion

Sand dams represent a viable rainwater harvesting and storage solution for many rural communities, but they are not universally appropriate. Performance varies widely, with reported failure rates in the range of 50%. This study supports the field observation that staged sedimentation would be expected to reduce the failure rate. Sand dam design should seek to balance costs and benefits, including risk of failure, and for many sites, this balance will include the use of spillway staging.

The application of staged dam design requires the understanding and participation of all stakeholders. Funding organizations need to understand that the long-term benefits provided by a successful sand dam may require many years to develop, and so flexible funding options—possibly including general funding for annual stage additions or funding which spans multiple project cycles—should be made available to sand dam-building NGOs. Sand dam practitioners need to either develop new strategies for project planning, monitoring and evaluation which incorporate multi-year staging campaigns, or develop stricter guidelines for the sites deemed appropriate for sand dams. Community members need to better understand the sedimentation processes associated with their sand dams, including the risks of building dams in too few stages, and must be willing to commit to multi-year construction phases despite potentially-limited initial results. Researchers can continue to contribute to increasing success rates by helping to better quantify uncertainty and risks, studying inter-dam and bank management influences on sedimentation, and evaluating options for sand dam rehabilitation.

Despite the challenges, I believe sand dam practitioners can continue to improve the performance of the structures they design. I hope the principles outlined in this report will prove useful towards that aim, and ultimately towards improving the livelihoods of rural communities throughout the world's drylands.

Bibliography

Aerts, J., R. Lasage, W. Beets, H. de Moel, G. Mutiso, S. Mutiso and A. de Vries (2007), Robustness of Sand Storage Dams under Climate Change, *Vadose Zone J.*, 6, 572-580, doi:10.2136/vzj2006.0097.

Al-Shemmeri, T. (2012), *Engineering Fluid Mechanics*, Ventus Publishing ApS, Amsterdam, the Netherlands.

Alexandrov, Y., J. B. Laronne and I. Reid (2003), Suspended sediment concentration and its variation with water discharge in a dryland ephemeral channel, northern Negev, Israel, *J. Arid Environ.*, 53, 73–84, doi:10.1006/jare.2002.1020.

Arnold, E., C. A. van den Dool and J. F. Joosse (2002), Retaining water in the Black Cotton Soil Area near Ikanga, Kenya, a study carried out by SaSol, Final report, 41 p., Delft University of Technology, the Netherlands.

ASTM Committee E-29 on Particle Size Measurement and American Society for Testing and Materials (1985), *Manual on test sieving methods*, American Society for Testing and Materials, Philadelphia, Pa.

Beimers, P. B., A. J. van Eick, K. S. Lam and B. Roos (2001), Improved design sand-storage dams, Kitui District, Kenya, Project report, 125 p., Delft University of Technology, the Netherlands.

Borst, L. and S. A. de Haas (2006), Hydrology of sand storage dams: A case study in the Kiindu catchment, Kitui District, Kenya, M.Sc. thesis, 146 pp., Vrije Universiteit, Amsterdam, the Netherlands, 1 Feb.

Bossenbroek J. and T. Timmermans (2003), Setting up a measuring program at Kisayani, to measure the effected area by sand storage dams, Traineeship Report, 87 p., Delft University of Technology, the Netherlands.

Burger, A. S., W. Malda, H. C. Winsemius (2003), Research to Sand-storage dams in Kitui district, 94 p. Delft University of Technology, the Netherlands.

Burger, S. W. and R. D. Beaumont (1970), Sand Storage Dams for Water Conservation, Convention: Water for the Future, Water Year 1970, Pretoria, Republic of South Africa.

Castro-Orgaz, O., J. V. Giráldez, L. Mateos and S. Dey (2012), Is the von Kármán constant affected by sediment suspension?, *J. Geophys. Res.*, 117, F04002, doi:10.1029/2011JF002211.

Chanson, H. (2004), *Hydraulics of open channel flow*, Butterworth-Heinemann, Oxford, England.

Chow, V. T. (1959), *Open Channel Hydraulics*, McGraw-Hill Book Company, Inc., New York.

Edwards, K. A., G. A. Classen and E. H. J. Schrotten (1983), *The Water Resource in Tropical Africa and Its Exploitation*, International Livestock Centre for Africa, Addis Ababa, Ethiopia.

- Engelund, F. and E. Hansen (1967), *A monograph on sediment transport in alluvial streams*, Teknisk Forlag, Copenhagen, Denmark.
- Ertsen, M.W., B. Biesbrouck, L. Postma, M. van Westerop (2005). Participatory design of sand storage dams, in *Coalitions and Collisions*, edited by T. Goessling, R.J.G. Jansen and L.A.G. Oerlemans, pp. 175–185, Wolf Publishers, Nijmegen, the Netherlands.
- Ertsen, M. and R. Hut (2009), Two waterfalls do not hear each other: Sand-storage dams, science and sustainable development in Kenya, *Phys. Chem. Earth Pt A/B/C*, 34, 14–22, doi:10.1016/j.pce.2008.03.009
- Food and Agriculture Organization of the United Nations (2012), Multipurpose Landcover Database for Kenya - AFRICOVER (GeoLayer), FAO GeoNetwork. Rome, Italy.
- Forzieri G., M. Gardenti, F. Caparrini and F. Castelli (2008), A methodology for the pre-selection of suitable sites for surface and underground small dams in arid areas: A case study in the region of Kidal, Mali, *Phys. Chem. Earth Pt A/B/C*, 33, 74–85, doi:10.1016/j.pce.2007.04.014.
- Frima, G. A. J., M. A. Huijsmans, N. van der Sluijs and T. E. Wiersma (2002), A research on the possibilities to construct sand-storage dams on black cotton soil, Kitui District, Project report, 121 p., Delft University of Technology, the Netherlands.
- Gaudio, R., A. Miglio and S. Dey (2010), Non-universality of von Kármán's κ in fluvial streams. *J. Hydraul. Res.*, 48, 658–663, doi:10.1080/00221686.2010.507338.
- Gee, G.W. and J. W. Bauder (1986), Particle Size Analysis, in *Methods of Soil Analysis, Part 1, Physical and Mineralogical Methods, Agronomy Monograph No 9*, 2nd ed., edited by A. Klute, pp. 383-411, American Society of Agronomy, Madison, Wisconsin.
- Gijsbertsen, C. (2007), A study to upscaling of the principle and sediment transport processes behind sand storage dams, Kitui District, Kenya, M.Sc. thesis, 146 pp., Vrije Universiteit, Amsterdam, the Netherlands, August.
- Grant, G. E. (1997), Critical flow constrains flow hydraulics in mobile-bed streams: A new hypothesis, *Water Resour. Res.*, 33, 349-358, doi:10.1029/96WR03134.
- Heath, R. C. (1987), *Basic ground-water hydrology (4th ed.)*, U.S. Geol. Surv. Water-Supply Paper 2220, United States Geological Survey, Alexandria, Virginia.
- Hellwig, D. H. R. (1973), Evaporation of water from sand, 3: The loss of water into the atmosphere from a sandy river bed under arid climatic conditions, *J. of Hydrology*, 18, 305–316, doi:10.1016/0022-1694(73)90054-1.
- Hellwig, D. H. R. (1973), Evaporation of water from sand, 4: The influence of the depth of the water-table and the particle size distribution of the sand, *J. of Hydrology*, 18, 317–327, doi:10.1016/0022-1694(73)90054-1.
- Hofkes, E. H. and J. T. Visscher (1986), Artificial Groundwater Recharge for Water Supply of Medium-Size Communities in Developing Countries, International Reference Centre for Community Water Supply and Sanitation, The Hague, the Netherlands.

Hoogmoed, M. (2007), Analyses of impacts of a sand storage dam on groundwater flow and storage. Groundwater flow modelling in Kitui District, Kenya, M.Sc. thesis, Vrije Universiteit, Amsterdam, the Netherlands.

Hudson, N. (1971), *Soil Conservation*, Cornell University Press, Ithaca, New York.

Hussey, S.W. (1997), Small-scale sand abstraction systems, paper presented at 23rd WEDC Conference Water and Sanitation for All, WEDC, Durban, Republic of South Africa.

Hut, R., M. Ertsen, N. Joeman, N. Vergeer, H. Winsemius and N. van de Giesen (2008), Effects of sand storage dams on groundwater levels with examples from Kenya, *Phys. Chem. Earth Pt A/B/C*, 33, 56–66, doi:10.1016/j.pce.2007.04.006.

Jansen, J. (2007), The influence of sand dams on rainfall-runoff response and water availability in the semi-arid Kiindu catchment, Kitui District, Kenya, M.Sc. Thesis, Vrije Universeit, Amsterdam, the Netherlands, 1 Jul.

Kinnell, P. I. A (2000), The Effect of Slope Length on Sediment Concentrations Associated with Side-Slope Erosion, *Soil Sci. Soc. Am. J.*, 64, 1004-1008, doi:10.2136/sssaj2000.6431004x.

Lane, E. W. (1955), The importance of fluvial morphology in hydraulic engineering, *P. Am. Soc. Civ. Eng.*, 81, 1-17.

Lasage, R., J. Aerts, G.-C. M. Mutiso and A. de Vries (2008), Potential for community based adaptation to droughts: Sand dams in Kitui, Kenya, *Phys. Chem. Earth Pt A/B/C*, 33, 67–73, doi:10.1016/j.pce.2007.04.009.

Maddrell, S. and Neal, I. (2012), *Sand Dams: a Practical Guide*, Excellent Development, London, England.

Mansell, M. G. and S. W. Hussey (2005), An investigation of flows and losses within the alluvial sands of ephemeral rivers in Zimbabwe. *J. Hydrol.*, 314, 192–203, doi:10.1016/j.jhydrol.2005.03.015.

Mao, L. (2012), The effect of hydrographs on bed load transport and bed sediment spatial arrangement, *J. Geophys. Res.*, 117, F03024, doi:10.1029/2012JF002428.

Marks, S. J., K. Onda and J. Davis (2013), Does sense of ownership matter for rural water system sustainability? Evidence from Kenya. *J. Water. Sanit. Hyg. Dev.*, 3, 122-133, doi:10.2166/washdev.2013.098.

Mays, L. W. (2011), *Water Resources Engineering*, John Wiley & Sons, Inc., Hoboken, New Jersey.

McCutcheon, S.C., J.L Martin and T.O. Barnwell, Jr. (1993), Water quality, in *Handbook of Hydrology*, edited by D.R. Maidment, Chapter 11, McGraw-Hill, New York, New York.

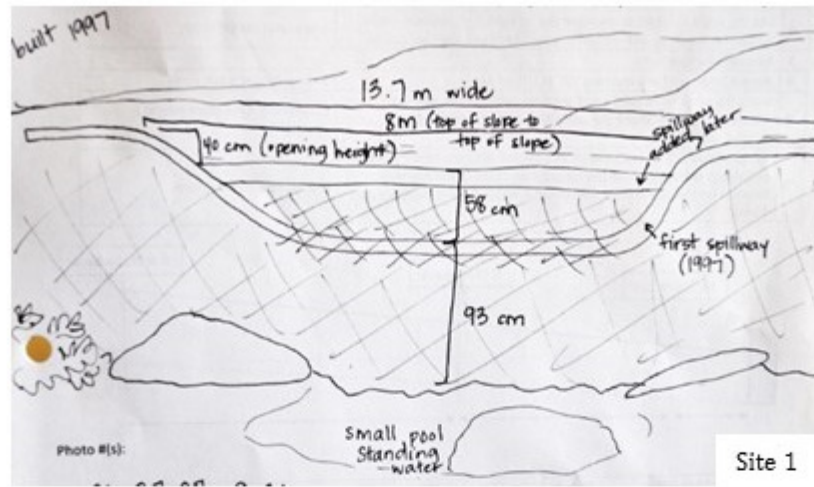
Moore, T. R. (1979), Rainfall Erosivity in East Africa. *Geogr. Ann. A*, 61, 147–156, doi:10.2307/520909.

- Morris, G. L. and J. Fan (1998). *Reservoir sedimentation handbook: design and management of dams, reservoirs, and watersheds for sustainable use*, McGraw-Hill Book Co., New York, New York.
- National Academy of Sciences (1974), *More Water for Arid Lands: Promising Technologies and Research Opportunities*, Washington D.C.
- Negev, M. (1969), *Analysis of data on suspended sediment discharge in several streams in Israel*, Hydrological Paper No. 12, Israel Hydrological Service, Jerusalem, Israel.
- Nilsson, A. (1988), *Groundwater Dams for Small-Scale Water Supply*, Intermediate Technology Publications, London, England.
- Nimmo, J. (2004), Porosity and pore size distribution, in *Encyclopedia of Soils in the Environment*, edited by D. Hillel, 295–303, Elsevier, London, England.
- Nissen-Petersen, E. (2006), *Water from Dry Riverbeds*, ASAL Consultants Ltd. for the Danish International Development Agency, Nairobi, Kenya.
- Powell, D.M., I. Reid, J.B. Laronne and L.E. Frostick (1996), Bedload as a component of sediment yield from a semiarid watershed of the northern Negev, in *Erosion and Sediment Yield: Global and Regional Perspectives*, edited by D.E Walling and B. Webb, 389–397 *International Association of Hydrological Sciences Publication No. 236*.
- Quilis, R. O., M. Hoogmoed, M. Ertsen, J. W. Foppen, R. Hut and A. de Vries (2009), Measuring and modeling hydrological processes of sand-storage dams on different spatial scales, *Phys. Chem. Earth Pt A/B/C*, 34, 289–298, doi:10.1016/j.pce.2008.06.057.
- R Core Team (2015), *R: A language and environment for statistical computing*. R Foundation for Statistical Computing, Vienna, Austria.
- RAIN Foundation (2008), *A practical guide to sand dam implementation: Water supply through local structures as adaptation to climate change*, Rainwater Harvesting Implementation Network, Amsterdam, the Netherlands.
- Rodier, J.A. (1994), *General characteristics of surface hydrology in arid and semi-arid areas of Africa and their consequences for development*, ORSTOM, Paris, France.
- Reid, I. and L. E. Frostick (1987), Flow dynamics and suspended sediment properties in arid zone flash floods, *Hydrol. Process.*, 1, 239–253, doi:10.1002/hyp.3360010303.
- Salem, B. B. (1989), *Arid zone forestry: a guide for field technicians*, Food and Agricultural Organization of the United Nations, Rome, Italy.
- The County Government of Kitui (2015), *Welcome: Facts About Kitui*, Kitui, Kenya.
- Todd, D. K. (1964), Groundwater, in *Handbook of applied hydrology*, edited by V. T. Chow, pp. 13-8, 13-9, 13-10, McGraw-Hill, New York, New York.
- USGS (2004), Shuttle Radar Topography Mission, 1 Arc Second scene SRTM_u03_n008e004, Unfilled Unfinished 2.0, Global Land Cover Facility, University of Maryland, College Park, Maryland, February 2000.

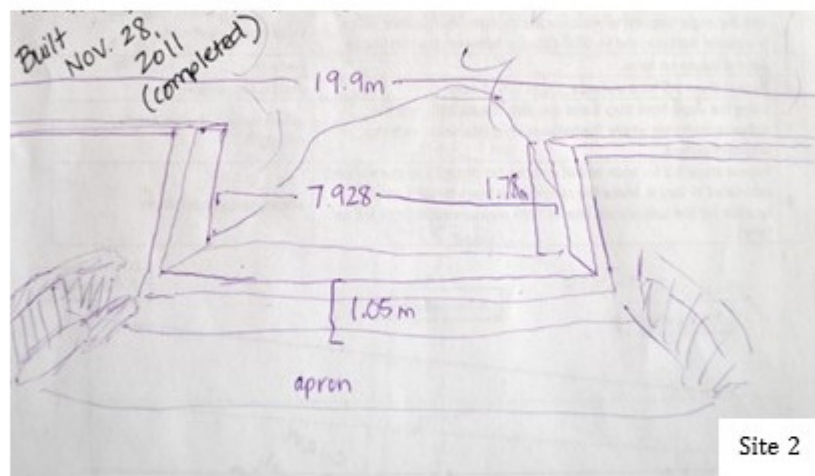
- USGS (2013), *SLC-off Products: Background*, Landsat Missions, January 2013.
- Van Haveren, B. P. (2004), Dependable Water Supplies from Valley Alluvium in Arid Regions, *Environ Monit Assess*, 99, 259–266, doi:10.1007/s10661-004-4031-5.
- Vanoni, V. (2006), *Sedimentation Engineering*, ASCE Manuals and Reports on Engineering Practice No. 54, American Society of Civil Engineers, Reston, Virginia.
- Voytenko, D. (2011), Modeling Direct Runoff Hydrographs with the Surge Function, M.S. Thesis, University of South Florida, Florida, 17 May.
- Wipplinger, O. (1953), The storage of water in sand: An investigation of the properties of natural and artificial sand reservoirs and of methods of developing such reservoirs, D. Sc. Thesis, Stellenbosch University, Stellenbosch, Republic of South Africa.
- Wipplinger, O. (1958), *Storage of Water in Sand*, South West Africa Administration, Water Affairs Branch, Windhoek, Namibia.
- Wu, L. (1987), Relationship between pore size, particle size, aggregate size and water characteristics, M.S. Thesis, Oregon State University, Corvallis, Oregon.

APPENDICES

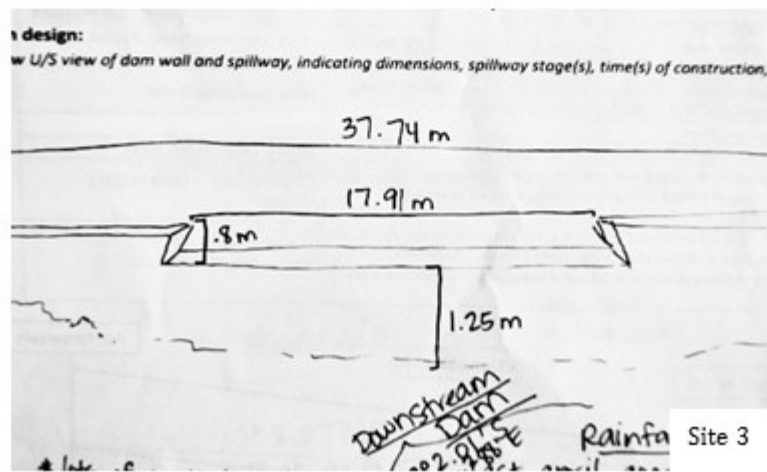
Appendix 1: Site drawings



Site 1

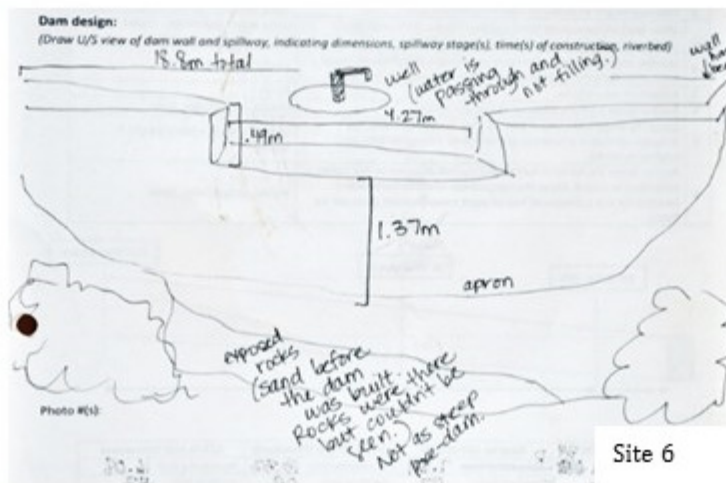
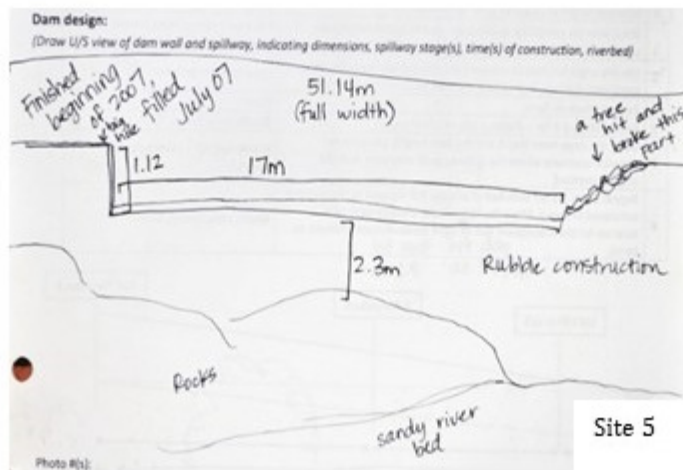
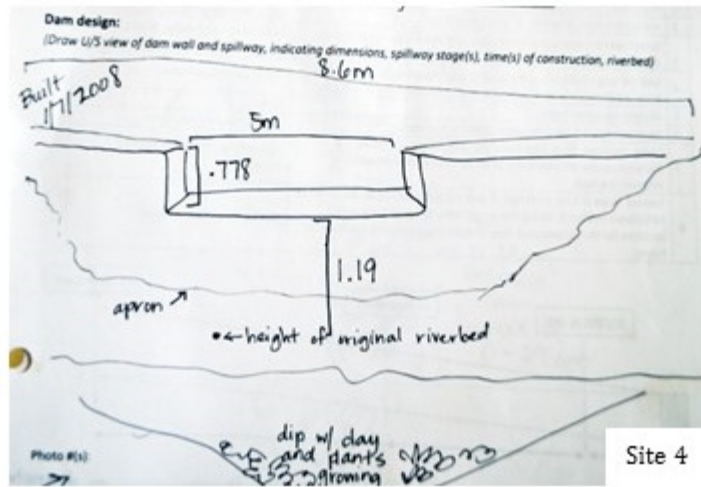


Site 2

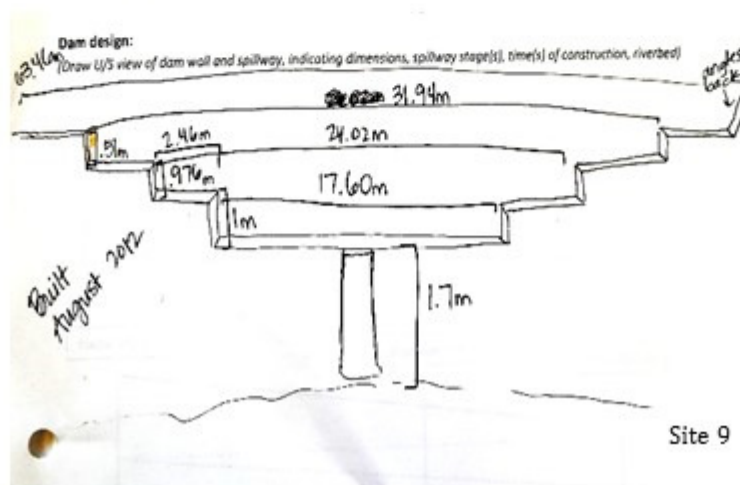
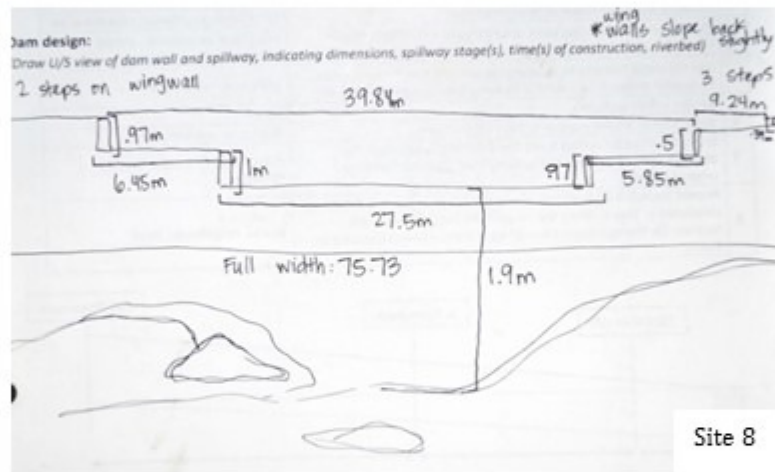
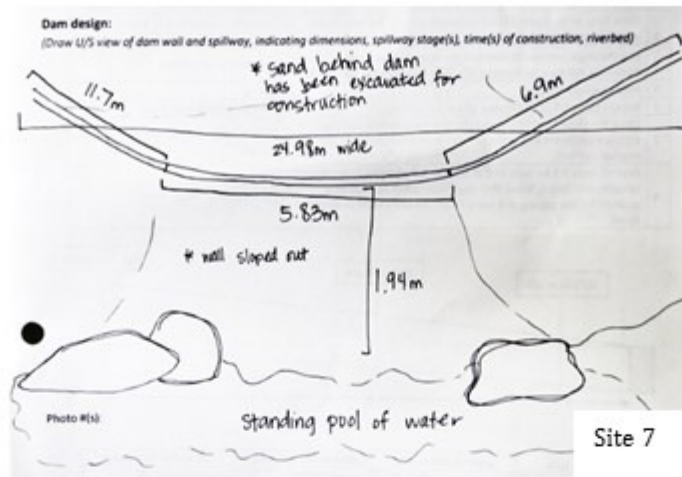


Site 3

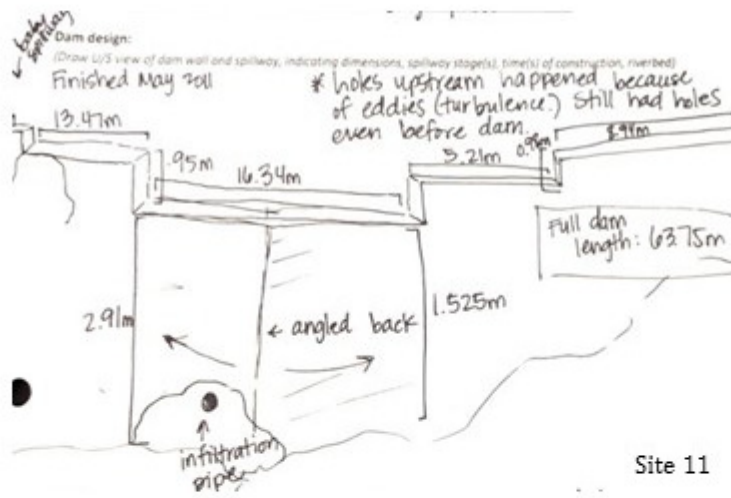
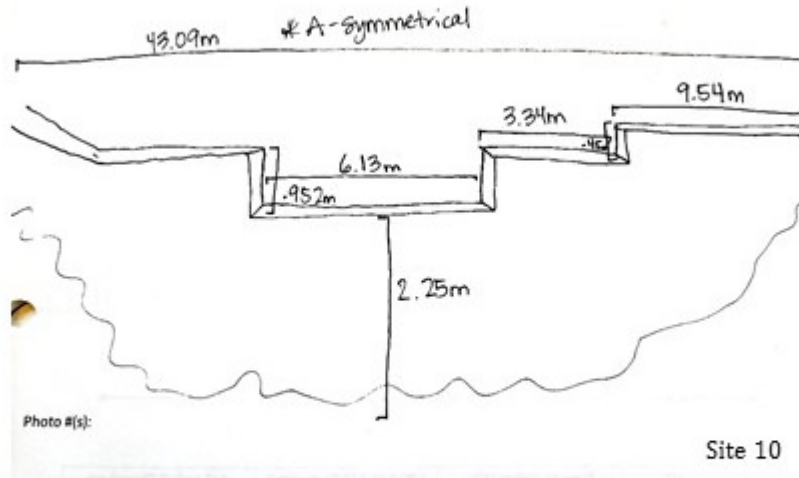
Appendix 1 (Continued): Site drawings



Appendix 1 (Continued): Site drawings



Appendix 1 (Continued): Site drawings



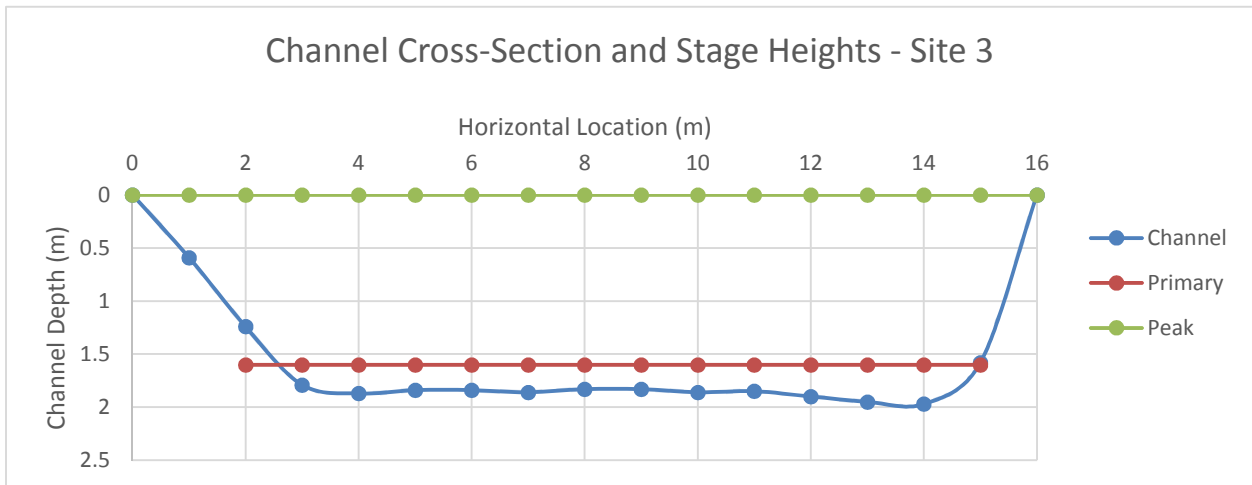
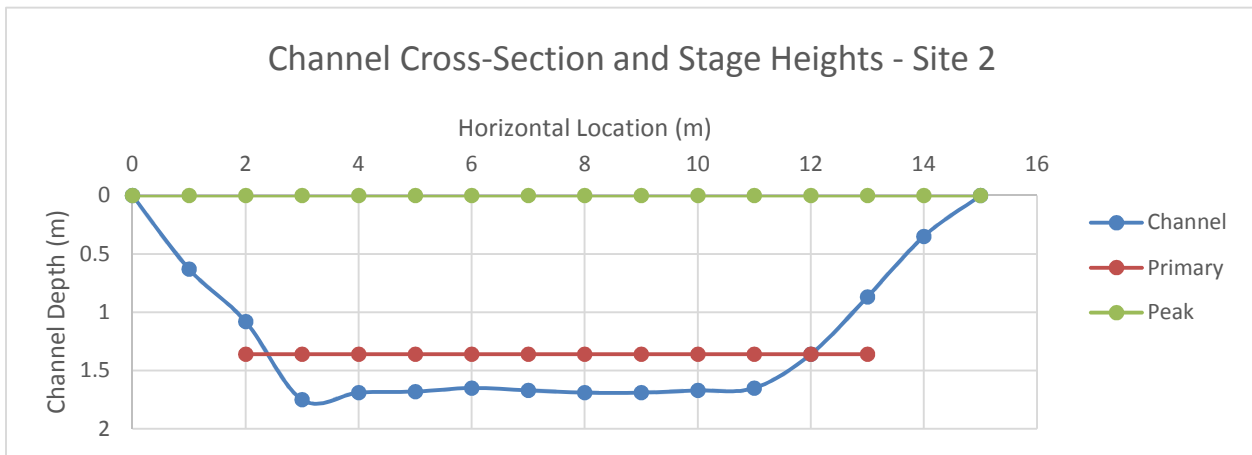
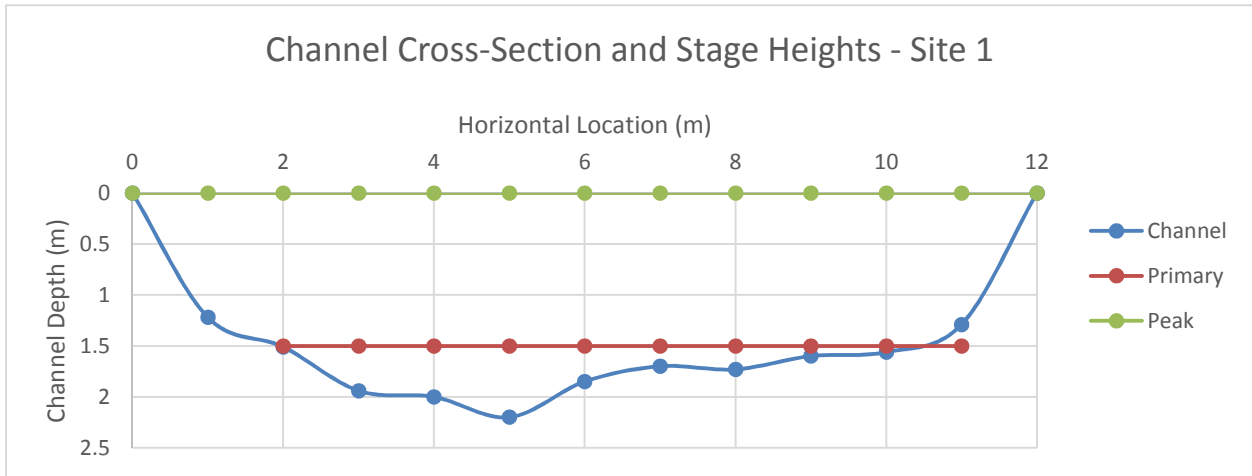
Appendix 2: Site photos



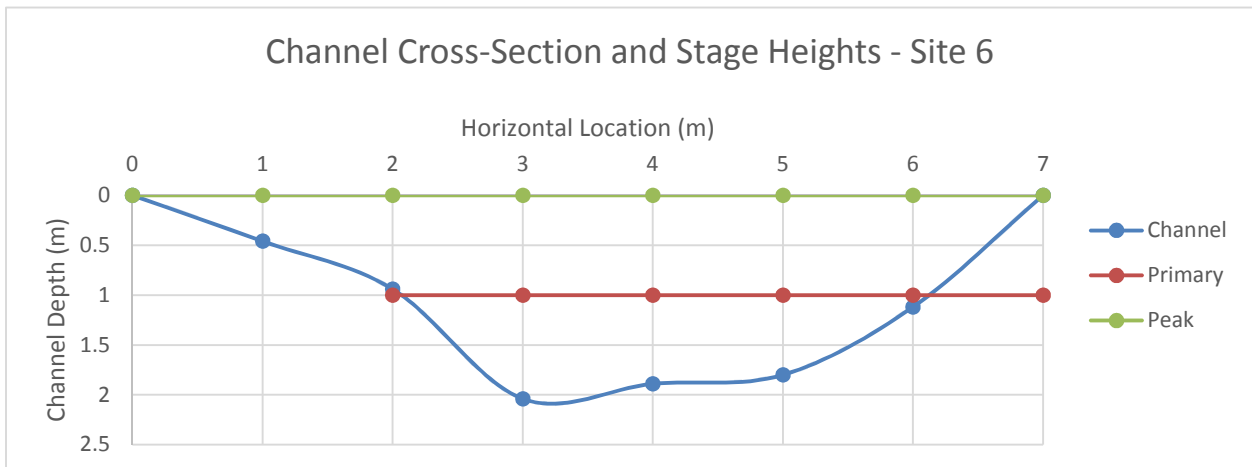
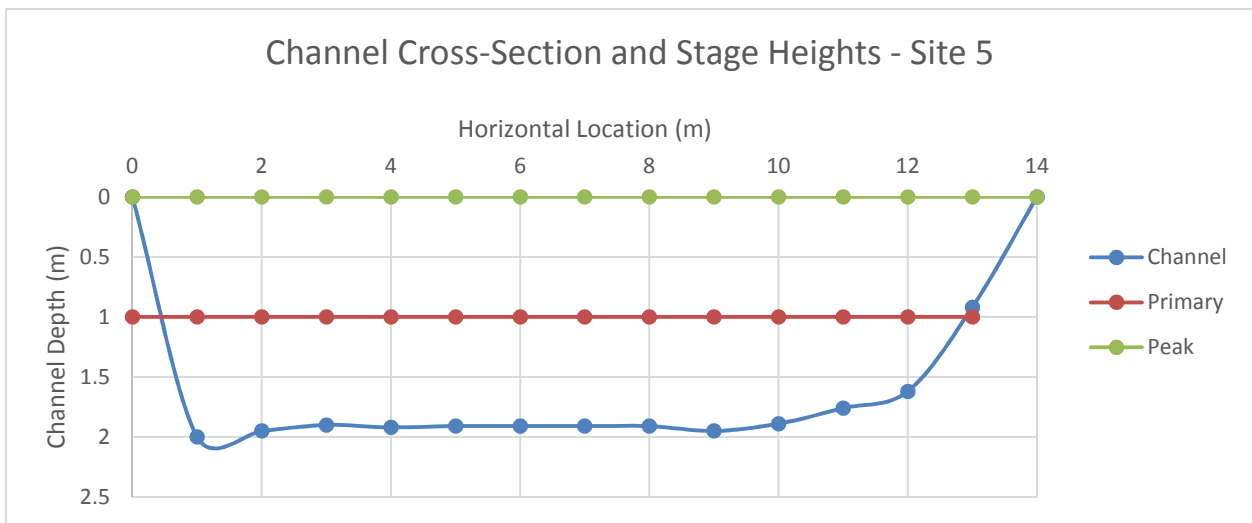
Appendix 2 (Continued): Site photos



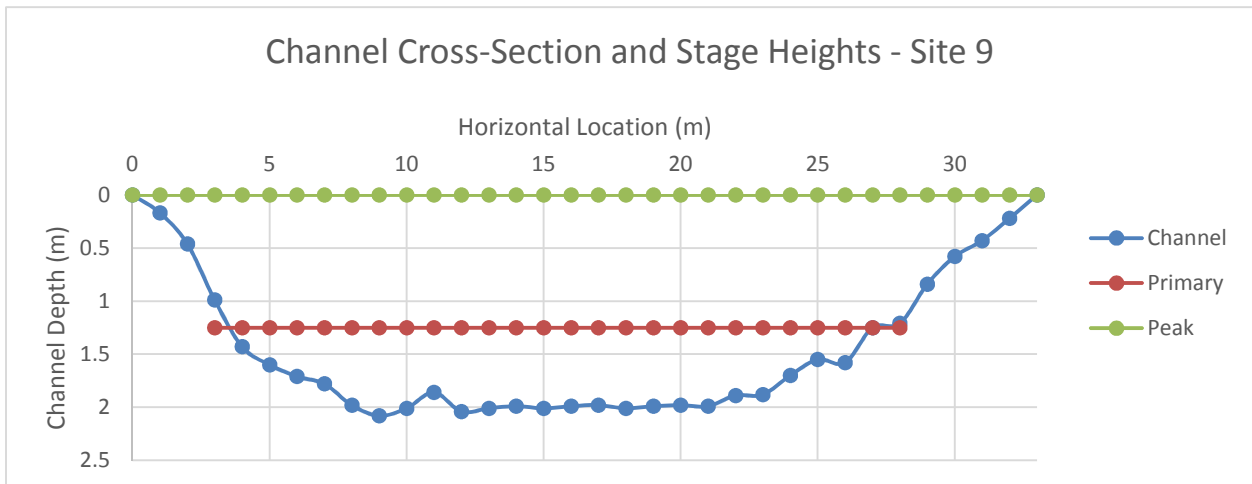
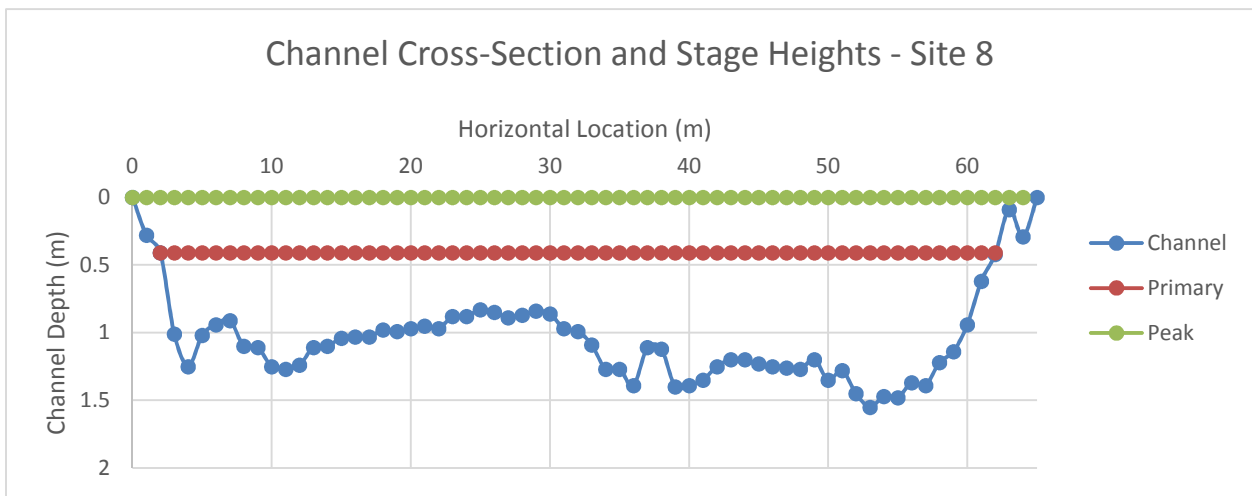
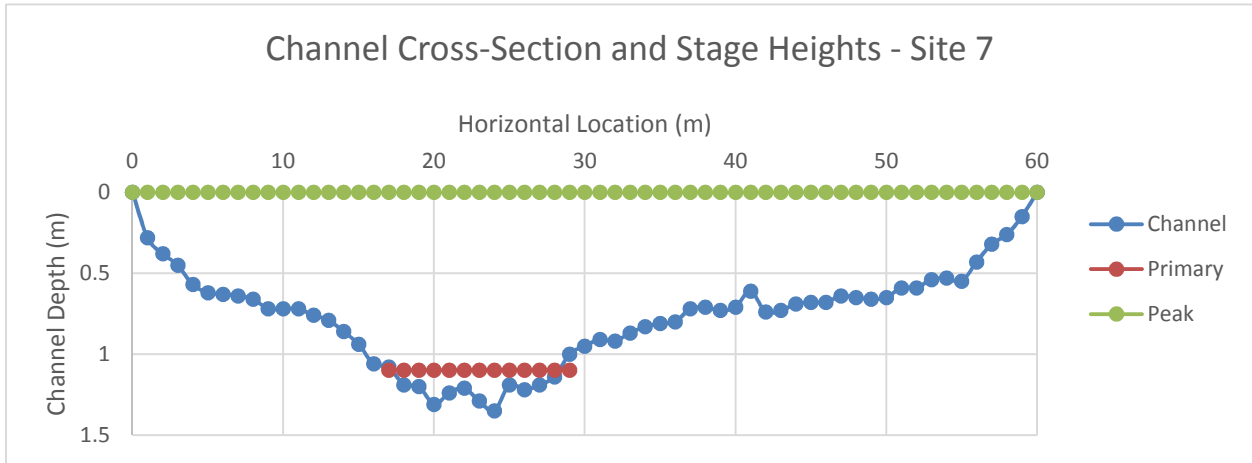
Appendix 3: Channel cross-section and stage profiles



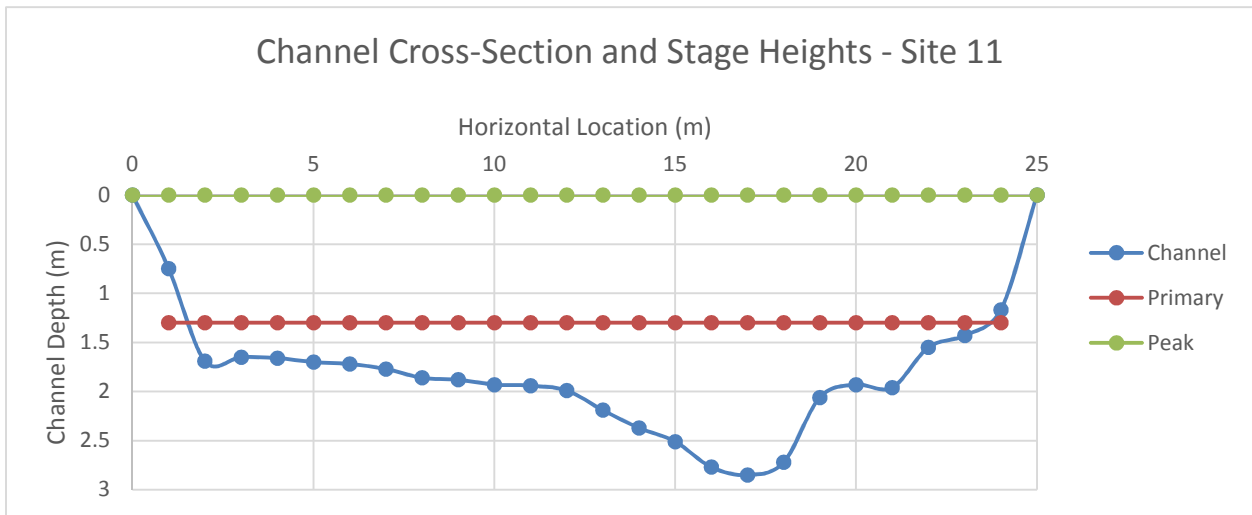
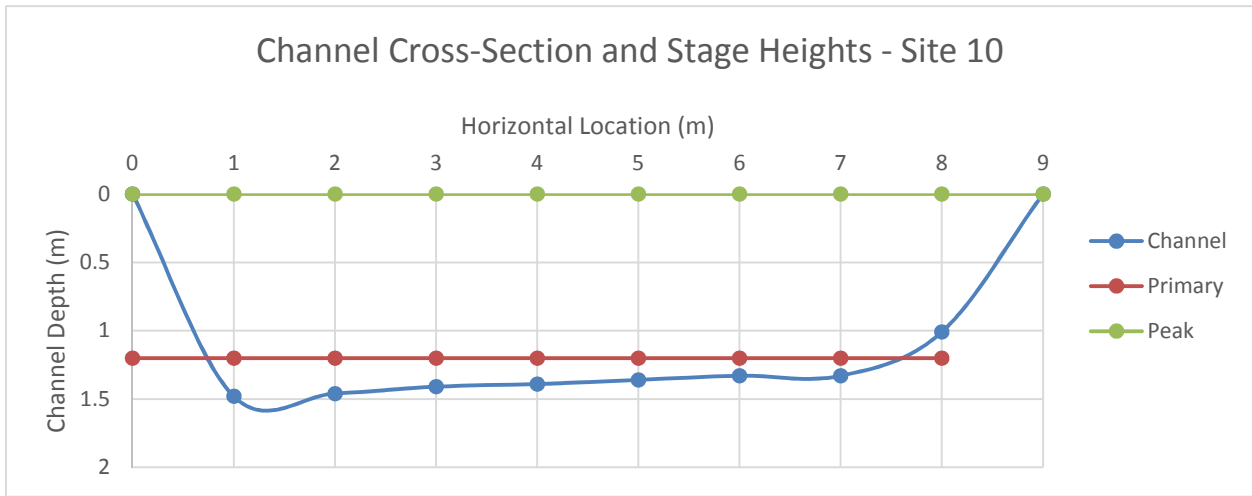
Appendix 3 (Continued): Channel cross-section and stage profiles



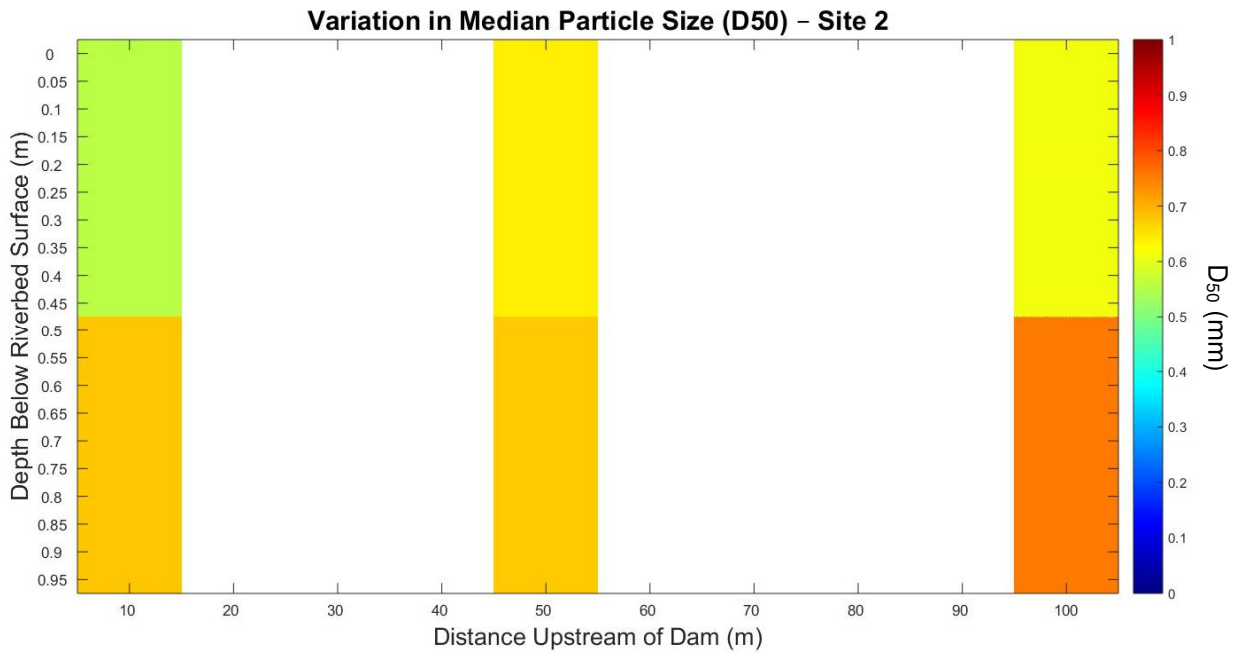
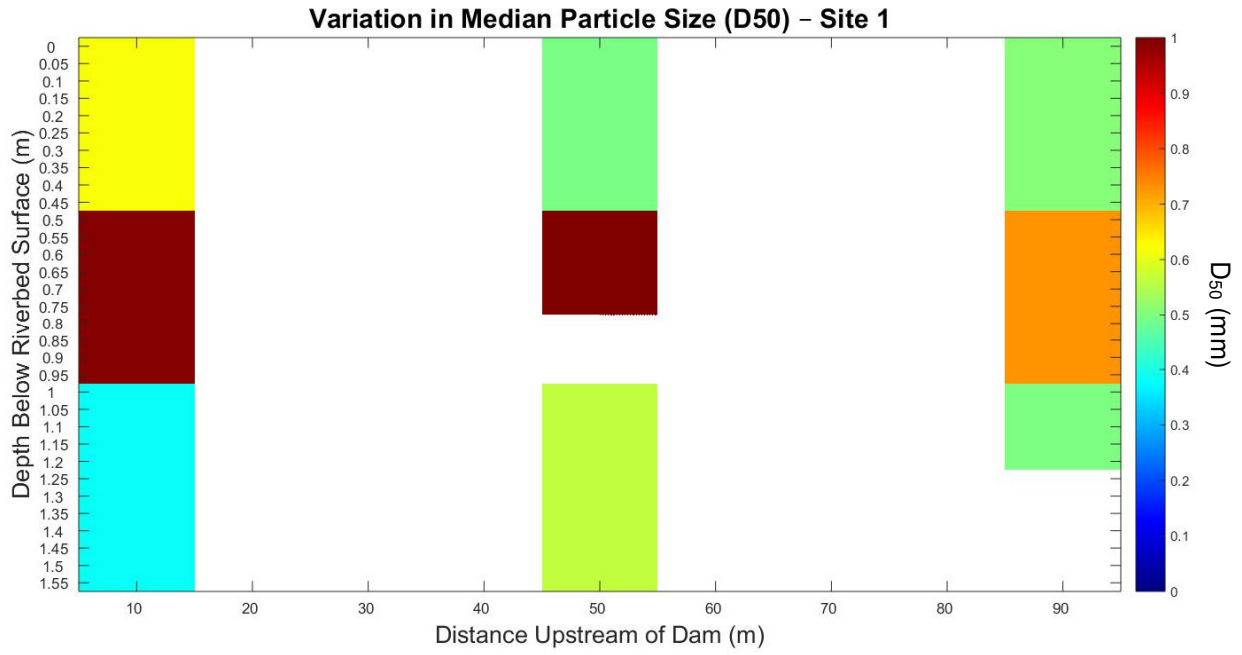
Appendix 3 (Continued): Channel cross-section and stage profiles



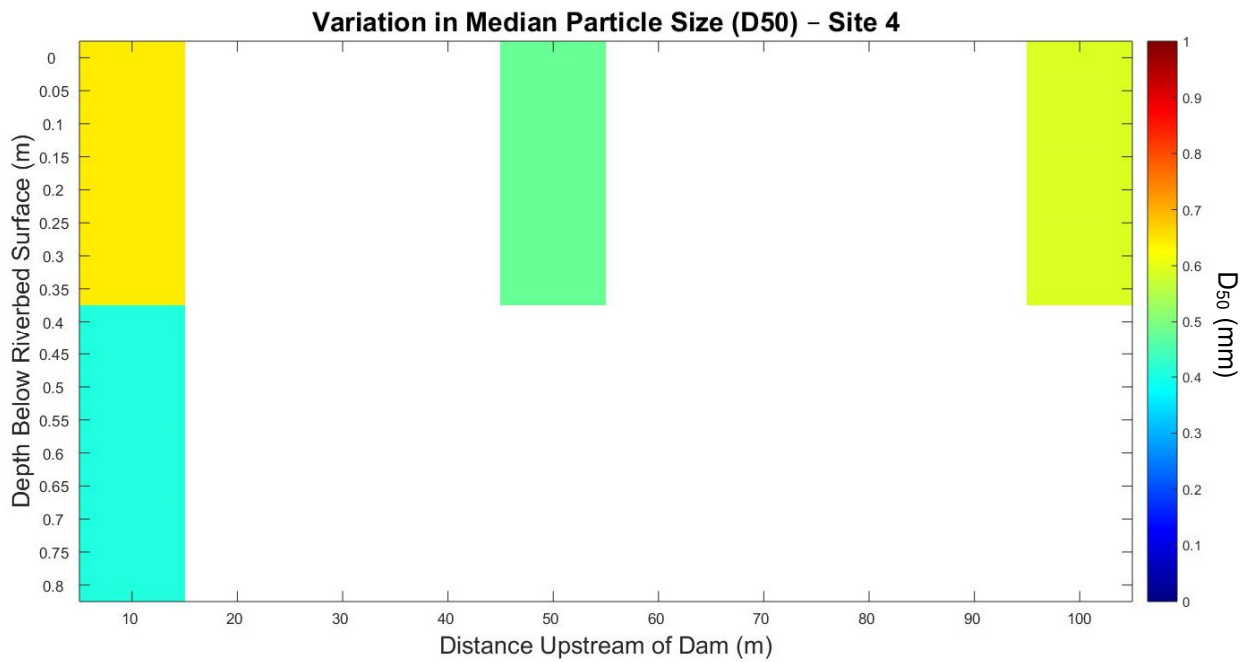
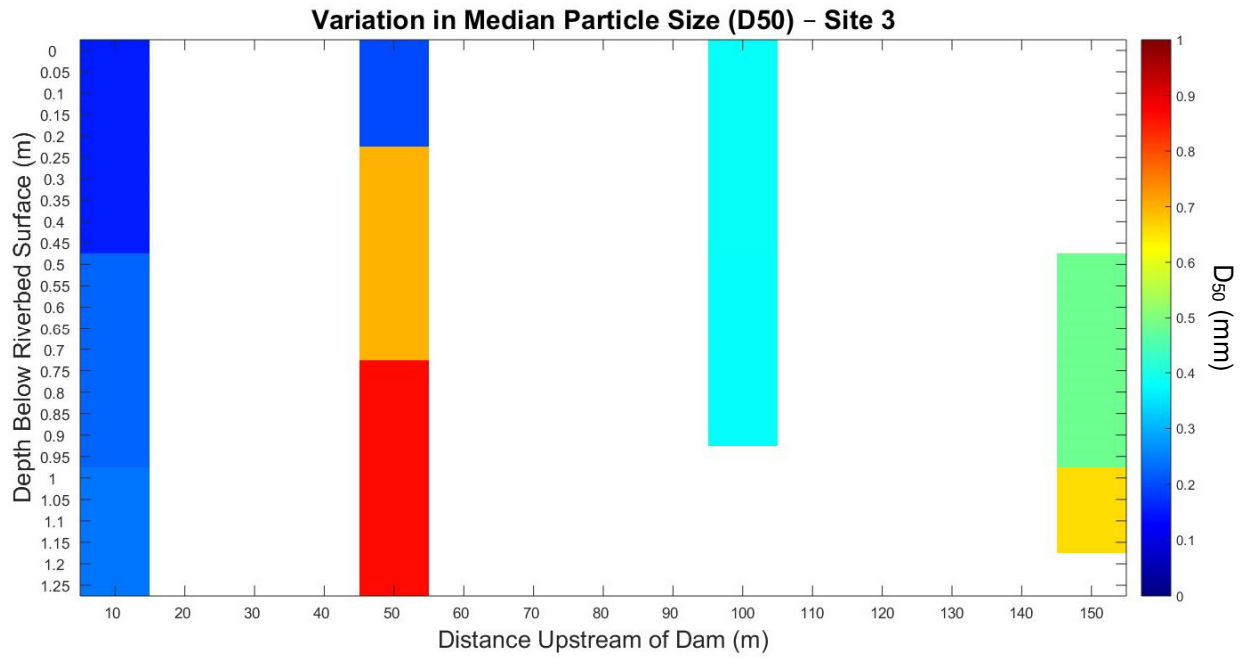
Appendix 3 (Continued): Channel cross-section and stage profiles



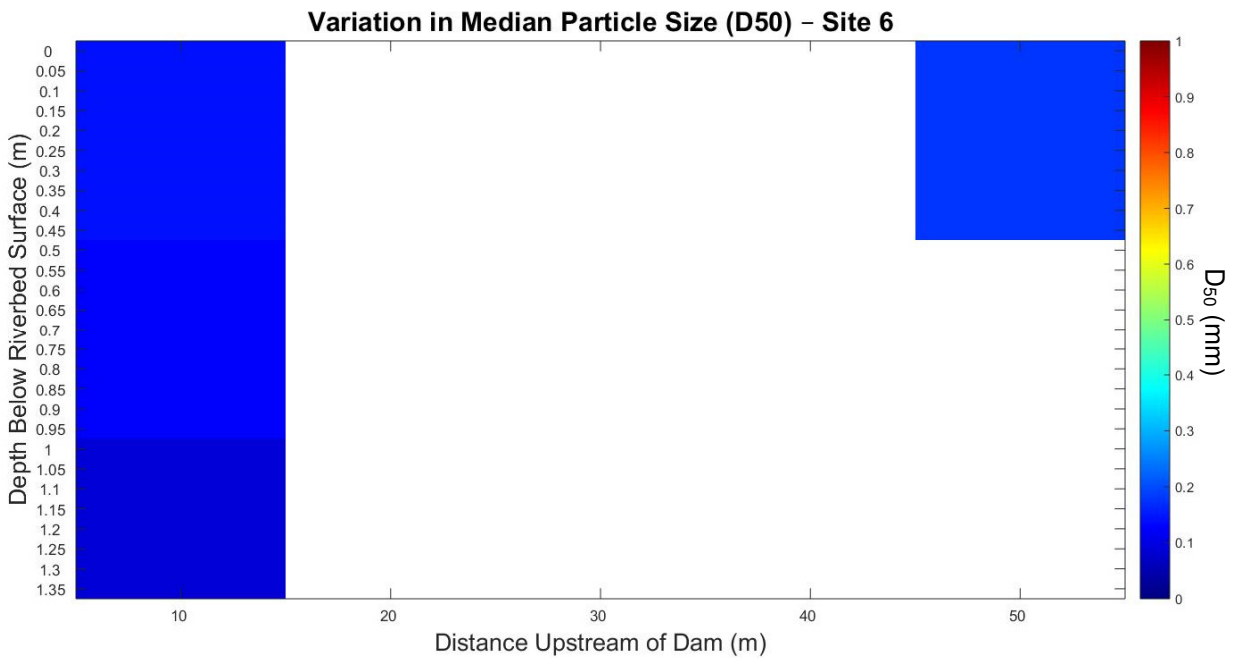
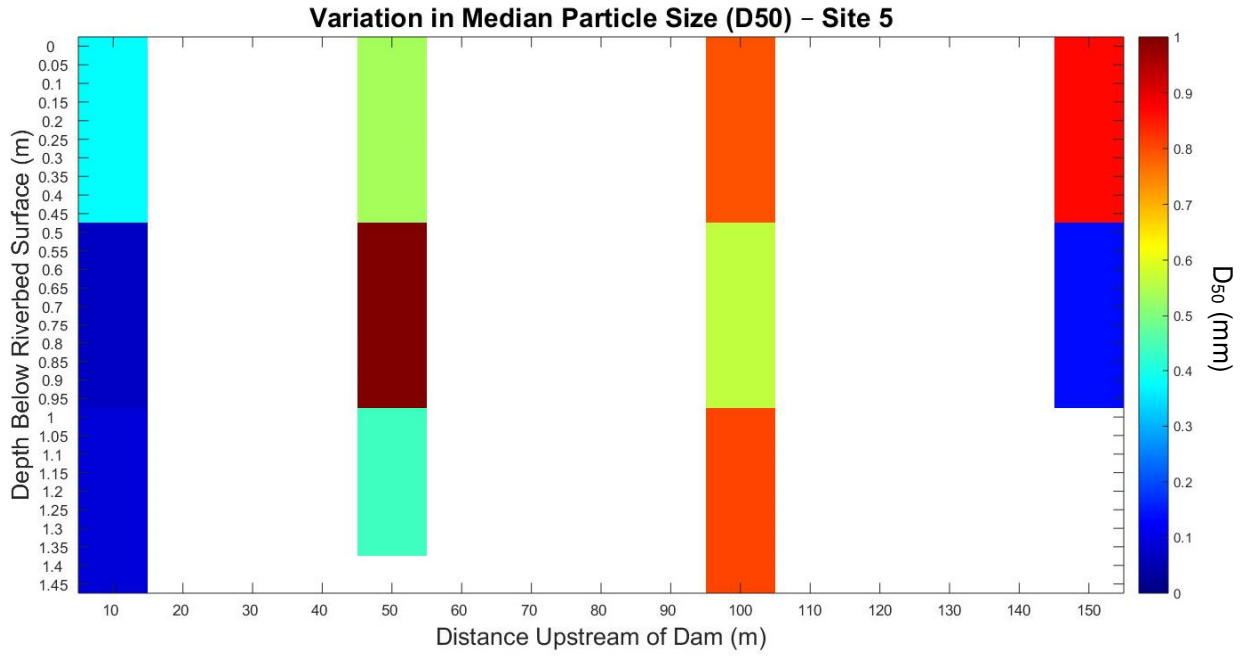
Appendix 4: Variation in median particle size by location and depth



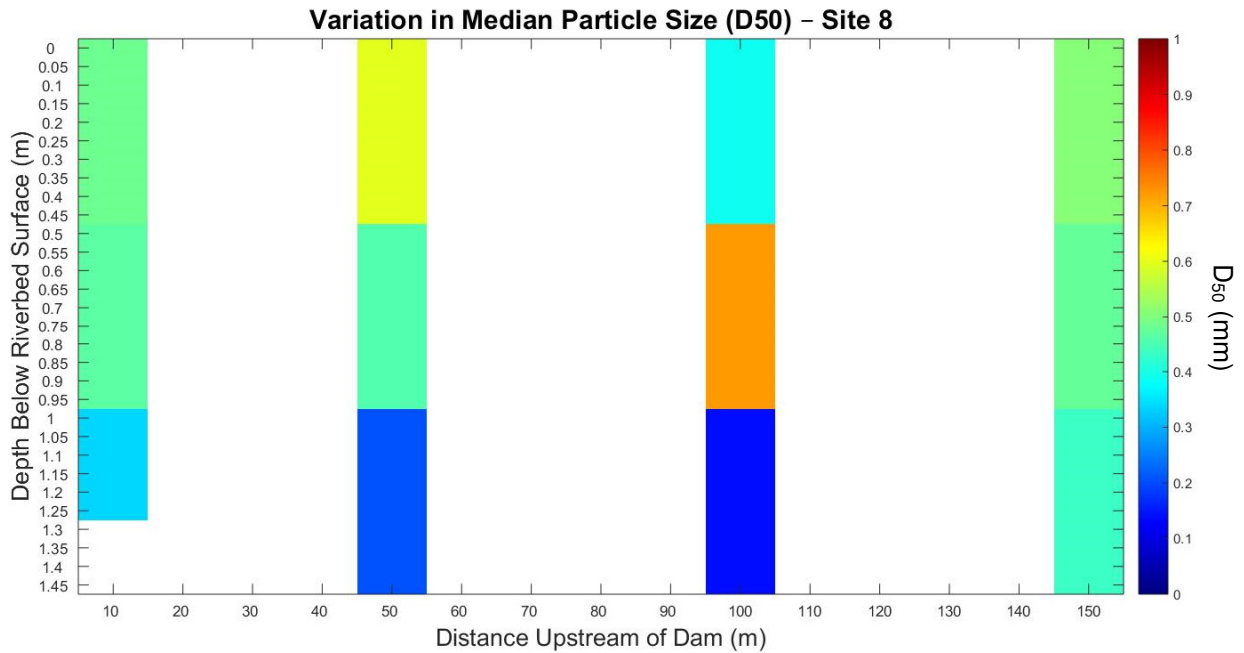
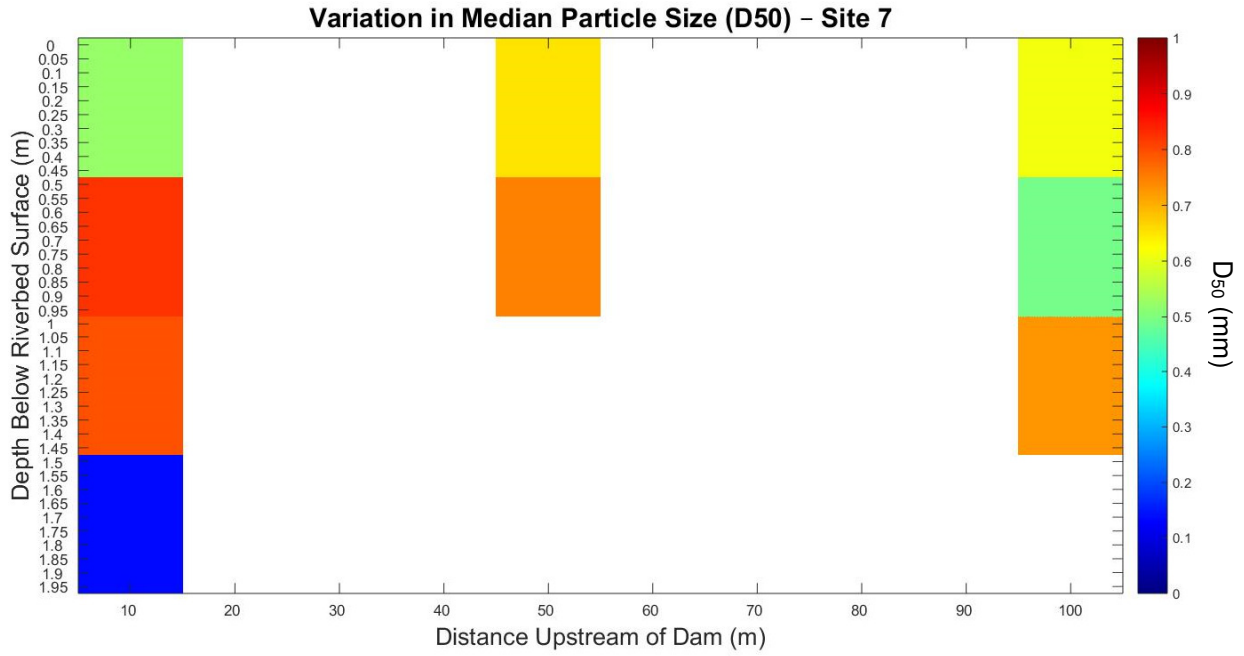
Appendix 4 (Continued): Variation in median particle size by location and depth



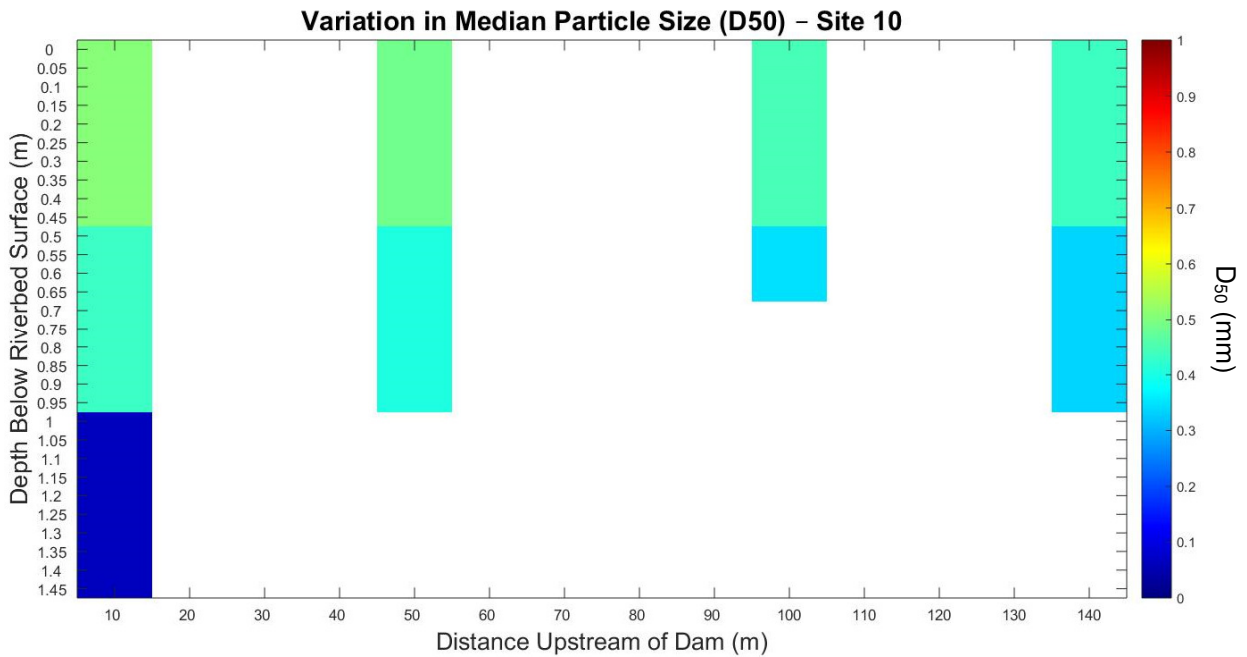
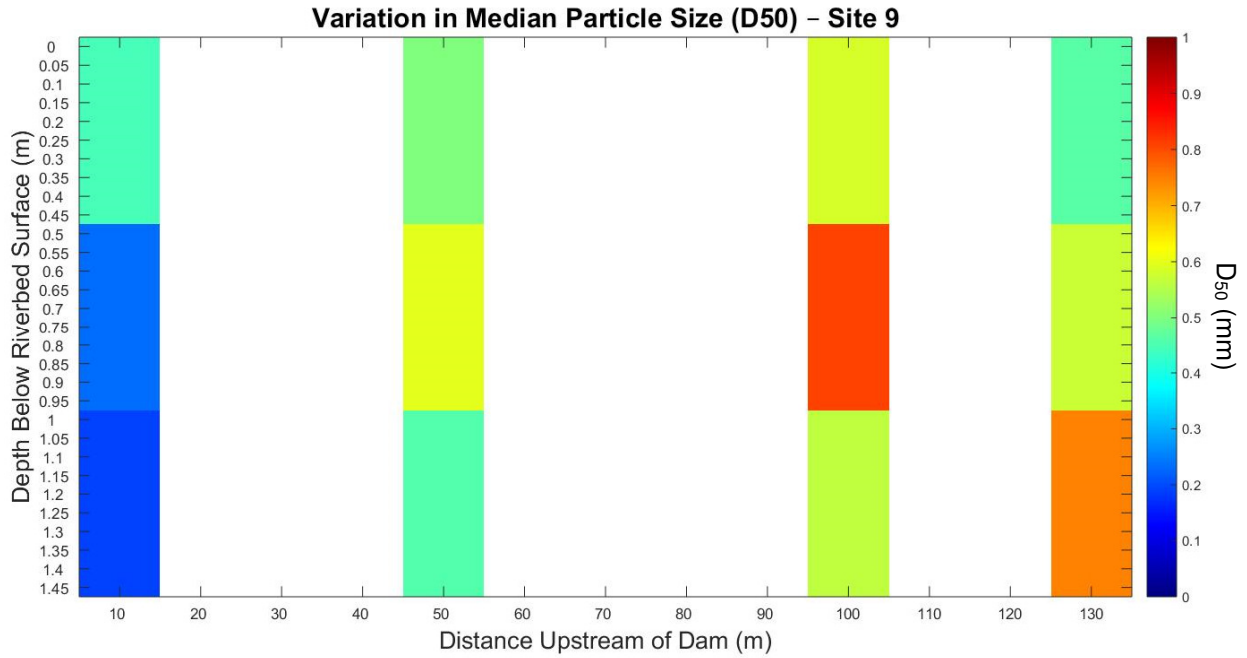
Appendix 4 (Continued): Variation in median particle size by location and depth



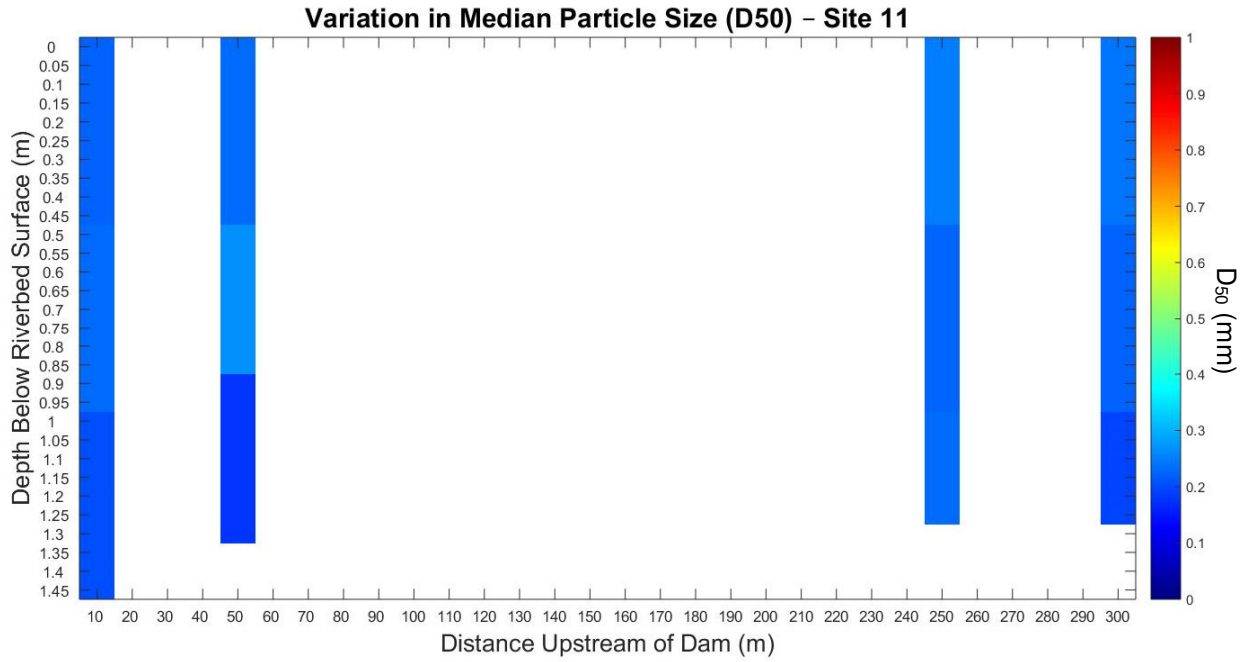
Appendix 4 (Continued): Variation in median particle size by location and depth



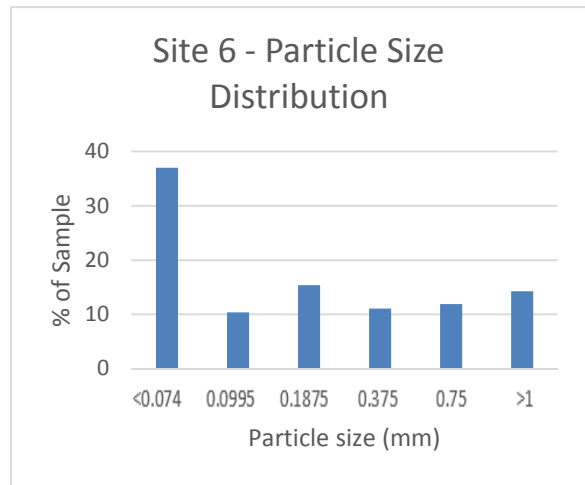
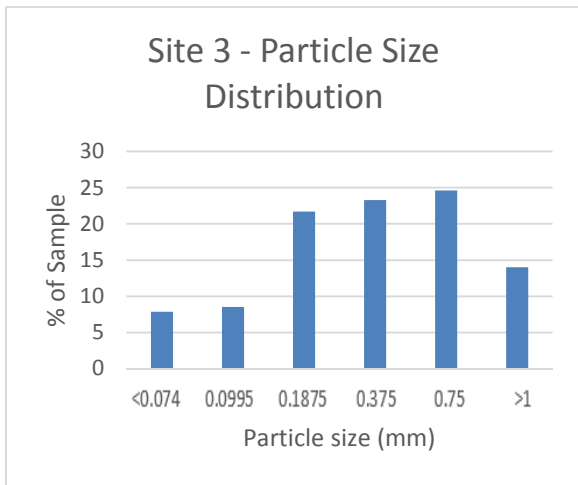
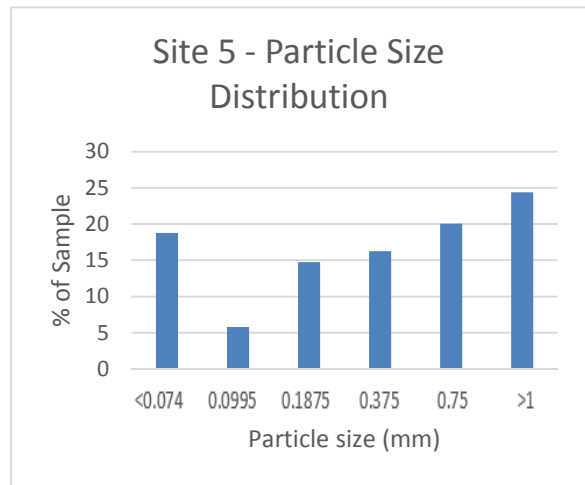
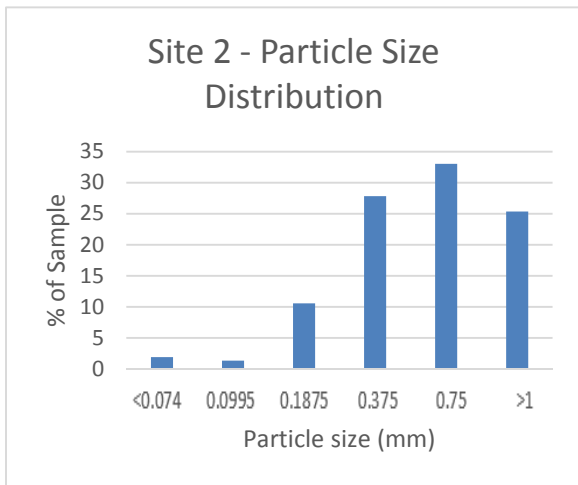
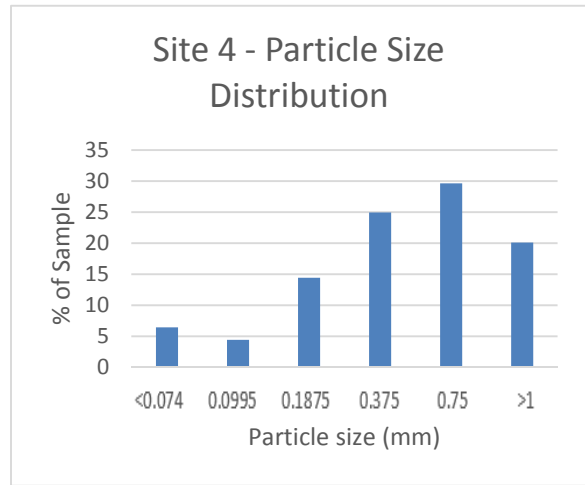
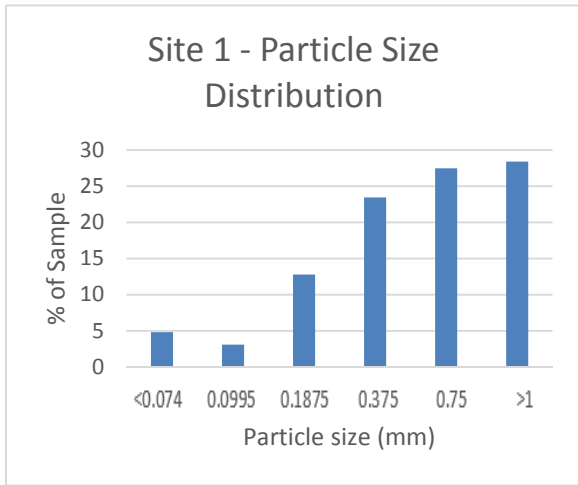
Appendix 4 (Continued): Variation in median particle size by location and depth



Appendix 4 (Continued): Variation in median particle size by location and depth



Appendix 5: Particle size distribution plots for bulk site sediment



Appendix 5 (Continued): Particle size distribution plots for bulk site sediment

